Geometric transition from hyperbolic to Anti-de Sitter structures in dimension four

Stefano Riolo, Andrea Seppi

HAL Id: hal-03000924
https://hal.science/hal-03000924

GEOMETRIC TRANSITION FROM HYPERBOLIC TO ANTI-DE SITTER STRUCTURES IN DIMENSION FOUR

STEFANO RIOLO AND ANDREA SEPPI

ABSTRACT. We provide the first examples of geometric transition from hyperbolic to Anti-de Sitter structures in dimension four, in a fashion similar to Danciger's three-dimensional examples. The main ingredient is a deformation of hyperbolic 4-polytopes, discovered by Kerckhoff and Storm, eventually collapsing to a 3-dimensional ideal cuboctahedron. We show the existence of a similar family of collapsing Anti-de Sitter polytopes, and join the two deformations by means of an opportune half-pipe orbifold structure. The desired examples of geometric transition are then obtained by gluing copies of the polytope.

1. INTRODUCTION

In this paper we provide explicit examples of geometric transition in dimension four. Before stating the main result (Theorem 1.1 below), we begin with some motivational preliminaries in dimension three.

Degeneration and transition. In his famous notes [Thu79], Thurston introduced a phenomenon called *degeneration* of hyperbolic structures. Several contributions have then been given on this topic [Hod86, Por98, HPS01, Por02, Ser05, PW07, Por13, Koz13, LMA15a, LMA15b, Koz16], which plays an important role in the proof of the celebrated Orbifold Theorem [BLP05, CHK00].

As an example, for some closed hyperbolic 3-orbifolds $\mathcal{X}$, singular along a knot $\Sigma \subset \mathcal{X}$ with cone angle $\frac{2\pi}{m}$, the following holds. There is a path $\theta \mapsto \mathcal{X}_\theta$ of hyperbolic cone-manifold structures on $\mathcal{X}$ with singular locus Σ and cone angle $\theta \in \left[\frac{2\pi}{m}, 2\pi\right)$, such that $\mathcal{X}_\theta$ collapses to a lower-dimensional orbifold as $\theta \to 2\pi$. This holds, for instance, when $\mathcal{X}$ is an exceptional Dehn filling of the figure-eight knot complement admitting a Seifert fibration $\mathcal{X} \to \mathcal{N}$ with base a hyperbolic 2-orbifold $\mathcal{N}$. As $\theta \to 2\pi$, the cone-manifold $\mathcal{X}_\theta$ collapses to $\mathcal{N}$, whose hyperbolic structure is said to *regenerate* to 3-dimensional hyperbolic structures.

The familiar idea of going from spherical to hyperbolic geometry, through Euclidean geometry, was known since Klein [AP15]. This is a continuous process inside projective geometry, seen as a common "ambient" geometry. This phenomenon, called *geometric transition*, has been recently studied in greater generality by Cooper Danciger and Wienhard [CDW18] (see also [Tre19]) through the notion of *limit geometry*. For example, among others, Euclidean geometry is a limit of both spherical and hyperbolic geometries inside projective geometry.

Let us come back to our hyperbolic cone 3-manifolds $\mathcal{X}_\theta$ collapsing to the hyperbolic 2-orbifold $\mathcal{N}$. The work of Danciger [Dan11, Dan13, Dan14] shows that in many such cases the hyperbolic structure of $\mathcal{N}$ regenerates to Anti-de Sitter (AdS for short, the Lorentzian analogue of hyperbolic geometry) structures on $\mathcal{X}$, where the singular locus Σ is a spacelike geodesic. Moreover, the two deformations are joined continuously via projective geometry so

as to have geometric transition. To this purpose, Danciger introduced the so called *half-pipe* (HP for short) geometry, which is a limit geometry [CDW18] inside projective geometry of both hyperbolic and Anti-de Sitter geometry. Half-pipe space naturally identifies with the space of spacelike hyperplanes in Minkowski space $\mathbb{R}^{1,n-1}$, and its group of transformations, which is a Chabauty limit of both $\mathrm{Isom}(\mathbb{H}^n)$ and $\mathrm{Isom}(\mathbb{A}\mathrm{d}\mathbb{S}^n)$, is isomorphic to $\mathrm{Isom}(\mathbb{R}^{1,n-1})$ by means of this duality. Suitable projective transformations are used to "rescale" the hyperbolic and AdS metric along the direction of collapse, thus obtaining geometric transition via half-pipe geometry.

In [Dan13, Theorem 1.1], Danciger provides an infinite class of Seifert 3-manifolds $\mathcal{X}$ (unit tangent bundles of some hyperbolic 2-orbifolds) supporting such a kind of geometric transition. Also, [Dan13, Theorem 1.2] is a regeneration result of half-pipe structures under a fairly general condition: the 1-dimensionality of the twisted cohomology group $H^1_{\mathrm{Ad}\,\rho}(\pi_1(\mathcal{X} \smallsetminus \Sigma), \mathfrak{so}(1,2))$, where $\rho \colon \pi_1(\mathcal{X} \smallsetminus \Sigma) \to \mathrm{Isom}(\mathbb{H}^2)$ is the representation associated to the degenerate structure and $\mathrm{Ad} \colon \mathrm{Isom}(\mathbb{H}^2) \to \mathrm{Aut}(\mathfrak{so}(1,2))$ is the adjoint representation.

Examples of transition in dimension four. It seems natural to ask whether this phenomenon is purely three-dimensional, or if it can happen also in higher dimension, where hyperbolic structures are typically more rigid. In this paper we answer affirmatively in dimension four. We indeed build some examples of geometric transition from hyperbolic to AdS structures. The construction is explicitly obtained by gluing copies of a hyperbolic or AdS collapsing 4-polytope.

The study of deformations of 4-dimensional hyperbolic cone-manifolds is quite recent, and in general very little is known on this topic. Recently, Martelli and the first author [MR18, Theorem 1.2] provided the first example of degeneration of hyperbolic cone structures on a 4-manifold to a 3-dimensional hyperbolic structure. We show that in this case there is geometric transition from hyperbolic to AdS structures, and provide an infinite class of such examples. The existence of such a phenomenon is a novelty in dimension four. Precisely, we show the following:

Theorem 1.1. *Let $\mathcal{N}$ be a hyperbolic 3-manifold that finitely orbifold-covers the ideal right-angled cuboctahedron. There exists a C^1 family $\{\sigma_t\}_{t \in (-\epsilon,\epsilon]}$ of simple projective cone-manifold structures on the 4-manifold*

$$\mathcal{X} = \mathcal{N} \times S^1,$$

singular along a compact foam $\Sigma \subset \mathcal{X}$, such that σ_t is conjugated to a geodesically complete, finite-volume,

- *hyperbolic orbifold structure with cone angles π as $t = \epsilon$,*
- *hyperbolic cone structure with decreasing cone angles $\alpha_t \in [\pi, 2\pi)$ as $t > 0$,*
- *half-pipe structure with spacelike singularity as $t = 0$,*
- *Anti-de Sitter structure with spacelike singularity of increasing magnitude $\beta_t \in (-\infty, 0)$ as $t < 0$.*

As $t \to 0^+$ (resp. $t \to 0^-$), we have $\alpha_t \to 2\pi$ (resp. $\beta_t \to 0$) and the induced hyperbolic (resp. AdS) structures on $\mathcal{X} \smallsetminus \Sigma$ degenerate to the complete hyperbolic structure of $\mathcal{N}$.

Similarly to Danciger's [Dan13, Theorem 1.1], but in higher dimension, there is a circle bundle $\mathcal{X} \to \mathcal{N}$ over a hyperbolic orbifold $\mathcal{N}$, and geometric transition from hyperbolic to AdS singular structures on $\mathcal{X}$ with collapse to $\mathcal{N}$. Let us briefly explain some terminology used in the statement of Theorem 1.1.
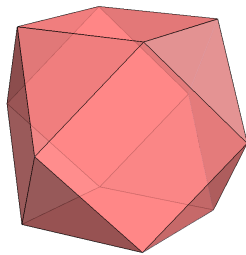
FIGURE 1. A cuboctahedron in $\mathbb{R}^3$. The ideal right-angled cuboctahedron in $\mathbb{H}^3$ can be seen as a cusped hyperbolic 3-orbifold.
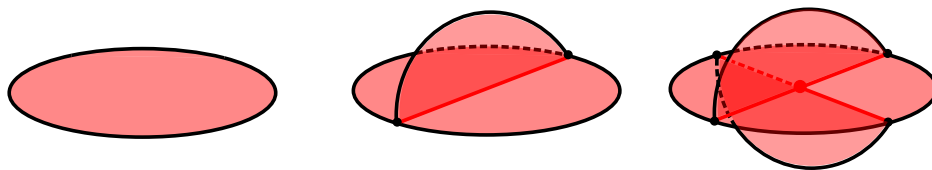

FIGURE 2. In red, the local models of a foam Σ, seen as open cones over some graphs (drawn in black). From left to right, a neighbourhood in Σ of a point in a 2-, 1-, and 0-stratum of Σ, respectively. Note that the third local model includes the other two. A foam in a 4-manifold is somehow the analogue of a trivalent graph in a 3-manifold.

The *cuboctahedron*, drawn in Figure 1, is a well-known uniform polyhedron whose *ideal* hyperbolic counterpart $\mathcal{C} \subset \mathbb{H}^3$ is *right-angled*. As such, the polyhedron $\mathcal{C}$ can be seen as a cusped hyperbolic 3-orbifold.

Roughly speaking, *simple projective cone-manifolds* (Definition 5.3) are singular real projective manifolds locally modelled on the double of a simple polytope in projective space. The singular locus $\Sigma \subset \mathcal{X}$ of an n-dimensional simple projective cone-manifold $\mathcal{X}$ is an $(n-2)$-complex with generic singularities: if $n = 1, 2, 3$ or 4, the set Σ is empty, discrete, a trivalent graph or a foam, respectively. A *foam* is a 2-complex locally modelled on the cone over the 1-skeleton of the tetrahedron; see Figure 2. Our singular locus is not a surface, as it has edges and vertices. However foams are quite natural objects in dimension four (like trivalent graphs in 3-manifolds). To the best of our knowledge, it is not known whether there can even exist deformations of 4-dimensional, finite-volume, hyperbolic cone-manifolds with singular locus an embedded surface.

The holonomy of a meridian $\gamma \in \pi_1(\mathcal{X} \smallsetminus \Sigma)$ of a 2-stratum of Σ has a totally geodesic 2-plane as fixed point set. We have a rotation in $\mathbb{H}^4$ of angle α_t when $t > 0$, and a Lorentz boost in $\mathbb{A}\mathrm{d}\mathbb{S}^4$ of magnitude β_t as $t < 0$. In the half-pipe case, we have a transformation that can be interpreted as an infinitesimal rotation (resp. boost) in $\mathbb{H}^4$ (resp. $\mathbb{A}\mathrm{d}\mathbb{S}^4$).

It is worth remarking that the cone-manifolds of Theorem 1.1 are non-compact, but of finite volume. (See [FS19, Chapter 5] and [BF18] for the notion of volume in half-pipe geometry.) Nevertheless, the singularity Σ is compact, or in other words, it does not enter into the ends of the cone-manifolds. These ends are (non-singular) *cusps* in a suitable sense: while for hyperbolic manifolds this notion is well-established, we propose here an analogue definition for AdS and half-pipe manifolds (Definition 3.6). As a direct consequence of our methods, we achieve a nice description of the geometry of the cusps. A section of the cusps will indeed naturally support a geometric transition from Euclidean to Minkowski (non-singular) structures — going through an intermediate geometry which is a "flat version" of

half-pipe geometry and is the so-called *Galilean geometry* [Yag79]. The curious reader might want to have a preliminary look at Figure 20 at page 40.

Also the *links* (the "spheres of directions") of the points of $\mathcal{X}$ naturally carry a geometric transition, which enlightens the structure of Σ itself, and will be described in Figures 25, 26 and 27 at page 48.

Finally, we remark that the statement of Theorem 1.1 can be made slightly more general by our methods, just assuming that $\mathcal{N}$ is a *cuboctahedral manifold*, namely a hyperbolic manifold tessellated by ideal right-angled cuboctahedra. We however chose to keep the statement in this simpler version. See Remark 7.29 for more details.

The proof: extending Kerckhoff and Storm's construction. The essential ingredient for the proof of Theorem 1.1 is a deforming 4-polytope $\mathcal{P}_t \subset \mathbb{H}^4$ parametrised by $t \in (0, 1]$, introduced by Kerckhoff and Storm [KS10]. For a particular choice of the 3-manifold $\mathcal{N}$, the hyperbolic cone structures σ_t that degenerate were shown to exist by Martelli and the first author [MR18, Theorem 1.2] by gluing eight copies of $\mathcal{P}_t$.

A fundamental property of $\mathcal{P}_t$ is that most of its dihedral angles are right for all values of t, while the remaining dihedral angles are all equal and tend to π as $t \to 0$, i.e. when $\mathcal{P}_t$ collapses to the aforementioned cuboctahedron. The presence of many right angles is essential in order to glue copies of $\mathcal{P}_t$ without creating a too complicated singular locus.

To prove Theorem 1.1, we first show that the path of hyperbolic polytopes extends for negative times $t \in (-1, 0)$ to a path of AdS polytopes with the same combinatorics of $\mathcal{P}_t \subset \mathbb{H}^4$ with $t \in (0, \epsilon]$, and sharing similar properties on the dihedral angles and on the collapse. A remarkable difference is that, since the AdS metric is Lorentzian, some of the bounding hyperplanes are spacelike, and some others timelike.

The construction is however quite complicated and involves several computations. To prove that the combinatorics of the AdS polytopes remains constant, we needed to implement a SAGE [The17] worksheet to prove Lemma 7.8. The proof of the analogous property on the hyperbolic side [KS10, MR18] circumvented this amount of computations relying on Vinberg's theory of hyperbolic polytopes with non-obtuse dihedral angles.

By opportunely rescaling $\mathcal{P}_t$ inside projective space along the direction of collapse, as suggested by the work of Danciger, we show that the resulting path of rescaled projective polytopes extends as $t = 0$ to a half-pipe 4-polytope. This whole deformation can be interpreted as a geometric transition of "cone-orbifold" structures. More precisely, the subset

$$\mathcal{P}_t^\times \subset \mathcal{P}_t$$

obtained by removing the ridges (the codimension-2 faces) with non-constant dihedral angles has a natural structure of hyperbolic (when $t > 0$) or AdS (when $t < 0$) orbifold. To show that these structures are linked by geometric transition, we construct an opportune half-pipe orbifold structure on the "rescaled limit" of $\mathcal{P}_t^\times$ as $t \to 0$.

Then, inspired by [MR18], we glue several copies of $\mathcal{P}_t$ in the following way. Any d-sheeted orbifold cover $\mathcal{N} \to \mathcal{C}$ of the the ideal right-angled cuboctahedron naturally induces a way to pair certain facets of d copies of $\mathcal{P}_t$. When $t < 0$, these facets are precisely the timelike facets of the AdS polytope. The resulting space is homeomorphic to $\mathcal{N} \times [0, 1]$, and its two boundary components contain all the ridges of the copies of $\mathcal{P}_t$ with non-constant dihedral angle. The final step is to double this manifold, thus obtaining $\mathcal{X} = \mathcal{N} \times S^1$ with a structure of hyperbolic, or AdS, cone-manifold. The singular locus Σ consists of the union of the copies of the ridges with non-constant dihedral angle.

We would like to stress here a particular caveat of this construction. The fact that the polytope $\mathcal{P}_t$, suitably rescaled, converges when $t \to 0$ to a half-pipe polytope is *not* sufficient to produce a half-pipe orbifold structure on the rescaled limit of $\mathcal{P}_t^\times$. Indeed, in contrast with the hyperbolic or AdS case, a hyperplane in half-pipe space does not uniquely determine a half-pipe reflection: there is a one-parameter family of reflections which fix a non-spacelike (i.e. *degenerate*) hyperplane. This counterintuitive phenomenon, which often occurs in the realm of real projective geometry, highlights the fact that half-pipe geometry is neither Riemannian, nor pseudo-Riemannian. Hence finding the "half-pipe glueings" is somehow subtler, and will be achieved by analysing the behaviour of the holonomy representations of the hyperbolic and AdS structures infinitesimally, near the collapse.

This analysis of the holonomy representations "nearby" the collapse, which is important in our construction of half-pipe structures, is one of the motivations of our work [RSa]. In general, a half-pipe structure is never rigid, because one can always conjugate with a transformation which "stretches" the degenerate direction, and obtain a new structure equivalent to the initial one *as a real projective structure*, but inequivalent *as a half-pipe structure*. We discover *a posteriori* in [RSa] that such "stretchings" are the only possible deformations of the HP orbifold structure we found, which is therefore essentially unique.

Organisation of the paper. We first develop some tools which will be useful in the following. In Section 2 we recall the relevant notions of geometric structures and geometric transition in any dimension. We introduce AdS and HP cusps in Section 3, hyperplanes, rotations and reflections in Section 4, and cone-manifolds in Section 5.

Then, we construct our examples of geometric transition. More precisely, in Section 6 we study some examples in dimension three, which are of fundamental importance to the understanding of the four-dimensional construction. The latter is developed in Section 7, which provides the proof of Theorem 1.1.

2. Geometric transition from $\mathbb{H}^n$ to $\mathbb{AdS}^n$

In this first part of the paper, we recall the relevant notions of geometric structures and geometric transition in any dimension, and we develop some tools which will be useful in the following.

We start by recalling the basic definitions concerning projective structures, in particular hyperbolic, Anti-de Sitter and half-pipe structures, and geometric transition.

2.1. **(G,X)-structures.** Recall that, given a Lie group G of analytic diffeomorphisms of a manifold X, a (G, X)-*structure* $\mathscr{P}$ on a smooth manifold $\mathcal{M}$ consists of an atlas

$$\mathscr{A} = \{\varphi^U : U \to X \,|\, U \in \mathscr{U}\}$$

where $\mathscr{U}$ is an open covering of $\mathcal{M}$, the maps φ are diffeomorphisms onto their images, and the transition functions are restrictions of elements of G.

Let $\widetilde{\mathcal{M}} \to \mathcal{M}$ the universal covering. It is well-known that a (G, X)-structure on $\mathcal{M}$ is equivalent to the data of a *developing map*

$$\mathrm{dev}\colon \widetilde{\mathcal{M}} \to X \ ,$$

which is a local diffeomorphism, and a *holonomy representation*

$$\rho\colon \pi_1 \mathcal{M} \to G \ ,$$

satisfying the condition that dev is equivariant for the holonomy representation. The pair (dev, ρ) is well-defined up to the action of G on such pairs, where G is acting on local diffeomorphisms from $\widetilde{\mathcal{M}}$ to X by post-composition and on G-valued representations by conjugation.

We say that a family $\mathscr{P}_t$ of (G, X)-structures on $\mathcal{M}$ is C^k if it admits a family of pairs (dev_t, ρ_t) such that $t \mapsto \mathrm{dev}_t \in C^\infty(\widetilde{\mathcal{M}}, X)$ is continuous for the C^k-norm on any compact set of $\widetilde{\mathcal{M}}$, and $t \mapsto \rho_t(\gamma) \in G$ is C^k for every $\gamma \in \pi_1 \mathcal{M}$.

2.2. **Real projective structures.** In this paper, we are interested in *real projective structures* on manifolds — namely, structures locally modelled on the real projective space P^n.

We denote by $\mathrm{Aut}(\mathsf{P}^n)$ the group of projective transformations of P^n, which is identified to $\mathrm{PGL}_{n+1}(\mathbb{R})$.

Definition 2.1. A *real projective structure* on an n-manifold $\mathcal{M}$ is an $(\mathrm{Aut}(\mathsf{P}^n), \mathsf{P}^n)$-structure. A *real projective manifold* is a manifold endowed with a real projective strucure.

The goal of this paper is to produce families of real projective structures on a fixed smooth manifold. Our structures will be obtained by gluing several copies of a projective polytope. In general, (convex) polytopes are conveniently defined as the intersection of some half-spaces (see Section 5.1). Since in P^n there is no notion of half-space, we will work with its double cover, namely the *projective sphere*

$$\mathsf{S}^n = \{x \in \mathbb{R}^{n+1} \smallsetminus \{0\}\}/\mathbb{R}_{>0} \ ,$$

where the group $\mathbb{R}_{>0}$ acts by multiplication. We will always use the notation

$$x = (x_0, \ldots, x_n) \in \mathbb{R}^{n+1}, \quad [x] = [x_0 : \ldots : x_n] \in \mathsf{S}^n.$$

The projective sphere S^n is clearly endowed with a real projective structure induced by the double covering $\mathsf{S}^n \to \mathsf{P}^n$. We will denote by $\mathrm{Aut}(\mathsf{S}^n)$ the group of projective automorphisms of S^n, which is the double cover of $\mathrm{Aut}(\mathsf{P}^n)$ induced by $\mathsf{S}^n \to \mathsf{P}^n$.

An *affine chart* is a subset of S^n defined by an equation of the form $\alpha(x) > 0$, for some nonzero linear form $\alpha \in \mathbb{R}^{n+1,*}$. Throughout the paper, we will mostly consider the following affine chart:

$$\mathsf{A}^n = \{[x_0 : \ldots : x_n] \in \mathsf{S}^n \,|\, x_0 > 0\} \ .$$

We will also denote the affine coordinates of A^n by

$$(y_1, \ldots, y_n) = \left(\frac{x_1}{x_0}, \ldots, \frac{x_n}{x_0}\right).$$

Remark 2.2. To be precise, in this paper we will construct families of $(\mathrm{Aut}(\mathsf{S}^n), \mathsf{S}^n)$-structures. Actually, for the structures we will construct, the restriction of the projection $\mathsf{S}^n \to \mathsf{P}^n$ on the image of the developing map will be injective. Thus the $(\mathrm{Aut}(\mathsf{S}^n), \mathsf{S}^n)$-structures we will construct will be automatically equivalent to $(\mathrm{Aut}(\mathsf{P}^n), \mathsf{P}^n)$-structures.

Our deformations of projective structures interpolate between *hyperbolic* and *Anti-de Sitter* structures, going through *half-pipe* structures. These are introduced in the following sections.

2.3. Hyperbolic structures.

We introduce the hyperbolic n-space as follows:

$$\mathbb{H}^n = \{[x] \in \mathsf{S}^n \,|\, q_1(x) < 0 \,,\, x_0 > 0\} \,,$$

where q_1 is the quadratic form

$$q_1(x) = -x_0^2 + x_1^2 + \ldots + x_n^2 \,.$$

Observe that $\mathbb{H}^n$ is well-defined as a subset of S^n, since both conditions

$$q_1(x) < 0 \qquad \text{and} \qquad x_0 > 0$$

are invariant under multiplication by a positive number. By construction, $\mathbb{H}^n$ is contained in the affine chart A^n defined in Section 2.2, and is expressed in affine coordinates as the unit ball $\{y_1^2 + \ldots + y_n^2 < 1\}$.

The *boundary at infinity* of $\mathbb{H}^n$ is its topological frontier:

$$\partial\mathbb{H}^n = \{[x] \in \mathsf{S}^n \,|\, q_1(x) = 0 \,,\, x_0 > 0\} \,,$$

which in affine coordinates is the sphere $\{y_1^2 + \ldots + y_n^2 = 1\}$.

It is well-known that $\mathbb{H}^n$ carries a Riemannian metric of constant sectional curvature -1, which is obtained by pulling-back the standard bilinear form b_1 of signature $(-, +, \ldots, +)$ on $\mathbb{R}^{n+1}$ (whose associated quadratic form is q_1) via the immersion $\sigma \colon \mathbb{H}^n \to \mathbb{R}^{n+1}$ which maps the class $[x]$ to the unique positive multiple of x such that $q_1(x) = -1$.

It then turns out that the group $\mathrm{Isom}(\mathbb{H}^n)$ of isometries of $\mathbb{H}^n$, endowed with the Riemannian metric $\sigma^* b_1$ as above, coincides with the subgroup of $\mathrm{Aut}(\mathsf{S}^n)$ which preserves $\mathbb{H}^n \subset \mathsf{S}^n$. The group $\mathrm{Isom}(\mathbb{H}^n)$ is also identified to an index two subgroup of $\mathrm{O}(q_1)$, the group of linear isometries of the quadratic form q_1. In conclusion, we have the following definition:

Definition 2.3. A *hyperbolic structure* on an n-dimensional manifold $\mathcal{M}$ is an $(\mathrm{Isom}(\mathbb{H}^n), \mathbb{H}^n)$-structure.

As a consequence of the above discussion, a hyperbolic structure on $\mathcal{M}$ is a particular case of real projective structure, as we can consider it as a S^n-valued atlas with transition functions in $\mathrm{Aut}(\mathsf{S}^n)$.

2.4. Anti-de Sitter structures.

Let us now introduce the Anti-de Sitter n-space, in a somewhat parallel way to $\mathbb{H}^n$. We define it as:

$$\mathbb{A}\mathrm{d}\mathbb{S}^n = \{[x] \in \mathsf{S}^n \,|\, q_{-1}(x) < 0\} \,,$$

where now q_{-1} is the quadratic form of signature $(-, +, \ldots, +, -)$:

$$q_{-1}(x) = -x_0^2 + x_1^2 + \ldots + x_{n-1}^2 - x_n^2 \,.$$

The *boundary at infinity* of $\mathbb{A}\mathrm{d}\mathbb{S}^n$ is then naturally defined as

$$\partial\mathbb{A}\mathrm{d}\mathbb{S}^n = \{[x] \in \mathsf{S}^n \,|\, q_{-1}(x) = 0\} \,.$$

Remark 2.4. Anti-de Sitter space is more often defined as the image of what we defined $\mathbb{A}\mathrm{d}\mathbb{S}^n$ through the double covering $\mathsf{S}^n \to \mathsf{P}^n$. Nevertheless, the polytopes we will construct are contained in the affine chart $\mathsf{A}^n = \{x_0 > 0\}$ (although $\mathbb{A}\mathrm{d}\mathbb{S}^n$ is not), hence this choice will make no substantial difference with the more frequent definition.

As already said, $\mathbb{A}\mathrm{d}\mathbb{S}^n$ is not contained in a single affine chart. However, we can easily describe its intersection with A^n as the internal region of the one-sheeted hyperboloid

$$\mathbb{A}\mathrm{d}\mathbb{S}^n \cap \mathsf{A}^n = \{y_1^2 + \ldots + y_{n-1}^2 - y_n^2 < 1\},$$

while $\partial\mathbb{A}\mathrm{d}\mathbb{S}^n \cap \mathsf{A}^n$ is the one-sheeted hyperboloid $\{y_1^2 + \ldots + y_{n-1}^2 - y_n^2 = 1\}$ itself.

Similarly to $\mathbb{H}^n$, the space $\mathbb{A}\mathrm{d}\mathbb{S}^n$ is endowed with a metric, which is now Lorentzian, obtained as the pull-back the standard bilinear form b_{-1} of signature $(-, +, \ldots, +, -)$ on $\mathbb{R}^{n+1}$ by the immersion $\sigma \colon \mathbb{A}\mathrm{d}\mathbb{S}^n \to \mathbb{R}^{n+1}$ mapping the class $[x]$ to the unique positive multiple of x such that $q_{-1}(x) = -1$. Again, the group $\mathrm{Isom}(\mathbb{A}\mathrm{d}\mathbb{S}^n)$ of isometries of $\mathbb{A}\mathrm{d}\mathbb{S}^n$ coincides with the subgroup of $\mathrm{Aut}(\mathsf{S}^n)$ preserving $\mathbb{A}\mathrm{d}\mathbb{S}^n$, and is identified to $\mathrm{O}(q_{-1})$.

We give the following definition of Anti-de Sitter structure, which will be another particular case of projective structure:

Definition 2.5. An *Anti-de Sitter* (or *AdS*) *structure* on an n-dimensional manifold $\mathcal{M}$ is an $(\mathrm{Isom}(\mathbb{A}\mathrm{d}\mathbb{S}^n), \mathbb{A}\mathrm{d}\mathbb{S}^n)$-structure.

2.5. **Half-pipe structures.** In [Dan11], Danciger introduced half-pipe geometry as a limit (in the sense of [CDW18]; see Section 2.7) of both hyperbolic and Anti-de Sitter geometries inside real projective geometry. Its definition is the following. Let us denote by q_0 the degenerate quadratic form on $\mathbb{R}^{n+1}$:

$$q_0(x) = -x_0^2 + x_1^2 + \ldots + x_{n-1}^2 \ .$$

Then we define

$$\mathsf{HP}^n = \{[x] \in \mathsf{S}^n \,|\, q_0(x) < 0 \,, \, x_0 \geq 0\} \ ,$$

This is again well-defined by homogeneity of the two conditions, and the *boundary at infinity* of half-pipe space is:

$$\partial\mathsf{HP}^n = \{[x] \in \mathsf{S}^n \,|\, q_0(x) = 0 \,, \, x_0 \geq 0\} \ .$$

By construction, HP^n is contained in the affine chart $\mathsf{A}^n = \{x_0 > 0\}$, where it is represented as a solid cylinder, defined by the equation $y_1^2 + \ldots + y_{n-1}^2 < 1$ in affine coordinates. Its boundary at infinity is topologically a sphere, consisting of the frontier of the solid cylinder in A^n and two additional points at infinity.

In analogy with the hyperbolic and Anti-de Sitter construction, we can introduce a degenerate metric on HP^n by means of the embedding of $\sigma \colon \mathsf{HP}^n \to \mathbb{R}^{n+1}$ sending $[x]$ to the unique positive multiple of x on which q_0 takes value -1. Then one pulls-back the degenerate bilinear form b_0 of signature $(-, +, \ldots, +, 0)$. The symmetric 2-tensor $\sigma^* b_0$ obtained in this way actually corresponds to the splitting $\mathsf{HP}^n = \mathbb{H}^{n-1} \times \mathbb{R}$, where $\sigma^* b_0$ coincides with the hyperbolic metric when restricted to the first factor, and is zero whenever one of the two arguments is in the $\mathbb{R}$ factor.

One would be tempted to define the transformation group of HP^n as the group $\mathrm{Aut}(\mathsf{HP}^n) < \mathrm{Aut}(\mathsf{S}^n)$ of projective transformations that preserve $\mathsf{HP}^n \subset \mathsf{S}^n$. However, we are interested in a more rigid geometry, which will be the limit of both hyperbolic and Anti-de Sitter geometry. One then *defines* the group of half-pipe transformations as:

$$G_{\mathsf{HP}^n} = \{A \in \mathrm{O}(q_0) \,|\, A(e_n) = \pm e_n \,, \, (A(e_0))_0 > 0\} \ .$$

Here we used $e_0, \ldots, e_n$ to denote the standard basis of $\mathbb{R}^{n+1}$. The last condition means that the first coordinate of $A(e_0)$ in the standard basis is positive. Together with the fact that $A \in \mathrm{O}(q_0)$, this implies that A preserves $\mathsf{HP}^n \subset \mathsf{S}^n$.

As a consequence of the definition, one sees that elements of G_{HP^n} are of the form:

$$
A = \left[\begin{array}{c|c} \widehat{A} & \begin{matrix} 0 \\ \vdots \\ 0 \end{matrix} \\ \hline \star \quad \dots \quad \star & \pm 1 \end{array} \right] , \tag{1}
$$

where $\widehat{A}$ is a linear isometry for the quadratic form of signature $(-, +, \dots, +)$, and the stars denote the entries of any vector in $\mathbb{R}^n$. The square brackets denote the projective class of a matrix in $\mathrm{GL}_{n+1}(\mathbb{R})/\mathbb{R}_{>0}$.

Remark 2.6. In contrast with $\mathbb{H}^n$ and $\mathbb{A}\mathrm{d}\mathbb{S}^n$ (where in place of the strict inclusions there are equalities), we have

$$
G_{\mathsf{HP}^n} \subsetneq \mathrm{Aut}(\mathsf{HP}^n) \subsetneq \mathrm{Isom}(\mathsf{HP}^n),
$$

where by $\mathrm{Isom}(\mathsf{HP}^n)$ we denote the group of self-homeomorphisms of HP^n which preserve the degenerate symmetric 2-tensor $\sigma^* b_0$. Indeed, from (1), the condition that e_n is eigenvector with eigenvalue ± 1 implies that A cannot "stretch" in the degenerate direction. Moreover, the group $\mathrm{Isom}(\mathsf{HP}^n)$ is infinite-dimensional, and so it cannot even embed into $\mathrm{Aut}(\mathsf{S}^n)$.

This finally enables us to provide the definition of half-pipe structures, which is the third special type of projective structures of our interest:

Definition 2.7. A *half-pipe* (or *HP*) *structure* on an n-manifold $\mathcal{M}$ is a $(G_{\mathsf{HP}^n}, \mathsf{HP}^n)$-structure.

2.6. **Relation with Minkowski geometry.** There are two main motivations behind this definition of half-pipe geometry. One motivation is that half-pipe geometry is transitional from hyperbolic to Anti-de Sitter geometry, as explained in detail in Section 2.7 below.

The other motivation comes from the fact that HP^n is naturally the dual space of Minkowski space $\mathbb{R}^{1,n-1}$, which is the vector space $\mathbb{R}^n$ endowed with the quadratic form

$$
\widehat{q}(\widehat{x}) = -x_0^2 + x_1^2 + \dots + x_{n-1}^2 ,
$$

where $\widehat{x} = (x_0, \dots, x_{n-1})$. Indeed, if $\widehat{b}$ denotes the bilinear form of $\mathbb{R}^{1,n-1}$ whose associated quadratic form is $\widehat{q}$, then any spacelike hyperplane in $\mathbb{R}^{1,n-1}$ writes as

$$
\{ p \in \mathbb{R}^{1,n-1} \,|\, \widehat{b}(p, \widehat{x}) = a \} , \tag{2}
$$

where $\widehat{x}$ is a future-directed normal vector to the hyperplane, hence satisfying

$$
\widehat{q}(\widehat{x}) = -x_0^2 + x_1^2 + \dots + x_{n-1}^2 < 0 \qquad \text{and} \qquad x_0 > 0 ,
$$

and $a \in \mathbb{R}$. This means that the class of the pair $(\widehat{x}, a)$ belongs to HP^n. Moreover, two pairs $(\widehat{x}, a)$ and $(\widehat{x}', a')$ determine the same spacelike hyperplane if and only if they differ by multiplication by a positive number.

In conclusion, HP^n parameterises the spacelike hyperplanes in $\mathbb{R}^{1,n-1}$. Similarly, $\partial \mathsf{HP}^n$ consists of a cylinder (homeomorphic to $S^{n-2} \times \mathbb{R}$) which naturally parametrises lightlike hyperplanes of $\mathbb{R}^{1,n-1}$, plus two additional points at infinity. Moreover, we have:

Lemma 2.8. *The action of* $\mathrm{Isom}(\mathbb{R}^{1,n-1})$ *on the set of spacelike hyperplanes of* $\mathbb{R}^{1,n-1}$ *induces a group isomorphism between* $\mathrm{Isom}(\mathbb{R}^{1,n-1})$ *and* G_{HP^n}.

Although this fact has already been observed, for instance in [FS19] and [BF18], we provide a complete proof since the explicit computation of the isomorphism will be useful in the remainder of the paper.

Proof. Our purpose is to construct a group isomorphism

$$\phi \colon \mathrm{Isom}(\mathbb{R}^{1,n-1}) \to G_{\mathsf{HP}^n} \ .$$

Let us first check that it is well-defined, i.e. its image is actually composed of elements of G_{HP^n}. It will then be obvious from the definition that ϕ is a group homomorphism, and that it is injective, since clearly only the identity element of $\mathrm{Isom}(\mathbb{R}^{1,n-1})$ fixes all spacelike hyperplanes.

For this purpose, we denote by $(\widehat{A}, v)$ an isometry of $\mathbb{R}^{1,n-1}$, of the form

$$p \mapsto \widehat{A} \cdot p + v \ ,$$

for $\widehat{A} \in \mathrm{O}(\widehat{q})$, and let us compute its action on HP^n. We need to distinguish two cases. If $\widehat{A}$ is future-preserving, namely $(\widehat{A}(e_0))_0 > 0$, then the hyperplane parameterised (up to positive multiples) by $(\widehat{x}, a)$, namely

$$P = \{p \in \mathbb{R}^{1,n-1} \,|\, \widehat{b}(p, \widehat{x}) = a\}$$

is mapped to the hyperplane

$$\widehat{A} \cdot P + v = \{q \in \mathbb{R}^{1,n-1} \,|\, \widehat{b}(q, \widehat{A} \cdot \widehat{x}) = a + \widehat{b}(v, \widehat{A} \cdot \widehat{x})\} \ ,$$

which is parameterised by $(\widehat{A} \cdot \widehat{x}, a + \widehat{b}(v, \widehat{A} \cdot \widehat{x}))$. From (1), this shows that $(\widehat{A}, v)$ corresponds to the following element of G_{HP^n}:

$$\phi(\widehat{A}, v) = \left[\begin{array}{ccc|c} & & & 0 \\ & \widehat{A} & & \vdots \\ & & & 0 \\ \hline \cdots & v^T J \widehat{A} & \cdots & 1 \end{array}\right] \ ,$$

where $J = \mathrm{diag}(-1, 1, \ldots, 1)$ is the matrix which represents the bilinear form $\widehat{b}$. Similarly, one checks that the induced action of $(-\widehat{A}, v)$, with $(\widehat{A}(e_0))_0 > 0$, gives the following element of G_{HP^n}:

$$\phi(-\widehat{A}, v) = \left[\begin{array}{ccc|c} & & & 0 \\ & \widehat{A} & & \vdots \\ & & & 0 \\ \hline \cdots & v^T J \widehat{A} & \cdots & -1 \end{array}\right] \ .$$

It thus follows from (1) that ϕ is well-defined and surjective, and this concludes the proof. $\quad\square$

2.7. **Rescaled limits and geometric transition.** Let us consider the family $\mathfrak{r}_t \in \mathrm{Aut}(\mathsf{S}^n)$, depending on the real parameter $t \neq 0$, defined by:

$$\mathfrak{r}_t = \left[\mathrm{diag}\left(1, \ldots, 1, \frac{1}{t}\right)\right] \in \mathrm{GL}_{n+1}(\mathbb{R})/\mathbb{R}_{>0} \ .$$

Let us denote by q_t the quadratic form:

$$q_t(x) = -x_0^2 + x_1^2 + \ldots + x_{n-1}^2 + \mathrm{sign}(t) t^2 x_n^2 \ .$$

(Observe that the notation is consistent with the definitions of q_{-1}, q_0, q_1 in the previous sections.) Then it follows that, for $t > 0$, $\mathfrak{r}_t(\mathbb{H}^n)$ is the domain $\mathbb{X}_t^n$ in S^n defined as follows:

$$\mathbb{X}_t^n = \{[x] \in \mathsf{S}^n \,|\, q_t(x) < 0 \,,\, x_0 > 0\} \ .$$

In particular, $\mathbb{X}_1^n = \mathbb{H}^n$. Moreover, if we endow $\mathbb{X}_t^n$ with a Riemannian metric induced by the quadratic form q_t as we did for $\mathbb{H}^n$, then $\mathfrak{r}_t$ is an isometry between $\mathbb{H}^n$ and $\mathbb{X}_t^n$, and
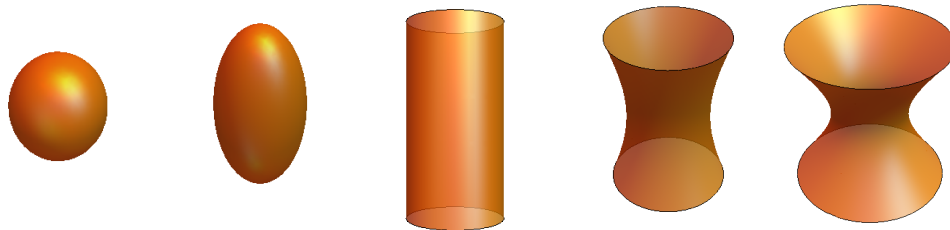
FIGURE 3. The transition from the ball model of $\mathbb{H}^n$ to the hyperboloid model of $\mathbb{AdS}^n$, in an affine chart (for $n = 3$).

therefore conjugates the isometry group of $\mathbb{H}^n$ to the isometry group of $\mathbb{X}_t^n$:

$$\mathrm{Isom}(\mathbb{X}_t^n) = \mathfrak{r}_t \mathrm{Isom}(\mathbb{H}^n) \mathfrak{r}_t^{-1} \ .$$

The following lemma says that half-pipe geometry is a "limit" of hyperbolic geometry:

Lemma 2.9 ([CDW18, FS19]). *When $t \to 0^+$, the closure $\overline{\mathbb{X}_t^n}$ converges to $\overline{\mathsf{HP}^n}$ in the Hausdorff topology of S^n, and the groups $\mathrm{Isom}(\mathbb{X}_t^n)$ converge to G_{HP^n} in the Chabauty topology on closed subgroups of $\mathrm{Aut}(\mathsf{S}^n)$.*

If we project to P^n, the situation is exactly the same for $t < 0$. However, in our setting there is a small difference due to the fact that we defined $\mathbb{AdS}^n$ as the double cover of what is usually defined as Anti-de Sitter space inside P^n (recall Remark 2.4). In particular, $\mathbb{AdS}^n$ is invariant by the antipodal map $a = [\mathrm{diag}(-1, \ldots, -1)] \in \mathrm{Aut}(\mathsf{S}^n)$ (which is in the centre of $\mathrm{Aut}(\mathsf{S}^n)$), while HP^n is contained in the affine chart $\{x_0 > 0\}$ and is therefore clearly not invariant by a. Nevertheless, if we define, for $t < 0$:

$$\mathbb{X}_t^n = \{[x] \in \mathsf{S}^n \mid q_t(x) < 0\} \ ,$$

then again $\mathfrak{r}_{|t|}$ defines an isometry between $\mathbb{AdS}^n$ and $\mathbb{X}_t^n$ endowed with the Lorentzian metric induced by q_t, so that

$$\mathrm{Isom}(\mathbb{X}_t^n) = \mathfrak{r}_{|t|} \mathrm{Isom}(\mathbb{AdS}^n) \mathfrak{r}_{|t|}^{-1} \ .$$

Similarly to the hyperbolic case, we have:

Lemma 2.10 ([CDW18, FS19]). *When $t \to 0^-$, $\overline{\mathbb{X}_t^n \cap \mathsf{A}^n}$ converges to $\overline{\mathsf{HP}^n}$, and the groups $\mathrm{Isom}(\mathbb{X}_t^n)$ converge to a central $\mathbb{Z}/2\mathbb{Z}$-extension of G_{HP^n} by means of the antipodal map.*

See also Figure 3. Motivated by this construction, we have the following definition of *geometric transition*:

Definition 2.11. [Dan13, Definition 3.8] Given an n-dimensional manifold $\mathcal{M}$, a *geometric transition* on $\mathcal{M}$ from hyperbolic to Anti-de Sitter structures is a continuous path $\{\mathscr{P}_t\}_{t \in (-\epsilon, \epsilon)}$ of real projective structures on $\mathcal{M}$ such that $\mathscr{P}_t$ is conjugate to a hyperbolic structure for $t > 0$, to a half-pipe structure for $t = 0$, and to an Anti-de Sitter structure for $t < 0$.

In fact, the geometric transitions we construct in this paper will be C^1 deformations of geometric structures.

Remark 2.12. Theorem 1.1 shows that there exists a cusped hyperbolic 3-manifold $\mathcal{N}$, a foam $\Sigma \subset \mathcal{X} = \mathcal{N} \times S^1$, and a geometric transition on the 4-manifold $\mathcal{M} = \mathcal{X} \smallsetminus \Sigma$ (see

Corollary 7.26). As in [Dan11, Dan13], the geometric structures of $\mathcal{M}$ extend to $\mathcal{X}$ with some special kinds of singularities along Σ. Such singular structures will be described in Section 5.2.

2.8. **A recipe to construct examples.** A direct way to construct examples of geometric transition from hyperbolic to Anti-de Sitter structures, which is essentially the strategy we will use in this paper, is the following. Observe that there is an isometric embedding ι of $\mathbb{H}^{n-1}$ into both $\mathbb{H}^n$ and $\mathbb{A}\mathrm{d}\mathbb{S}^n$, which is given by:

$$\iota([x_0 : \ldots : x_{n-1}]) = [x_0 : \ldots : x_{n-1} : 0] \ . \tag{3}$$

Hence $\iota(\mathbb{H}^{n-1})$ is a totally geodesic hyperplane in $\mathbb{H}^n$ (resp. $\mathbb{A}\mathrm{d}\mathbb{S}^n$), whose image is $\mathbb{H}^n \cap \{x_n = 0\}$ (resp. $\mathbb{A}\mathrm{d}\mathbb{S}^n \cap \{x_n = 0\} \cap \{x_0 > 0\}$), and the embedding ι extends to an embedding of $\partial\mathbb{H}^{n-1}$ into $\partial\mathbb{H}^n$ (resp. $\partial\mathbb{A}\mathrm{d}\mathbb{S}^n$). The same formula (3) defines also a copy of $\mathbb{H}^{n-1}$ inside HP^n.

In fact, observe that the subgroup

$$G_0 = \left\{ \left[\begin{array}{ccc|c} & & & 0 \\ & \widehat{A} & & \vdots \\ & & & 0 \\ \hline 0 & \ldots & 0 & \pm 1 \end{array} \right] \ \middle| \ \widehat{A} \in \mathrm{O}(\widehat{q}), (\widehat{A}(e_0))_0 > 0 \right\} , \tag{4}$$

is simultaneously a subgroup of $\mathrm{Isom}(\mathbb{H}^n)$, $\mathrm{Isom}(\mathbb{A}\mathrm{d}\mathbb{S}^n)$ and G_{HP^n} in $\mathrm{Aut}(\mathsf{S}^n)$, composed precisely of those elements of $\mathrm{Isom}(\mathbb{H}^n)$, $\mathrm{Isom}(\mathbb{A}\mathrm{d}\mathbb{S}^n)$ and G_{HP^n} which preserve the image of ι. The group G_0 is isomorphic to $\mathrm{Isom}(\mathbb{H}^{n-1}) \times \mathbb{Z}/2\mathbb{Z}$. The reflection $r = \mathrm{diag}(1, \ldots, 1, -1)$, along the hyperplane $\iota(\mathbb{H}^{n-1})$ of $\mathbb{H}^n$, $\mathbb{A}\mathrm{d}\mathbb{S}^n$, or HP^n is indeed central. The group G_0 is also isomorphic to $\mathrm{O}(\widehat{q})$, the isomorphism being given by

$$r^i \begin{bmatrix} \widehat{A} & 0 \\ 0 & 1 \end{bmatrix} \in G_0 \mapsto (-1)^i \widehat{A} \in \mathrm{O}(\widehat{q}) \tag{5}$$

for $i = 0, 1$. We will sometimes implicitly use this isomorphism in the paper.

With these premises, one then constructs a continuous family of projective structures $\mathscr{P}_t$ on a manifold $\mathcal{M}$, with pairs developing map-holonomy (dev_t, ρ_t) such that:

- For $t > 0$, dev_t takes values in $\mathbb{H}^n$ and ρ_t in $\mathrm{Isom}(\mathbb{H}^n)$;
- For $t < 0$, dev_t takes values in $\mathbb{A}\mathrm{d}\mathbb{S}^n$ and ρ_t in $\mathrm{Isom}(\mathbb{A}\mathrm{d}\mathbb{S}^n)$;
- When $t \to 0^{\pm}$, dev_t converges to a submersion d_0 with image in $\iota(\mathbb{H}^{n-1})$, which is h_0-equivariant for a representation h_0 of $\pi_1\mathcal{M}$ into the subgroup G_0 preserving $\iota(\mathbb{H}^{n-1})$.

Then by applying the projective transformations $\mathfrak{r}_{|t|}$, the pair $(\mathfrak{r}_{|t|} \circ \mathrm{dev}_t, \mathfrak{r}_{|t|}\rho_t\mathfrak{r}_{|t|}^{-1})$ determines a path of projective structures which, by construction, are conjugate to a hyperbolic structure when $t > 0$, and to an Anti-de Sitter structure when $t < 0$. If the pair $(\mathfrak{r}_{|t|} \circ \mathrm{dev}_t, \mathfrak{r}_{|t|}\rho_t\mathfrak{r}_{|t|}^{-1})$ converges to a pair developing map-holonomy (dev_0, ρ_0), then, as a consequence of Lemma 2.9 and Lemma 2.10, this will determine a half-pipe structure on $\mathcal{M}$.

3. GEOMETRY OF THE CUSPS

Since the cone-manifolds of Theorem 1.1 are cusped, in this section we introduce the notion of cusp in AdS and half-pipe manifolds.

3.1. **Horospheres.** Let us start with the notion of horosphere in the three geometries of our interest.
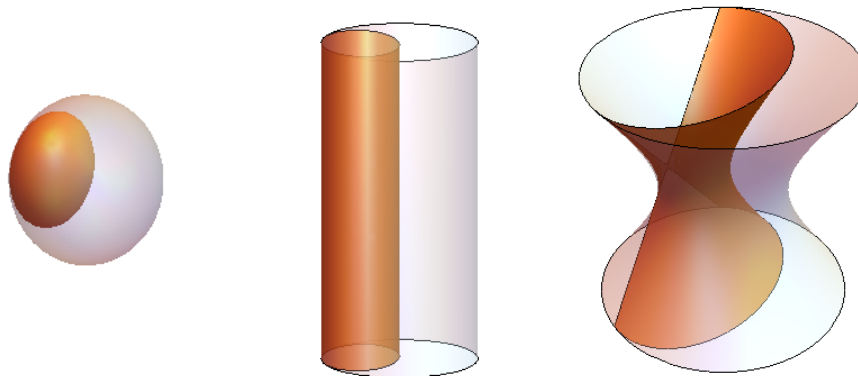
FIGURE 4. Hyperbolic, half-pipe, and Anti-de Sitter horospheres in an affine chart.

Definition 3.1. A *horosphere* in $\mathbb{H}^n$ is a smooth surface $H \subset \mathbb{H}^n$ which is orthogonal to all the geodesics with the same endpoint $p \in \partial \mathbb{H}^n$. A *horosphere* in $\mathbb{AdS}^n$ is a smooth timelike surface $H \subset \mathbb{AdS}^n$ which is orthogonal to all the spacelike geodesics with the same endpoint $p \in \partial \mathbb{AdS}^n$.

Since there is no notion of orthogonality in HP^n, the half-pipe notion is slightly different.

Definition 3.2. A *horosphere* in HP^n is the union of all the degenerate lines going through a hyperbolic horosphere $\widehat{H}$ contained in a spacelike hyperplane.

See Figure 4 to visualise the horospheres in the affine models of $\mathbb{H}^n$, HP^n and $\mathbb{AdS}^n$. In each of the three geometries, we call *boundary at infinity* of a horosphere H the set

$$\partial_\infty H = \overline{H} \smallsetminus H$$

(here $\overline{H}$ denotes the closure of H in S^n), which consists of a single point in $\partial \mathbb{H}^n$ for the hyperbolic case, a pair of antipodal points in $\partial \mathbb{AdS}^n$ for the AdS case, and of a closed interval in $\partial \mathsf{HP}^n$ for the half-pipe geometry.

In fact, in terms of the duality with $\mathbb{R}^{1,n-1}$, a horosphere in HP^n can be described as the space of all spacelike hyperplanes in $\mathbb{R}^{1,n-1}$ whose normal vector (which is a point of $\mathbb{H}^{n-1}$) lies in a horosphere of dimension $n-2$. Hence the boundary at infinity of a half-pipe horosphere consists of a degenerate (vertical) line, which corresponds to all lightlike hyperplanes in $\mathbb{R}^{1,n-1}$ containing the same lightlike direction, plus the two additional points which lie outside the affine chart A^n.

3.2. **Metric expressions and upper half-space models.** Let us now give a parameterisation of horospheres and recover their Euclidean, Minkowski, or Galilean geometry. Recall that we defined

$$\mathbb{X}_t^n = \{ [x] \in \mathsf{S}^n \mid q_t(x) < 0 \} \ ,$$

where

$$q_t(x) = -x_0^2 + x_1^2 + \ldots + x_{n-1}^2 + t|t|x_n^2 \ .$$

For $t \neq 0$, $\mathbb{X}_t^n$ is endowed with a pseudo-Riemannian metric (Riemannian for $t > 0$ and Lorentzian for $t < 0$) of constant curvature -1, given by pulling back the bilinear form b_t

on $\mathbb{R}^{n+1}$ associated to q_t by the embedding that sends $[x]$ to the unique positive multiple of x on which q_t takes the value -1. Let us thus consider the embedding

$$\eta_t \colon \mathbb{R}^{n-1} \to \mathbb{R}^{n+1}$$

given by

$$\eta_t(y_2, \ldots, y_n) = (f_t(y_2, \ldots, y_n) + 1, f_t(y_2, \ldots, y_n), y_2, \ldots, y_n) \ ,$$

where the function $f_t \colon \mathbb{R}^{n-1} \to \mathbb{R}$ is given by

$$f_t(y_2, \ldots, y_n) = \frac{1}{2}(y_2^2 + \ldots + y_{n-1}^2 + t|t|y_n^2) \ .$$

(Note that f_t is determined by the condition $q_t \circ \eta_t \equiv -1$.) By pulling back the bilinear form $b_t = -dx_0^2 + dx_1^2 + \ldots + t|t|dx_n^2$, we obtain

$$\eta_t^* b_t = dy_2^2 + \ldots + dy_{n-1}^2 + t|t|dy_n^2 \ .$$

In particular we obtained:

- for $t = 1$, a horosphere in $\mathbb{H}^n$ is isometric to Euclidean space $\mathbb{R}^{n-1}$;
- for $t = -1$ a horosphere in $\mathbb{A}d\mathbb{S}^n$ is isometric to Minkowski space $\mathbb{R}^{1,n-2}$;
- for $t = 0$ a horosphere in HP^n is isometric to $\mathbb{R}^{n-1}$, endowed with a degenerate metric of signature $+ \ldots + 0$ (the pull-back of the degenerate metric of HP^n).

In all cases, we have

$$p = [1 : 1 : 0 : \ldots : 0] \in \partial_\infty \eta_t(\mathbb{R}^{n-1}).$$

In fact, applying the projective transformation $\mathfrak{r}_t$ one sees that the half-pipe horosphere which is the image of η_0 is the rescaled limit of hyperbolic and AdS horospheres.

With a little more effort, we can use the embeddings η_t to obtain an upper half-plane model for the spaces $\mathbb{X}_t$. Let us define a parameterization $\zeta_t \colon \mathbb{R}_{>0} \times \mathbb{R}^{n-1} \to \mathbb{X}_t^n$ (this is only a local parameterization if $t < 0$, see Remark 3.4 below):

$$\zeta_t(y_1, \ldots, y_n) = \begin{pmatrix} \frac{1}{2}\left(y_1 + \frac{1}{y_1}\right) & \frac{1}{2}\left(y_1 - \frac{1}{y_1}\right) & 0 & \ldots & 0 \\ \frac{1}{2}\left(y_1 - \frac{1}{y_1}\right) & \frac{1}{2}\left(y_1 + \frac{1}{y_1}\right) & 0 & \ldots & 0 \\ 0 & 0 & 1 & & \vdots \\ \vdots & & & \ddots & \\ 0 & & \ldots & \ldots & 1 \end{pmatrix} \eta_t\left(\frac{y_2}{y_1}, \ldots, \frac{y_n}{y_1}\right) \ . \qquad (6)$$

A tedious but elementary computation shows that

$$\zeta_t^* b_t = \frac{dy_1^2 + \ldots + dy_{n-1}^2 + t|t|dy_n^2}{y_1^2} \ .$$

Remark 3.3. To explain how the expression (6) is obtained, let us observe that the big matrix in Equation (6) is an isometry for every $\mathbb{X}_t^n$, translating along the geodesic $x_2 = \ldots = x_n = 0$, which is orthogonal to the horosphere parameterised by η_t.

Hence ζ_t provides a upper half-space model for $\mathbb{H}^n$ ($t = 1$), $\mathbb{A}d\mathbb{S}^n$ ($t = -1$) and HP^n ($t = 0$). It is moreover evident that the multiplication of the last coordinate by $|t|$ provides an isometry between the upper half-space model for $\mathbb{X}_t^n$ and $\mathbb{H}^n$ (if $t > 0$) and for $\mathbb{X}_t^n$ and $\mathbb{A}d\mathbb{S}^n$ (if $t < 0$). The (spacelike, for the AdS and HP case) geodesics with endpoint at infinity $p = [1 : 1 : 0 : \ldots : 0]$ are represented by vertical lines, as expected.

Remark 3.4. The upper half-space model for $\mathbb{A}d\mathbb{S}^3$ has been described in [Dan11, Appendix A], although obtained in a different way. We remark here that, with our definition of $\mathbb{A}d\mathbb{S}^n$, the upper half-space model only covers a part of $\mathbb{A}d\mathbb{S}^n$ — roughly speaking, half of $\mathbb{A}d\mathbb{S}^n$.

A little trick to visualise a larger portion is to allow $y_1 \in \mathbb{R} \smallsetminus \{0\}$ in the parameterization ζ_{-1}. In this way, one gets a parameterization of the complement of the lightlike hyperplane $\{x_0 = x_1\}$ as the union of the upper half-space and the lower half-space. However, the boundary at infinity is somewhat more complicated to describe in this model.

3.3. **Cusps.** From the upper half-space models we constructed, we see that every isometry of $\mathbb{H}^n$ or $\mathbb{A}\mathrm{d}\mathbb{S}^n$ which preserves a horosphere H acts on H by isometries for its intrinsic (Euclidean or Minkowski) metric. Conversely, every isometry of H extends uniquely to a global isometry.

Given a horosphere H of $\mathbb{X}_t^n$, we thus define:

- for $t = 1$, the subgroup $P_1 := \mathrm{Stab}_{\mathbb{H}^n}(H) \cong \mathrm{Isom}(\mathbb{R}^{n-1})$ of $\mathrm{Isom}(\mathbb{H}^n)$;
- for $t = -1$, the subgroup $P_{-1} := \mathrm{Stab}_{\mathbb{A}\mathrm{d}\mathbb{S}^n} \cong \mathrm{Isom}(\mathbb{R}^{1,n-2})$ of $\mathrm{Isom}(\mathbb{A}\mathrm{d}\mathbb{S}^n)$;
- for $t = 0$, the subgroup $P_0 := \mathrm{Stab}_{\mathsf{HP}^n}(H) \cap \mathrm{Stab}_{\mathsf{HP}^n}(p)$ of G_{HP^n}, for some $p \in \partial_\infty H$ that is not a vertex of the closed interval $\partial_\infty H$.

The third point needs some explication. First, recall that the boundary at infinity of a half-pipe horosphere does not consist of a single point, but of a closed interval. It is for this reason that we need to specify that P_0 is the stabiliser of *both* H and $p \in \partial_\infty H$. Moreover, the condition that p is an interior point of $\partial_\infty H$ means that p is not one of the two points which lie outside the affine chart A^n (the two points at infinity in Figure 4). In other words, in the usual duality with Minkowski space, p corresponds to a lightlike hyperplane in $\mathbb{R}^{1,n-1}$.

The geometry $(G, X) = (P_0, H)$ of a half-pipe horosphere H is called *Galilean geometry* [Yag79]. It can be checked that P_0 is the limit of $\mathfrak{r}_{|t|} P_1 \mathfrak{r}_{|t|}^{-1}$ and $\mathfrak{r}_{|t|} P_{-1} \mathfrak{r}_{|t|}^{-1}$. In other words, Galilean geometry is transitional between Euclidean and Minkowski geometry.

Remark 3.5. It turns out that P_0 is isomorphic to the semidirect product $\mathrm{Isom}(\mathbb{R}^{n-2}) \ltimes \mathbb{R}^{n-1}$. (An explicit geometric interpretation can be given using the duality with Minkowski space.) We omit the precise details here, as we will explain concretely some examples of interest for this paper — see Example 3.8 below.

We are now ready for the definition of cusp in each of the three cases.

Definition 3.6. A *cusp* in a hyperbolic (resp. Anti-de Sitter, half-pipe) manifold is a region isometric to the quotient of $\{y_1 > 1\}$ in the upper half-space model, by a subgroup Γ of P_1 (resp. P_{-1}, P_0) acting properly and co-compactly on $H = \{y_1 = 1\}$.

Remark 3.7. By a standard computation, one sees that a cusp in a hyperbolic or Anti-de Sitter manifold has finite volume. For half-pipe geometry, there is a canonical volume form as well [FS19], and in the same way it is immediate to check that the volume of a cusp is finite also in this case.

Example 3.8. Simple examples are *toric cusps*, where $\Gamma \cong \mathbb{Z}^{n-1}$ lies in the normal subgroup $\mathbb{R}^{n-1}$ of P_1, P_{-1}, or P_0, and the section $^H/\Gamma$ is a Euclidean, Minkowski, or Galilean $(n-1)$-torus, respectively. In hyperbolic geometry, $\mathbb{Z}^{n-1}$ acts by translations on a Euclidean horosphere, where the standard generators of $\mathbb{Z}^{n-1}$ are linearly independent translations. Exactly the same construction goes through for the AdS case for actions on Minkowski horospheres.

Let us now provide a similar example for half-pipe geometry. Recall that a horosphere H in HP^n is the product of a horosphere $\widehat{H}$ in $\mathbb{H}^{n-1}$ and the degenerate direction, in the standard decomposition $\mathsf{HP}^n \cong \mathbb{H}^{n-1} \times \mathbb{R}$. We let $\mathbb{Z}^{n-1}$ act on H in the following way. The first $n-2$ standard generators $\gamma_1, \ldots, \gamma_{n-2}$ act on $\widehat{H}$ by translation as above. We now define the action of the remaining generator γ_{n-1}. Suppose $\widehat{H}$ is obtained as the intersection of

the hyperboloid in $\mathbb{R}^{1,n-1}$ with a lightlike hyperplane parallel to $w^\perp$, where w is a lightlike vector in $\mathbb{R}^{1,n-1}$ and $w^\perp$ is its orthogonal complement with respect to the Minkowski bilinear form $\widehat{b}$. Then we let γ_{n-1} act by translation by (a multiple of) w.

We now check, by means of the duality with Minkowski geometry (see Section 2.6), that this action of $\mathbb{Z}^{n-1}$ is faithful. Indeed, in the dual Minkowski picture, $\gamma_1, \ldots, \gamma_{n-2}$ act as

$$x \mapsto \widehat{A} \cdot x \ ,$$

where $\widehat{A}$ is a linear isometry such that $\widehat{A} \cdot w = w$. The generator γ_{n-1} acts as

$$x \mapsto x + \lambda w$$

for some $\lambda \in \mathbb{R}$. Since $\widehat{A} \cdot w = w$, it is clear that these actions commute. The resulting group $\Gamma < P_0$ thus provides an example of toric cusp in a half-pipe manifold.

The examples of geometric transition we construct in the second part of the paper will be examples of hyperbolic/Anti-de Sitter/half-pipe manifolds with cusps. We will describe the geometry of the cusps, and their transition, in terms of the geometric structures induced on the quotient of a horosphere, as in Section 7.3. We will therefore be able to visualise the corresponding transition from Euclidean to Minkowski structures of codimension one.

4. Half-spaces, reflections and rotations

In this section, we describe the behaviour of hyperplanes and half-spaces under geometric transition and introduce projective reflections. Finally, we introduce rotations, boosts and their infinitesimal analogues in half-pipe geometry.

4.1. Dual projective sphere. Let us introduce the necessary notation.

A *hyperplane* (resp. *subspace*) $H \subset \mathsf{S}^n$ of the projective sphere is the image through the quotient map $\mathbb{R}^{n+1} \smallsetminus \{0\} \to \mathsf{S}^n$ of a linear hyperplane (resp. *subspace*) of $\mathbb{R}^{n+1}$. A *half-space* $\boldsymbol{H} \subset \mathsf{S}^n$ of the projective sphere is the closure of one of the two connected components of $\mathsf{S}^n \smallsetminus H$, where H is a hyperplane. In other words, a half-space is the closure of an affine chart (see Section 2.2).

The *dual projective sphere* is defined as

$$\mathsf{S}^{n,*} = \{\alpha \in \mathbb{R}^{n+1,*} \smallsetminus \{0\}\}/\mathbb{R}_{>0} \ ,$$

where $\mathbb{R}^{n+1,*}$ is the vector space of linear forms on $\mathbb{R}^{n+1}$. We will use coordinates with respect to the dual basis of the standard basis, namely the basis $\{e_0^*, \ldots, e_n^*\}$ defined by $e_i^*(x_0, \ldots, x_n) = x_i$. We will also denote elements of $\mathsf{S}^{n,*}$ by

$$(\alpha) = (\alpha_0 : \ldots : \alpha_n) \in \mathsf{S}^{n,*}$$

if $\alpha = \alpha_0 e_0^* + \ldots + \alpha_n e_n^*$. The dual projective sphere $\mathsf{S}^{n,*}$ is identified to the space of half-spaces in S^n, by associating to the class of a linear form α the half-space defined by:

$$\boldsymbol{H} = \{[x] \in \mathsf{S}^n \,|\, \alpha(x) \leq 0\} \ .$$

By a small abuse of notation, we will sometimes denote a half-space $\boldsymbol{H} \subset \mathsf{S}^n$ with the corresponding point $(\alpha) \in \mathsf{S}^{n,*}$ of the dual sphere.

The following elementary lemma will be useful to control the behaviour of half-spaces under geometric transition.

Lemma 4.1. *Let* $\boldsymbol{H} = (\alpha_0 : \ldots : \alpha_n)$ *be a half-space in* S^n*. Then for every* $t > 0$*, the half-space* $\mathfrak{r}_t \boldsymbol{H}$ *has coordinates*

$$\mathfrak{r}_t \boldsymbol{H} = \left(\frac{\alpha_0}{t} : \ldots : \frac{\alpha_{n-1}}{t} : \alpha_n\right) \ .$$

Proof. Recall that the projective transformation $\mathfrak{r}_t$ is defined by

$$\mathfrak{r}_t = \left[\operatorname{diag}\left(1, \ldots, 1, \frac{1}{t} \right) \right] \ .$$

Given $[x] = [x_0 : \ldots : x_n]$, then $[x] \in \mathfrak{r}_t \boldsymbol{H}$ if and only if $[x] = \mathfrak{r}_t([x'])$ for some $[x'] \in \boldsymbol{H}$; namely:

$$[x_0 : \ldots : x_{n-1} : x_n] = \left[x_0' : \ldots : x_{n-1}' : \frac{x_n'}{t} \right] \ ,$$

where $[x_0' : \ldots : x_{n-1}' : x_n']$ satisfies the defining condition for $\boldsymbol{H}$, namely:

$$\alpha_0 x_0' + \ldots + \alpha_n x_n' \leq 0 \ .$$

By multiplying by $1/t$, this is equivalent to

$$\frac{\alpha_0}{t} x_0 + \ldots + \frac{\alpha_{n-1}}{t} x_{n-1} + \alpha_n x_n \leq 0 \ .$$

This proves the claim. $\qquad\square$

Definition 4.2. A *half-space* (resp. *hyperplane*, *subspace*) in $\mathbb{X}_t^n$ is a nonempty intersection of $\mathbb{X}_t^n$ with a half-space (resp. hyperplane, subspace) of S^n.

4.2. **Hyperplanes in $\mathbb{H}^n$ and $\mathbb{A}\mathrm{d}\mathbb{S}^n$.** We shall now provide a geometric description of hyperplanes and half-spaces in $\mathbb{H}^n$, $\mathbb{A}\mathrm{d}\mathbb{S}^n$ and HP^n. Let us start with the hyperbolic space. We have the following simple lemma.

Lemma 4.3. *Given a half-space $\boldsymbol{H} = (\alpha)$ of S^n, $\partial\boldsymbol{H}$ intersects $\mathbb{H}^n$ if and only if*

$$q_1(\alpha_0, \ldots, \alpha_n) > 0 \ .$$

Proof. It is well-known that a hyperplane in $\mathbb{R}^{n+1}$ intersects $\mathbb{H}^n$ if and only if its orthogonal complement for the bilinear form b_1 (whose associated quadratic form is q_1), seen as a line in Minkowski space $\mathbb{R}^{1,n}$, is spacelike. Compared to our lemma, there is only one small caveat: when choosing the dual basis of $\mathbb{R}^{n+1,*}$ as $\{e_0^*, \ldots, e_n^*\}$, we are essentially using the standard Euclidean product to identify $\mathbb{R}^{n+1,*}$ with $\mathbb{R}^{n+1}$. On the other hand, taking the orthogonal complement in $\mathbb{R}^{1,n}$ corresponds to choosing the basis $\{-e_0^*, e_1^*, \ldots, e_{n-1}^*, e_n^*\}$. However, the two choices differ by the following change of coordinates

$$(\alpha_0, \alpha_1, \ldots, \alpha_n) \mapsto (-\alpha_0, \alpha_1, \ldots, \alpha_n)$$

which is an isometry for the quadratic form q_1. Hence Lemma 4.3 follows. $\qquad\square$

By the same reason, we can also use the usual formulae to compute the dihedral angle between two half-spaces:

Lemma 4.4. *Given α, α' such that $q_1(\alpha), q_1(\alpha') < 0$ let $\boldsymbol{H} = (\alpha)$ and $\boldsymbol{H}' = (\alpha')$ be the corresponding half-spaces. The hyperplanes $\partial\boldsymbol{H}$ and $\partial\boldsymbol{H}'$ intersect transversely in $\mathbb{H}^n$ if and only if*

$$|b_1(\alpha, \alpha')| < \sqrt{|q_1(\alpha)|}\sqrt{|q_1(\alpha')|} \ .$$

In this case, the dihedral angle θ between the half-spaces $\boldsymbol{H}$ and $\boldsymbol{H}'$ satisfies

$$\cos\theta = -\frac{b_1(\alpha, \alpha')}{\sqrt{|q_1(\alpha)|}\sqrt{|q_1(\alpha')|}} \ .$$

One can also find similar formulae for the Anti-de Sitter case. It turns out that every hyperplane $\partial\boldsymbol{H}$ in S^n intersects $\mathbb{A}\mathrm{d}\mathbb{S}^n$ non-trivially. Moreover, recall that a hyperplane in Anti-de Sitter space is called *spacelike*, *timelike* or *lightlike* if the induced bilinear form is positive definite, indefinite or degenerate, respectively. One then has the following characterisation:

Lemma 4.5. *Let $\boldsymbol{H} = (\alpha_0 : \ldots : \alpha_n)$ be a half-space of S^n. Then $\partial\boldsymbol{H} \cap \mathbb{A}\mathrm{d}\mathbb{S}^n$ is:*

- *Spacelike if $q_{-1}(\alpha_0, \ldots, \alpha_n) < 0$. In this case, $\partial\boldsymbol{H} \cap \mathbb{A}\mathrm{d}\mathbb{S}^n$ consists of two disconnected totally geodesic copies of $\mathbb{H}^{n-1}$.*
- *Timelike if $q_{-1}(\alpha_0, \ldots, \alpha_n) > 0$. In this case, $\partial\boldsymbol{H} \cap \mathbb{A}\mathrm{d}\mathbb{S}^n$ consists of a totally geodesic copy of $\mathbb{A}\mathrm{d}\mathbb{S}^{n-1}$.*
- *Lightlike if $q_{-1}(\alpha_0, \ldots, \alpha_n) = 0$.*

One can then compute angles between hyperplanes by a direct formula in terms of the bilinear form b_{-1}. We provide here the formula for the case of two spacelike hyperplanes.

We recall that the *angle* between two spacelike hyperplanes in a Lorentzian space is a number $\varphi \in [0, +\infty)$, which is defined as the distance in a copy of $\mathbb{H}^{n-1}$ between the two points corresponding to the two future unit normal vectors in the tangent space at an intersection point. This notion of angle is used in Lemma 4.6 below. See also Figure 5.

Lemma 4.6. *Given α, α' such that $q_{-1}(\alpha), q_{-1}(\alpha') < 0$ let $\boldsymbol{H} = (\alpha)$ and $\boldsymbol{H}' = (\alpha')$ be the corresponding half-spaces. The hyperplanes $\partial\boldsymbol{H}$ and $\partial\boldsymbol{H}'$ intersect transversely in $\mathbb{A}\mathrm{d}\mathbb{S}^n$ if and only if*

$$|b_{-1}(\alpha, \alpha')| > \sqrt{|q_{-1}(\alpha)|}\sqrt{|q_{-1}(\alpha')|} \ .$$

In this case, the angle φ between the hyperplanes $\partial\boldsymbol{H}$ and $\partial\boldsymbol{H}'$ satisfies the equation:

$$\cosh\varphi = \frac{|b_{-1}(\alpha, \alpha')|}{\sqrt{|q_{-1}(\alpha)|}\sqrt{|q_{-1}(\alpha')|}} \ ,$$

where the sign of $b_{-1}(\alpha, \alpha')$ is negative if $\boldsymbol{H} \cap \boldsymbol{H}'$ contains timelike segments with endpoints in $\partial\boldsymbol{H} \cap \partial\boldsymbol{H}'$, and positive otherwise.

We also need to briefly analyse the situation for the intersection between two timelike hyperplanes. See also Figure 6.

Lemma 4.7. *Given α, α' such that $q_{-1}(\alpha), q_{-1}(\alpha') > 0$ let $\boldsymbol{H} = (\alpha)$ and $\boldsymbol{H}' = (\alpha')$ be the corresponding half-spaces. The hyperplanes $\partial\boldsymbol{H}$ and $\partial\boldsymbol{H}'$ always intersect in $\mathbb{A}\mathrm{d}\mathbb{S}^n$. Moreover:*

- *The intersection is spacelike (i.e. a totally geodesic copy of $\mathbb{H}^{n-2}$) if and only if*

$$|b_{-1}(\alpha, \alpha')| > \sqrt{|q_{-1}(\alpha)|}\sqrt{|q_{-1}(\alpha')|} \ .$$

- *The intersection is timelike (i.e. a totally geodesic copy of $\mathbb{A}\mathrm{d}\mathbb{S}^{n-2}$) if and only if*

$$|b_{-1}(\alpha, \alpha')| < \sqrt{|q_{-1}(\alpha)|}\sqrt{|q_{-1}(\alpha')|} \ .$$

4.3. **Hyperplanes in half-pipe geometry.** Let us now move to the case of hyperplanes in half-pipe space. In this case, we have two types of hyperplanes: *spacelike* hyperplanes, for which the induced bilinear form is positive definite (these are isometrically embedded copies of $\mathbb{H}^{n-1}$), and *degenerate* hyperplanes, for which the induced bilinear form is indeed degenerate. These two types are detected by the following lemma.

Lemma 4.8. *A half-space $\boldsymbol{H} = (\alpha_0 : \ldots : \alpha_n)$ in S^n intersects HP^n if and only if $\alpha_n \neq 0$ or $q_0(\alpha_0, \ldots, \alpha_n) > 0$. In this case, the hyperplane $\partial\boldsymbol{H} \cap \mathsf{HP}^n$ is:*

- *Spacelike if $\alpha_n \neq 0$. In this case, $\partial\boldsymbol{H} \cap \mathsf{HP}^n$ consists of a copy of $\mathbb{H}^{n-1}$.*
- *Degenerate if $\alpha_n = 0$ and $q_0(\alpha_0, \ldots, \alpha_n) > 0$. In this case, $\partial\boldsymbol{H} \cap \mathsf{HP}^n$ consists of a copy of HP^{n-1}.*

Proof. If $\alpha_n = 0$, then $\boldsymbol{H}$ is of the form

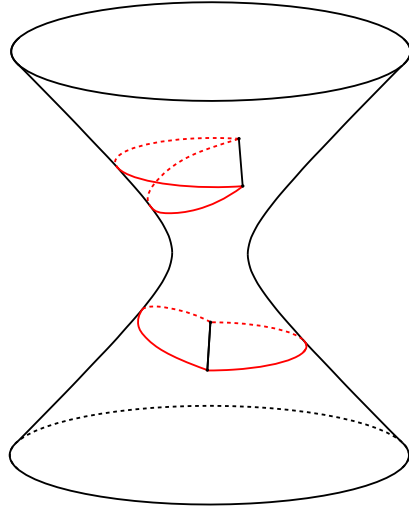$$\boldsymbol{H} = \{(\widehat{x} : x_n) \,|\, \widehat{x} \in \widehat{\boldsymbol{H}}, x_n \in \mathbb{R}\} \ ,$$

FIGURE 5. In an affine chart for Anti-de Sitter space, the two possibilities (above and below in the same figure) for the configuration of $\boldsymbol{H}$ and $\boldsymbol{H}'$ as in Lemma 4.6.
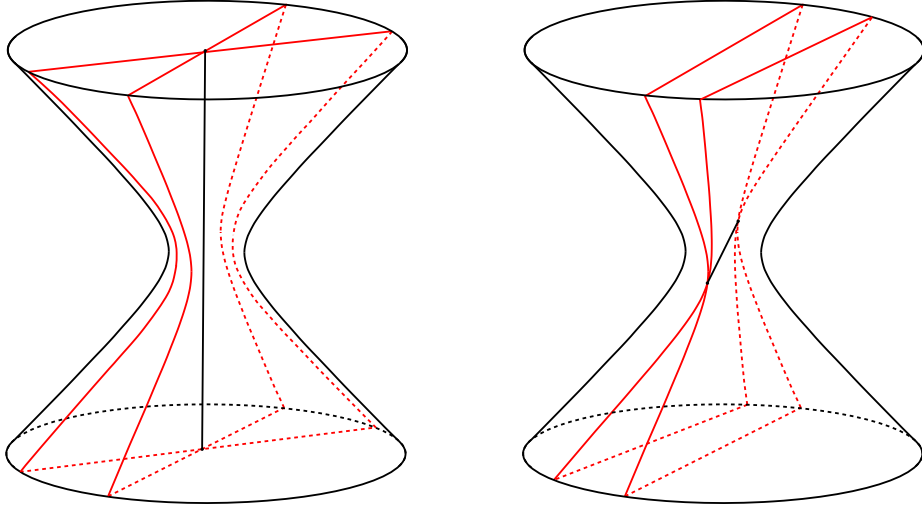

FIGURE 6. The two possibilities for the intersection of two timelike planes in $\mathbb{AdS}^3$: a timelike (left) or spacelike (right) line.

where $\widehat{\boldsymbol{H}}$ is a half-space of S^{n-1} defined by the condition $\alpha_0 x_0 + \ldots + \alpha_{n-1} x_{n-1} \leq 0$. Hence in the affine chart A^n, $\boldsymbol{H}$ is the product of a half-space in $\mathsf{A}^{n-1} \subset \mathsf{A}^n$ and $\mathbb{R}$. Since HP^n can be regarded in A^n as the product of $\mathbb{H}^{n-1} \times \mathbb{R}$, the condition that $\boldsymbol{H}$ intersects HP^n is equivalent to the condition that $\widehat{\boldsymbol{H}}$ intersects $\mathbb{H}^{n-1}$, which by Lemma 4.3 is $-\alpha_0^2 + \alpha_1^2 + \ldots + \alpha_{n-1}^2 > 0$, or equivalently,

$$q_0(\alpha_0, \ldots, \alpha_n) > 0 \ .$$

In this case, for each $\widehat{x} \in \widehat{\boldsymbol{H}}$, the "vertical" line $\{(\widehat{x}, t) \,|\, t \in \mathbb{R}\}$ is in $\partial \boldsymbol{H}$ and its tangent space coincides with the kernel of the degenerate form $\sigma^* b_0$ (see Section 2.5). Hence $\partial \boldsymbol{H} \cap \mathsf{HP}^n$ is degenerate, namely it is vertical in the affine chart A^n. See Figure 7, on the right.

The other case is thus $\alpha_n \neq 0$. In this case, the sign of α_n determines whether $\boldsymbol{H}$ is unbounded in the positive or negative x_n direction. In fact, up to multiplying by a positive
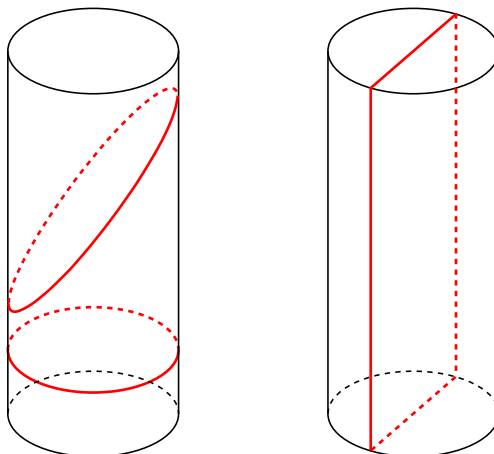
FIGURE 7. Hyperplanes in the affine (cylindric) model of HP^n: on the left, two space-like hyperplanes, on the right, a degenerate hyperplane.

number, we can assume

$$\boldsymbol{H} = (\alpha_0 : \ldots : \alpha_{n-1} : \pm 1) \ .$$

For instance, if $\alpha_n = 1$, we get that $\boldsymbol{H}$ is defined by the condition

$$\alpha_0 x_0 + \ldots \alpha_{n-1} x_{n-1} + x_n \leq 0 \ ,$$

and therefore $\partial \boldsymbol{H}$ is given by the condition

$$\alpha_0 x_0 + \ldots \alpha_{n-1} x_{n-1} + x_n = 0 \ . \tag{7}$$

This shows that $\partial \boldsymbol{H} \cap \mathsf{HP}^n$ is transverse to the degenerate direction, and it is therefore of spacelike type. $\qquad\square$

Remark 4.9. This discussion also gives a deeper insight into the duality between HP^n and Minkowski space. Recall that, as mentioned in Section 2.6, any point of HP^n corresponds to a spacelike hyperplane in Minkowski space $\mathbb{R}^{1,n-1}$. Dually, any spacelike hyperplane $\partial \boldsymbol{H}$ of HP^n corresponds to a point in $\mathbb{R}^{1,n-1}$, which turns out to be the intersection point of all the spacelike hyperplanes associated to points of $\partial \boldsymbol{H}$. Such a dual point is easily computed: if the hyperplane $\partial \boldsymbol{H}$ in HP^n is determined by the equation

$$\alpha_0 x_0 + \ldots + \alpha_{n-1} x_{n-1} + x_n = 0 \ ,$$

then its dual point is

$$p = (\alpha_0, -\alpha_1, \ldots, -\alpha_{n-1}) \ .$$

Moreover, this correspondence is again natural with respect to the action of the isometry groups G_{HP^n} and $\mathrm{Isom}(\mathbb{R}^{1,n-1})$.

As a consequence of the above remark, the condition that two spacelike hyperplanes $H, H' \subset \mathsf{HP}^n$ intersect is equivalent to the condition that the two dual points p and p' in $\mathbb{R}^{1,n-1}$ belong to the same spacelike hyperplane. Indeed, every point in the intersection $H \cap H'$ corresponds to a spacelike hyperplane in $\mathbb{R}^{1,n-1}$ which contains both p and p'. See also Figure 8. This shows the following:

Lemma 4.10. *Given $\widehat{\alpha}, \widehat{\alpha}'$ such that $\widehat{q}(\widehat{\alpha}), \widehat{q}(\widehat{\alpha}') < 0$, consider the half-spaces $\boldsymbol{H} = (\widehat{\alpha} : 1)$ and $\boldsymbol{H}' = (\widehat{\alpha}' : 1)$. The hyperplanes $\partial \boldsymbol{H}$ and $\partial \boldsymbol{H}'$ intersect transversely in HP^n if and only if $\widehat{\alpha} - \widehat{\alpha}'$ is a spacelike segment in Minkowski space.*
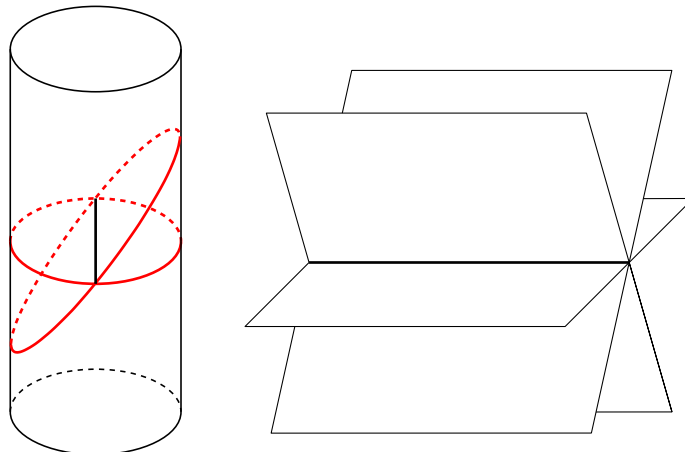
FIGURE 8. A sheaf of hyperplanes in HP^n (on the left) corresponds to the points of $\mathbb{R}^{1,n-1}$ lying on a spacelike line ℓ (on the right). Viceversa, the intersection of the sheaf is in bijection with the spacelike hyperplanes containing ℓ.

Recall that we denote by $\widehat{q}$ the quadratic form of signature $(-, +, \ldots, +)$ on $\mathbb{R}^n$, viewed as the subspace of $\mathbb{R}^{n+1}$ defined by the vanishing of the last coordinate.

In [Dan13] a notion of angle between spacelike hyperplanes in HP^n was introduced, which is the *infinitesimal version* of dihedral angles in $\mathbb{H}^n$ and $\mathbb{AdS}^n$ under the geometric transition we described above. In this setting, it is easy to give a definition of dihedral angle between two spacelike hyperplanes:

Definition 4.11. Given two HP spacelike half-spaces defined by $\boldsymbol{H} = (\widehat{\alpha} : 1)$ and $\boldsymbol{H}' = (\widehat{\alpha}' : 1)$ (i.e. such that $\widehat{q}(\widehat{\alpha}), \widehat{q}(\widehat{\alpha}') < 0$), the *angle* between $\partial\boldsymbol{H}$ and $\partial\boldsymbol{H}'$ is the number

$$\psi = \sqrt{\widehat{q}(\widehat{\alpha} - \widehat{\alpha}')} \in [0, +\infty) \ .$$

In other words, the angle is defined as the length of the segment connecting the two dual points, which is spacelike by Lemma 4.10. In Section 4.4 below we show that this notion actually coincides with the infinitesimal version of the angles between hyperplanes in $\mathbb{H}^n$ and $\mathbb{AdS}^n$.

4.4. **Rotations, boosts, and their infinitesimal analogues.** In this section we briefly introduce rotations and their analogues in AdS geometry (boosts) and in half-pipe geometry (infinitesimal rotations). This will be relevant for our Theorem 1.1, because the holonomy of the geometric structures on a peripheral loop around the singular locus Σ will consists of these elements.

Definition 4.12. A *rotation* (resp. *boost* or *infinitesimal rotation*) is a non-trivial orientation-preserving element of $\mathrm{Isom}(\mathbb{H}^n)$ (resp. $\mathrm{Isom}(\mathbb{AdS}^n)$ or G_{HP^n}) which fixes point-wise a co-dimension two subspace (which is required to be spacelike, for $\mathbb{AdS}^n$ and HP^n).

If r is such a rotation (resp. boost or infinitesimal rotation), the *angle* associated to r is defined as the angle between H and $r(H)$, where H is any (spacelike) hyperplane containing $\mathrm{Fix}(r)$.

Remark 4.13. To motivate the existence of infinitesimal rotations in HP^n, recall Lemma 4.10 and Figure 8. Two intersecting spacelike hyperplanes correspond precisely to two points $\widehat{\alpha}, \widehat{\alpha}' \in \mathbb{R}^{1,n-1}$ which are spacelike separated. Hence any translation in $\mathbb{R}^{1,n-1}$ in the

direction of $\widehat{\alpha} - \widehat{\alpha}'$ induces an infinitesimal rotation r of HP^n, which fixes the points of HP^n corresponding to spacelike hyperplanes P containing $\widehat{\alpha} - \widehat{\alpha}'$.

Observe that r also fixes pointwise an entire degenerate hyperplane in HP^n, corresponding to all the translates of the hyperplanes P as above. This is a qualitative difference with respect to hyperbolic and AdS geometries.

We now briefly show that the infinitesimal angle in half-pipe geometry is exactly the infinitesimal version of angle in $\mathbb{H}^n$ and $\mathbb{AdS}^n$. Let r_t be a smooth family of rotations of angle $\theta(t)$ with $\theta(0) = 0$. Up to isometries, we assume that

$$r_t = \begin{pmatrix} 1 & 0 & \dots & & 0 \\ 0 & \ddots & & & \vdots \\ \vdots & & \cos\theta(t) & \sin\theta(t) \\ 0 & \dots & -\sin\theta(t) & \cos\theta(t) \end{pmatrix}.$$

That is, r_t is a rotation which fixes the codimension two totally geodesic subspace defined by $x_{n-1} = x_n = 0$, and sends the hyperplanes $x_n = 0$ to another hyperplane forming an angle $\theta(t)$. By a direct computation, one sees that

$$\lim_{t\to 0} \mathfrak{r}_t r_t \mathfrak{r}_t^{-1} = \begin{pmatrix} 1 & 0 & \dots & 0 \\ 0 & \ddots & & \vdots \\ \vdots & & 1 & 0 \\ 0 & \dots & -\dot\theta & 1 \end{pmatrix},$$

which is a half-pipe infinitesimal rotation, corresponding under the usual isomorphism with $\mathrm{Isom}(\mathbb{R}^{1,n-1})$ to a translation of the vector $(0, \dots, 0, -\dot\theta)$. Hence in the limit the angle of the infinitesimal rotation is $|\dot\theta|$, by Definition 4.11. The computation can be done analogously for a boost in Anti-de Sitter space by replacing sin and cos by sinh and cosh, respectively.

This argument also explains the name "infinitesimal rotation", introduced in [Dan13].

4.5. **Reflections along hyperplanes.** More generally, the holonomy group of our geometric structures will be generated by compositions of reflections through the bounding hyperplanes of the polytopes that we will glue. In this section, we describe half-pipe limits of reflections in $\mathbb{H}^n$ or $\mathbb{AdS}^n$.

Definition 4.14. A *(projective) reflection* is a non-trivial involution $r \in \mathrm{Aut}(\mathsf{S}^n)$ that fixes point-wise a hyperplane.

Note that in $\mathrm{Isom}(\mathbb{H}^n)$ and $\mathrm{Isom}(\mathbb{AdS}^n)$ there is a unique reflection fixing a given hyperplane. This turns out not to be true in half-pipe geometry. Since this point will be very relevant in the following, let us explain this phenomenon more precisely.

Let H be a degenerate hyperplane in HP^n, as in the second point of Lemma 4.8. In the duality with Minkowski space, H corresponds to the set of all the spacelike hyperplanes P in $\mathbb{R}^{1,n-1}$ having normal vector in a totally geodesic hyperplane of $\mathbb{H}^{n-1}$, which is of the form $w^\perp \cap \mathbb{H}^{n-1}$, where w is some spacelike vector in $\mathbb{R}^{1,n-1}$ and $w^\perp$ is its orthogonal complement for the Minkowski product. Now, every reflection of $\mathbb{R}^{1,n-1}$ in a spacelike hyperplane orthogonal to w leaves (set-wise) invariant each such hyperplane P. See Figure 9.

In summary, the above argument shows the following proposition, which is a remarkable difference with respect to hyperbolic and AdS geometry.
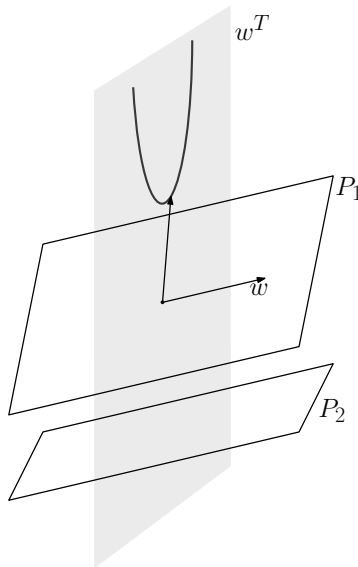
FIGURE 9. The argument of Proposition 4.15: Minkowski reflections in hyperplanes parallel to $w^\perp$ (in grey) leave set-wise invariant every spacelike hyperplane (like P_1 and P_2 in the figure) having normal vector in $w^\perp \cap \mathbb{H}^{n-1}$ (this intersection is pictured as a hyperbola here). They all induce half-pipe reflections fixing a degenerate hyperplane, as in Figure 7 on the right.

Proposition 4.15. *Given any degenerate hyperplane in* HP^n, *there is a one-parameter family of reflections in* G_{HP^n} *which fix the hyperplane pointwise.*

On the other hand, for spacelike hyperplanes uniqueness of the half-pipe reflection holds:

Proposition 4.16. *Given any spacelike hyperplane in* HP^n, *there is a unique reflection in* G_{HP^n} *which fix the hyperplane pointwise.*

To see this, recall that a spacelike hyperplane H in HP^n corresponds to all the spacelike hyperplanes P in $\mathbb{R}^{1,n-1}$ which contain a given point p, and we can assume that p is the origin. If an isometry $(\widehat{A}, v)$ of $\mathbb{R}^{1,n-1}$ fixes (set-wise) all the hyperplanes P going through the origin, it must also fix the origin itself, hence it must be linear (i.e. the translation part v is trivial). Since it fixes timelike normal directions, then $\widehat{A}$ is either id or $-$id. In conclusion, the unique half-pipe reflection fixing H is $(-\mathrm{id}, 0)$.

5. Polytopes and cone-manifolds

In this section, we provide some additional tools to prove Theorem 1.1. We first introduce projective polytopes and simple projective cone-manifolds. Then, we describe the singularities of such cone-manifolds in the hyperbolic, AdS, and HP cases by means of the (G, X)-structures given by the links of points.

5.1. **Polytopes.** We now introduce our main tool to provide examples of transition. Recall Section 4 about half-spaces of the projective sphere.

Definition 5.1. An n-dimensional *projective polytope* is a finite intersection of half-spaces

$$\mathcal{P} = \boldsymbol{H}_1 \cap \ldots \cap \boldsymbol{H}_N \subset \mathsf{S}^n$$

in the projective sphere such that the interior of $\mathcal{P}$ is non-empty.

We will always assume that the set of half-spaces defining $\mathcal{P}$ is minimal, that is, there is no $\boldsymbol{H}_i$ containing the intersection of the remaining half-spaces. In this case, each $\partial \boldsymbol{H}_i$ is called a *bounding hyperplane* of $\mathcal{P}$.

The polytope $\mathcal{P}$ is naturally stratified into k-*faces*, $k = 0, \ldots, n$, as follows. The unique n-face is $\mathcal{P}$ itself. The $(n-1)$-faces, called *facets*, are given by $\mathcal{F}_i = \mathcal{P} \cap \partial \boldsymbol{H}_i$, $i = 1, \ldots, N$. Now, each facet $\mathcal{F}_i$ is a projective $(n-1)$-polytope. The $(n-2)$-faces of $\mathcal{P}$, called *ridges*, are by definition the facets of each $\mathcal{F}_i$. One proceeds inductively in this way, until reaching the 1-faces, called *edges*, and the 0-faces, called *vertices*. The *combinatorics* of a polytope $\mathcal{P}$ is (the isomorphism class of) the poset of the faces of $\mathcal{P}$, ordered by set inclusion.

Given a point $p \in \mathcal{P}$, we have $p = [v]$ for some $v \in \mathbb{R}^{n+1} \smallsetminus \{0\}$. Each (possibly none) half-space $\boldsymbol{H}_i$ such that $p \in \partial \boldsymbol{H}_i$ determines a half-space of the projective sphere S^{n-1} over the quotient vector space $\mathbb{R}^{n+1}/\langle v \rangle$. The *link* of the point p is the $(n-1)$-dimensional projective polytope $\mathcal{L}_p \subset \mathsf{S}^{n-1}$ defined as the intersection of such half-spaces. (If p is in the interior of $\mathcal{P}$, then $\mathcal{L}_p$ is nothing but S^{n-1}.)

The polytope $\mathcal{P}$ is said to be *simple* if every k-face is contained in exactly $(n-k)$ bounding hyperplanes. Equivalently, the link of each vertex is a simplex.

Definition 5.2. A *hyperbolic* (resp. *half-pipe* or *Anti-de Sitter*) *polytope* is a non-empty subset

$$\hat{\mathcal{P}} = \mathcal{P} \cap \mathbb{H}^n \quad (\text{resp. } \hat{\mathcal{P}} = \mathcal{P} \cap \mathsf{HP}^n \text{ or } \hat{\mathcal{P}} = \mathcal{P} \cap \mathbb{A}\mathrm{d}\mathbb{S}^n),$$

where $\mathcal{P} \subset \mathsf{S}^n$ is a projective polytope.

5.2. **Simple projective cone-manifolds.** The process of geometric transition typically involves a path of *singular* geometric structures. In this section, we describe such structures in the special case of Theorem 1.1.

We call *stratified manifold* a topological n-manifold $\mathcal{X}$ together with a *stratification*, that is a partition

$$\mathcal{X} = \mathcal{X}^{[0]} \sqcup \ldots \sqcup \mathcal{X}^{[n]}$$

such that $\mathcal{X}^{[k]}$ is an embedded k-manifold with empty boundary. The connected components of $\mathcal{X}^{[k]}$ are called k-*strata*.

Let us fix n half-spaces $\boldsymbol{H}_1, \ldots, \boldsymbol{H}_n \subset \mathsf{S}^n$ such that the hyperplanes $\partial \boldsymbol{H}_1, \ldots, \partial \boldsymbol{H}_n$ are in general position. The intersection

$$\mathcal{P} = \boldsymbol{H}_1 \cap \ldots \cap \boldsymbol{H}_n \subset \mathsf{S}^n$$

is a simple projective polytope (see Section 5.1).

Let us now consider the *double* $D(\mathcal{P})$ of $\mathcal{P}$, that is, the space obtained from two copies of $\mathcal{P}$ by identifying the two copies of $\partial \mathcal{P}$ through the map induced by the identity. Note that $D(\mathcal{P})$ is homeomorphic to the n-sphere. By considering the natural stratification $\mathcal{P}^{[0]} \sqcup \ldots \sqcup \mathcal{P}^{[n]}$ of $\mathcal{P}$ induced by its faces, we define the following stratification of $D(\mathcal{P})$:

- $D(\mathcal{P})^{[k]} = \mathcal{P}^{[k]}$ for $k \leq n-2$,
- $D(\mathcal{P})^{[n-1]} = \emptyset$,
- $D(\mathcal{P})^{[n]} = D(\mathcal{P}^{[n-1]} \cup \mathcal{P}^{[n]})$.

Recalling now Section 2.2 about projective stuctures, we note that for $k \leq n-2$ each k-stratum is a projective manifold homeomorphic to $\mathbb{R}^k$, while the n-stratum $D(\mathcal{P})^{[n]}$ does not have a preferred projective structure. Choosing for each $i \in \{1, \ldots, n\}$ a projective reflection r_i (recall Definition 4.14) that fixes the hyperplane $\partial \boldsymbol{H}_i$, we have a well defined projective structure also on $D(\mathcal{P})^{[n]}$.

We call $\mathcal{D}$ the double $D(\mathcal{P})$ together with its stratification and such an additional projective structure on each of its strata. This will be the local model for our cone-manifolds.

Definition 5.3. A *simple projective cone-manifold* is a stratified manifold $\mathcal{X}$ with an atlas of stratum-preserving charts, each with values in some $\mathcal{D}$ constructed as above, whose transition functions restrict to an isomorphism of projective manifolds on each stratum.

Remark 5.4. One could give a much more general definition of "projective cone-manifold", by induction on the dimension. We do not need this here. However, our notion of simple projective cone-manifold includes the one introduced by Danciger in his works on geometric transition. In contrast with the projective cone-manifolds of Theorem 1.1, the ones considered in [Dan11, Dan13, LMR19] are stratified as $\mathcal{X} = \mathcal{X}^{[n]} \sqcup \mathcal{X}^{[n-2]}$. In other words, the singular locus $\Sigma \subset \mathcal{X}$ is a codimension-two submanifold.

We note that each stratum of such a cone-manifold $\mathcal{X}$ is a real projective manifold. The set
$$\Sigma = \mathcal{X}^{[0]} \cup \ldots \cup \mathcal{X}^{[n-2]}$$
is called the *singular locus* of $\mathcal{X}$, while $\mathcal{X}^{[n-1]} = \emptyset$ and $\mathcal{X}^{[n]} = \mathcal{X} \smallsetminus \Sigma$ (which is the unique n-stratum if $\mathcal{X}$ connected) is called the *regular locus* of $\mathcal{X}$. The singular locus Σ is an $(n-2)$-complex with generic singularities: Σ is empty if $n = 1$, a discrete set if $n = 2$, and is locally modelled on the cone over the $(n-3)$-skeleton of an $(n-1)$-simplex if $n \geq 3$. In particular, Σ is a trivalent graph if $n = 3$, and a so called *foam* if $n = 4$.

Given a point $p \in \mathcal{X} \smallsetminus \Sigma$, we define its *link* $\mathcal{L}_p$ to be the sphere of directions at p of the projective manifold $X \smallsetminus \Sigma$, that is, the projective sphere S^{n-1} over the tangent space at p. If instead $p \in \Sigma$, we define its *link* $\mathcal{L}_p$ to be the double of the link (see Section 5.1) of a corresponding point in $\partial \mathcal{P}$ through a chart. The link $\mathcal{L}_p$ is naturally a simple projective cone-manifold homeomorphic to the $(n-1)$-sphere.

For example, if $\mathcal{X}$ has dimension $n = 2$, then $\mathcal{L}_p$ is a projective circle, which is equivalent to S^1 if and only if p is non-singular. If $n = 3$, then $\mathcal{L}_p$ is a cone 2-sphere with 0, 2, or 3 singular points, depending on whether p belongs to a 3-, 1-, or 0-stratum, respectively. If $n = 4$, the singular locus of the cone 3-sphere $\mathcal{L}_p$ is empty, an unknotted cicle, an unknotted theta graph, or the 1-skeleton of a tetrahedron, depending whether p belongs to a 4-, 2-, 1-, or 0-stratum, respectively.

The *holonomy representation* and *developing map* of a projective cone-manifold $\mathcal{X}$ are by definition those of its regular locus. The holonomy $\rho(\gamma)$ of a meridian $\gamma \in \pi_1(\mathcal{X} \smallsetminus \Sigma)$ of an $(n-2)$-stratum is conjugated to a product of reflections $r_i r_j \in \mathrm{Aut}(\mathsf{S}^n)$ that fix a common $(n-2)$-subspace of S^n.

5.3. The hyperbolic, AdS, and HP case. We are interested in some special classes of simple projective cone-manifolds:

Definition 5.5. A simple projective cone-manifold $\mathcal{X}$ is said to be *hyperbolic* (resp. *half-pipe* or *Anti-de Sitter*) if

- each chart has values in some $D(\hat{\mathcal{P}}) \subset D(\mathcal{P}) = \mathcal{D}$, where $\hat{\mathcal{P}} = \mathcal{P} \cap \mathbb{H}^n$ (resp. $\hat{\mathcal{P}} = \mathcal{P} \cap \mathsf{HP}^n$ or $\hat{\mathcal{P}} = \mathcal{P} \cap \mathbb{A}\mathrm{d}\mathbb{S}^n$);
- for each $\mathcal{D}$, the reflections $r_1, \ldots, r_n$ belong to $\mathrm{Isom}(\mathbb{H}^n)$ (resp. G_{HP^n} or $\mathrm{Isom}(\mathbb{A}\mathrm{d}\mathbb{S}^n)$);
- the transition functions restrict to isometries (resp. G_{HP}-isomorphisms, isometries) on the strata.

A simple AdS or HP cone-manifold has *spacelike singularities* if every bounding hyperplane of each $\hat{\mathcal{P}}$ is spacelike.

We refer to [BLP05] (see also [Thu98, CHK00, McM17]) for the general definition of hyperbolic cone-manifold, and to [BBS11] for the 3-dimensional AdS case.

Recall now Section 4.4 about rotations, boosts and their infinitesimal counterpart. Given an n-dimensional simple projective cone-manifold $\mathcal{X}$, the holonomy of a meridian of an $(n-2)$-stratum is conjugated to:

- a rotation in $\mathrm{Isom}(\mathbb{H}^n)$ if $\mathcal{X}$ is hyperbolic,
- a boost in $\mathrm{Isom}(\mathbb{A}\mathrm{d}\mathbb{S}^n)$ if $\mathcal{X}$ is Anti-de Sitter and Σ is spacelike,
- their infinitesimal version in G_{HP^n} if $\mathcal{X}$ is half-pipe and Σ is spacelike.

In such cases, to each $(n-2)$-stratum is thus associated a number: the angle of rotation is called *cone angle*, the angle of the boost (with opposite sign) is called *magnitude*, and that of the infinitesimal rotation (again with opposite sign) is called *infinitesimal cone angle*, respectively. The sign convention is consistent with [Dan11, Dan13], where roughly speaking the negative sign corresponds to the fact that the singularity is a "defect" with respect to the non-singular case. We refer to [Dan13, Sections 2.5 and 4.2] for more details.

The transitional 3-dimensional AdS cone-manifolds in [Dan11, Dan13] have spacelike singularities — said "with tachyons" [BBS11], being each 1-stratum a spacelike geodesic, i.e. a "particle faster than light". In this case, the holonomy representation at a meridian is a AdS boost which fixes pointwise a spacelike geodesic.

The local structure of a point $p \in \mathcal{X}$ is determined by its link $\mathcal{L}_p$. We now briefly describe the situation in the three cases of interest for us.

In hyperbolic geometry. Given a point $x \in \mathbb{H}^n$, we have $\mathrm{Stab}_{\mathbb{H}^n}(x) \cong \mathrm{O}(n)$, and the link of x can be identified to the round sphere. Simple hyperbolic cone-manifolds can be defined as manifolds locally modelled on the hyperbolic cone [BH11] over a spherical cone-manifold one dimension less, which is the double of a spherical simplex.

In Anti-de Sitter geometry. The analogous geometry for $\mathbb{A}\mathrm{d}\mathbb{S}^n$ has been introduced in [BBS11], where it is called *HS geometry*. By identifying $T_x \mathbb{A}\mathrm{d}\mathbb{S}^n$ with $\mathbb{R}^{1,n-1}$, the link of a point $x \in \mathbb{A}\mathrm{d}\mathbb{S}^n$ is called HS^{n-1}, and is a projective $(n-1)$-sphere identified with the space of rays in $\mathbb{R}^{1,n-1}$. The stabiliser $\mathrm{Stab}_{\mathbb{A}\mathrm{d}\mathbb{S}^n}(x)$ is identified to $\mathrm{O}(1, n-1)$. The sphere HS^{n-1} is partitioned into (see Figure 10–right):

- the region of timelike rays, which corresponds to two copies of $\mathbb{H}^{n-1}$;
- the region of spacelike rays, which is a copy of de Sitter space $\mathrm{d}\mathbb{S}^{n-1}$;
- the set of lightlike rays, which is the common boundary of the two latter regions and is topologically the disjoint union of two $(n-2)$-spheres.

An *HS-structure* is by definition an $(\mathrm{O}(1, n-1), \mathsf{HS}^{n-1})$-structure. An HS manifold is thus partitioned into a hyperbolic region, a de Sitter region, and a null locus. In analogy with the hyperbolic case, simple AdS cone-manifolds are locally modelled on the AdS suspension [BBS11] over the double of an HS simplex of one dimension less. In the AdS case with spacelike singularities, the facets of the HS simplex are contained in the de Sitter region of HS^{n-1} and are spacelike.

In half-pipe geometry. The stabiliser in G_{HP^n} of a point $x \in \mathsf{HP}^n$ is isomorphic to $\mathrm{Isom}(\mathbb{R}^{n-1}) \times \mathbb{Z}/2\mathbb{Z}$. To see this, recall that by the usual duality (Section 2.6), the stabiliser of a point in HP^n is the same as the stabiliser of a spacelike hyperplane P in $\mathrm{Isom}(\mathbb{R}^{1,n-1})$. The $\mathbb{Z}/2\mathbb{Z}$ factor is generated by a reflection in P, while $\mathrm{Isom}(\mathbb{R}^{n-1})$ corresponds to Euclidean isometries of H which extend to $\mathbb{R}^{1,n-1}$ by preserving setwise each component of $\mathbb{R}^{1,n-1} \setminus P$. The link of a point in HP^n is thus endowed with a (G, X)-structure, where X is an $(n-1)$-sphere identified to the set of rays in $T_x \mathsf{HP}^n$, and $G = \mathrm{Stab}_{\mathsf{HP}^n}(x)$ is the stabiliser of x as described above. Note that such a (G, X)-structure has some distinguished points, which correspond
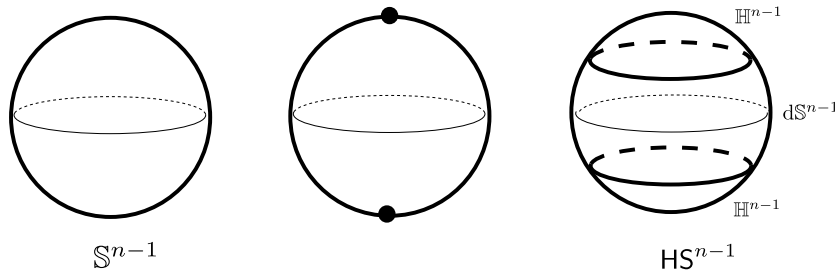
FIGURE 10. The link of a point in a hyperbolic, half-pipe, or Anti-de Sitter n-manifold. In the hyperbolic case (left), we have the round sphere $\mathbb{S}^{n-1}$. In the AdS case (right), the link is called HS^{n-1}, and is subdivided into two timelike regions (copies of $\mathbb{H}^{n-1}$), one spacelike region (copy of the de Sitter space $\mathrm{d}\mathbb{S}^{n-1}$), and two lightlike $(n-2)$-spheres. In the HP case (centre), we have just a sphere with two marked antipodal points, corresponding to the degenerate direction. In the transition from AdS to hyperbolic geometry the two timelike regions shrink to points and then disappear.

to the degenerate rays exiting from x. These are well-defined since they are preserved by the action of G (see Figure 10–centre).

Analogously to the hyperbolic and AdS case, one can visualise the link of a point in a simple half-pipe cone-manifold as the double of a simplex in the space of rays in $T_x \mathsf{HP}^n$. If the singularity Σ is spacelike, then the facets of such simplex are spacelike.

Remark 5.6. We omit the details here, but (similarly to Remark 3.5) it can be seen directly that the rescaled limits of the point stabilisers $\mathrm{Stab}_{\mathbb{H}^n}(x)$ and $\mathrm{Stab}_{\mathbb{A}\mathrm{d}\mathbb{S}^n}(x)$ are point stabilisers in half-pipe geometry. Hence a geometric transition from hyperbolic to AdS geometry on simple projective cone-manifolds induces a geometric transition from spherical to HS cone structures, going through the analogous structure for half-pipe geometry. This can be visualised in Figure 10 for non-singular points, and in Figures 25, 26, 27 for singular points in dimension four (as in Theorem 1.1).

6. WARM UP IN DIMENSION THREE

We are ready to build explicitly some examples of geometric transition. Section 6 is a warm up in dimension three, while in Section 7 we prove Theorem 1.1.

In this section, we describe two examples of 3-dimensional geometric transition from hyperbolic to an Anti-de Sitter structures, going through a half-pipe structure. These will serve as a toy model for the 4-dimensional geometric transition constructed in Section 7. In contrast with the deformations studied in [Dan13] and [Dan14], where the 3-manifold is closed and the singular locus is a knot, our examples are cusped and the singular locus is either a link or a trivalent graph. We will not provide all the proofs in this section, since they will actually follow from the results we prove in dimension four; the reader can also see the survey paper [Sep20] for more details on some examples in dimension two and three.

6.1. **Singularity along a link.** Consider an ideal right-angled octahedron $\mathcal{O}_0 \subset \mathbb{H}^3$, with the natural colouring of its facets in black and white in the chequerboard fashion. By doubling $\mathcal{O}_0$ along its white faces, and then doubling the resulting manifold with boundary, we get [KM13, Figure 2] a well-known complete, finite-volume, hyperbolic 3-manifold $\mathcal{M}$ homeomorphic to the complement in S^3 of the minimally twisted 6-chain link (see Figure 11). Note that $\mathcal{M}$ is tessellated by four copies of the octahedron $\mathcal{O}_0$.
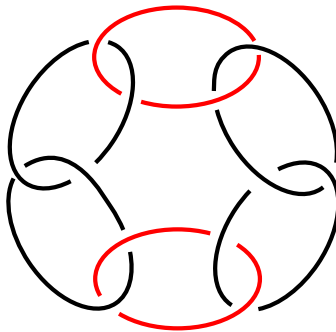
FIGURE 11. The minimally twisted 6-chain link in the 3-sphere. Its complement $\mathcal{M}$ is hyperbolic, and can be tessellated by four ideal right-angled octahedra. By 0-surgery on the two red components, we get a Dehn filling $\mathcal{X}$ of $\mathcal{M}$ homeomorphic to $\mathcal{S}_{0,4} \times S^1$, where $\mathcal{S}_{0,4}$ is a 4-times punctured sphere.
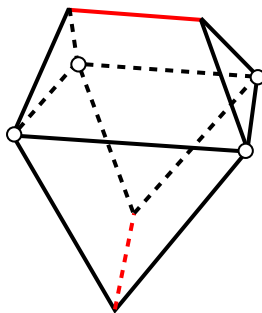

FIGURE 12. The polyhedron $\mathcal{O}_\theta \subset \mathbb{H}^3$. The white dots represent ideal vertices, the black edges are right-angled, and the red edges have dihedral angle $\theta \in (0, \pi)$. As $\theta \to 0$, the red edges disappear, and we have the original ideal octahedron $\mathcal{O}_0$. As $\theta \to \pi$, the polyhedron collapses to the horizontal ideal quadrilateral $\mathcal{Q}$. By rescaling and continuing the path, we have similarly an AdS polyhedron with the same combinatorics and the same convention on the dihedral angles, where now the quadrliateral faces are spacelike, and the triangular ones are timelike. The polyhedron $\mathcal{O}_\theta$ (and its AdS version) is isometric to a facet $\mathcal{F}_{\boldsymbol{X}}$, $\boldsymbol{X} \in \{\boldsymbol{A}, \ldots, \boldsymbol{F}\}$, of the 4-polytope $\mathcal{P}_t$ of Section 7. The quadrilateral faces are the ridges $\mathcal{R}_{\boldsymbol{X} i+}$ of $\mathcal{P}_t$, while the triangular faces are the ridges of type $\mathcal{R}_{\boldsymbol{X} i-}$ (see the end of Section 7.2 for the notation).

Let us now deform $\mathcal{O}_0$ by a path $\theta \mapsto \mathcal{O}_\theta \subset \mathbb{H}^3$ of polyhedra described in Figure 12, where the two red edges have varying dihedral angle θ and all the remaining edges are right-angled, while the white dots represent ideal vertices. Geometric models of this deformation are shown in Figure 13. The polyhedron $\mathcal{O}_\theta$ exists for all $\theta \in (0, \pi)$ by Andreev's Theorem [And70a, And70b]. As $\theta \to 0$, the red edges shrink and go to infinity, and we have the original octahedron $\mathcal{O}_0$.

More concretely, $\mathcal{O}_\theta$ can be defined as the intersection in S^3 of the half-spaces in Table 1, for $t \in (0, 1)$, using the notation introduced in Section 4.1. It can be checked directly that the correct orthogonality relations hold, and that the relation between the angle θ and the parameter $t \in (0, 1)$ (by applying Lemma 4.4 to the first and third vector in the left column, for instance) is given by:

$$\cos \theta_t = \frac{3t^2 - 1}{1 + t^2} \ .$$

By deforming simultaneously in this way each copy of $\mathcal{O}_0$ in $\mathcal{M}$, we get a *Dehn filling* $\mathcal{X}$ of the hyperbolic 3-manifold $\mathcal{M}$, i.e. $\mathcal{X} \smallsetminus \Sigma$ is homeomorphic to $\mathcal{M}$ for a link $\Sigma \subset \mathcal{X}$
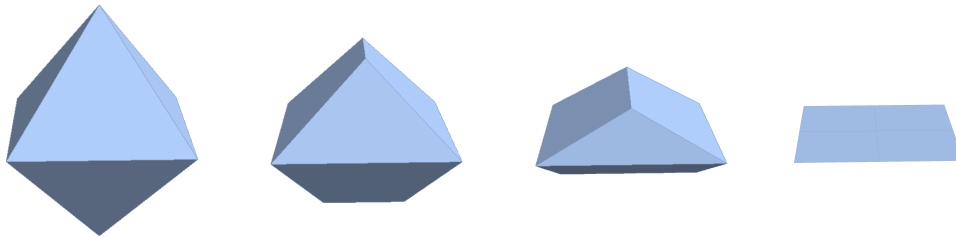
FIGURE 13. A movie of the collapse of the polyhedron $\mathcal{O}_\theta$ in an affine chart (Klein model of $\mathbb{H}^3$), from the ideal octahedron $\mathcal{O}_0$ to the ideal quadrilateral $\mathcal{Q}$.

$$\left(-|t| : -\sqrt{2}|t| : 0 : -1\right), \qquad \left(-1 : -\sqrt{2} : 0 : +t\right),$$
$$\left(-|t| : 0 : -\sqrt{2}|t| : +1\right), \qquad \left(-1 : 0 : -\sqrt{2} : -t\right),$$
$$\left(-|t| : +\sqrt{2}|t| : 0 : -1\right), \qquad \left(-1 : +\sqrt{2} : 0 : +t\right),$$
$$\left(-|t| : 0 : +\sqrt{2}|t| : +1\right), \qquad \left(-1 : 0 : +\sqrt{2} : -t\right).$$

TABLE 1. The half-spaces defining the deformation of the right-angled ideal octahedron, expressed as elements of $\mathsf{S}^{3,*}$. When $t < 0$, we have an AdS polyhedron.

(see Figure 11). Each component of Σ is the double of a red edge of $\mathcal{O}_\theta$. Moreover, the deformation describes a path of hyperbolic cone-structures on $\mathcal{X}$ with cone angles 2θ along Σ, converging to the hyperbolic manifold $\mathcal{M}$ as $\theta \to 0$.

The path of polyhedra is arranged in such a way that the four ideal vertices of $\mathcal{O}_\theta$ stay fixed, and belong to $\partial\mathbb{H}^2 \subset \partial\mathbb{H}^3$ for the fixed hyperplane $\mathbb{H}^2 = \{x_3 = 0\} \subset \mathbb{H}^3$ — this arrangement is indeed used in Table 1 and in Figure 13. In particular, we have a fixed ideal quadrilateral $\mathcal{Q} = \mathcal{O}_\theta \cap \mathbb{H}^2$. As $\theta \to \pi$, the polyhedron $\mathcal{O}_\theta$ collapses to the polygon $\mathcal{Q}$. The corresponding cone-manifolds collapse to the hyperbolic four-punctured sphere $\mathcal{S}_{0,4}$ obtained by doubling $\mathcal{Q}$. Note that there is a homeomorphism $\mathcal{O}_\theta \to \mathcal{Q} \times [-1, 1]$ wich sends the quadrilateral faces to $\mathcal{Q} \times \{1, -1\}$ and the triangular faces to $\partial\mathcal{Q} \times [-1, 1]$. It follows that $\mathcal{X}$ is homeomorphic to $\mathcal{S}_{0,4} \times S^1$. (In particular, $\mathcal{X}$ does not admit any complete hyperbolic structure.)

The reader can check that when $t \in (-1, 0)$, the polyhedron defined in Table 1 is Anti-de Sitter, its quadrliateral faces are spacelike, and the triangular ones are timelike. All the edges are right-angled, with the exception of the red ones (which are spacelike). By rescaling the polyhedron in the direction of collapse, i.e. orthogonally to the plane $\mathbb{H}^2 \subset \mathbb{H}^3$, we get transition from hyperbolic to AdS polyhedra with constant combinatorics. In the limit half-pipe polyhedron, the triangular faces are degenerate. The path of rescaled polyhedra is easily computed by applying Lemma 4.1 and pictured (in an affine chart) in Figure 14.

The essential point to prove the transition at the level of geometric structures on $\mathcal{M}$ is to show that for every plane in the list of Table 1 (which depends on the parameter t), if r_t is the hyperbolic (for $t > 0$) or AdS (for $t < 0$) reflection in the given plane, then $\mathfrak{r}_t r_t \mathfrak{r}_t^{-1}$ converges to a half-pipe reflection when $t \to 0$ (with the same limit for $t \to 0^+$ and $t \to 0^-$). This essentially shows the convergence at the level of holonomy representations, since the holonomy of any element of $\pi_1(\mathcal{M})$ is obtained by composition of a finite number of such
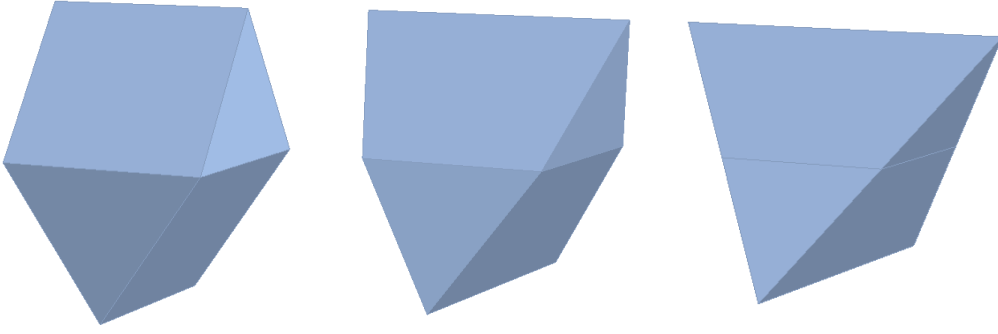
FIGURE 14. In an affine chart, the rescaled path of polyhedra for $t \leq 0$. In the left figure (t=0), the polyhedron is in half-pipe space and the triangular faces are degenerate (vertical). In the middle picture, an AdS polyhedron with timelike triangular faces and spacelike quadrilateral faces. When $t = -1$ (in the right), the faces become lightlike and the polyhedron is inscribed in the one-sheeted hyperboloid which is the boundary at infinity of $\mathbb{AdS}^3$.

reflections. This point is certainly non-trivial in general since, as we explained in Section 4.13, a (degenerate) plane in HP^3 does not determine uniquely a half-pipe reflection.

Although all the previous statements can be verified directly, we avoid detailed computations, since everything follows from the fact that, as $\theta \geq \frac{\pi}{2}$, the polyhedron $\mathcal{O}_\theta$ is a facet of the 4-polytope introduced in Section 7 (see also Remark 7.2 for the case $\theta < \frac{\pi}{2}$), and meets the adjacent facets of the 4-polytope orthogonally (see Propositions 7.3, 7.10, 7.11 and 7.12 in the sequel).

In particular, we get (all the details follow from the proof of Theorem 1.1 in Section 7):

Proposition 6.1. *There exists a C^1 family $\{\sigma_t\}_{t \in (-1,1]}$ of simple projective cone-manifold structures on the 3-manifold $\mathcal{X} = \mathcal{S}_{0,4} \times S^1$, singular along a link Σ with two components, such that σ_t is conjugated to a geodesically complete, finite-volume*

- *hyperbolic cone structure with decreasing cone angles $2\theta_t \in (0, 2\pi)$ as $t > 0$,*
- *half-pipe structure with spacelike singularity as $t = 0$,*
- *Anti-de Sitter structure with spacelike singularity of increasing magnitude $\varphi_t \in (-\infty, 0)$ as $t < 0$.*

As $t \to 1$, we have $2\theta_t \to 0$ and the hyperbolic structures on $\mathcal{M} = \mathcal{X} \setminus \Sigma$ converge to the complete one. As $t \to 0^+$ (resp. $t \to 0^-$), we have $2\theta_t \to 2\pi$ (resp. $\varphi_t \to 0$) and the hyperbolic (resp. AdS) structures degenerate to the hyperbolic structure of $\mathcal{S}_{0,4} = \mathrm{Double}(\mathcal{Q})$.

6.2. **Singularity along a graph.** Let now $\mathcal{S}_{0,3}$ be the hyperbolic thrice punctured sphere. Similarly to the previous section, we now provide an example of 3-dimensional transition where the singular locus is a theta-graph:

Proposition 6.2. *There exists a C^1 family $\{\sigma_s\}_{s \in (-1,\epsilon]}$ of simple projective cone-manifold structures on the 3-manifold $\mathcal{X} = \mathcal{S}_{0,3} \times S^1$, singular along a theta-graph Σ, such that σ_s is conjugated to a geodesically complete, finite-volume*

- *hyperbolic orbifold structure with cone angles π as $s = \epsilon > 0$,*
- *hyperbolic cone structure with decreasing cone angles $\vartheta_s \in [\pi, 2\pi)$ as $s > 0$,*
- *half-pipe structure with spacelike singularity as $s = 0$,*
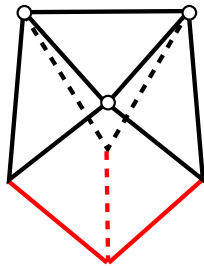- *Anti-de Sitter structure with spacelike singularity of increasing magnitude $\phi_s < 0$ as $s < 0$.*

FIGURE 15. A facet $\mathcal{F}_{i^-}$, $i^- \in \{0^-, \ldots, 7^-\}$, of the 4-polytope of Section 7 (see the end of Section 7.2 for the notation). The white dots represent ideal vertices, the black edges are right-angled, and the red edges have dihedral angle $\theta \in [\frac{\pi}{2}, \pi)$. As $\theta \to \pi$, the polyhedron collapses to the horizontal ideal triangle. By rescaling and continuing the path, we have similarly an AdS polyhedron with the same combinatorics and the same convention on the dihedral angles, where now the three vertical triangular faces (ridges of the 4-polytope of type $\mathcal{R}_{i^- X}$) are timelike, while the horizontal ideal triangle (the ridge $\mathcal{R}_{i^- i^+}$ of the 4-polytope) and the remaining three quadrilateral faces (ridges of type $\mathcal{R}_{i^- j^+}$) are spacelike.
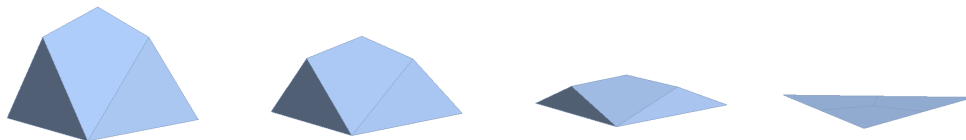

FIGURE 16. The collapse of the polyhedron $\mathcal{F}_\vartheta$ of Section 6.2, in the Klein model of $\mathbb{H}^3$. The leftmost polyhedron turns out to be also the rescaled limit, inside HP^3.

As $s \to 0^+$ (resp. $s \to 0^-$), we have $\vartheta_s \to 2\pi$ (resp. $\phi_s \to 0$) and the hyperbolic (resp. AdS) structures on $\mathcal{X} \smallsetminus \Sigma$ degenerate to the complete hyperbolic structure of $\mathcal{S}_{0,3}$.

Consider indeed the polyhedron $\mathcal{F}_\vartheta$ in Figure 15, where the red edges have varying dihedral angle $\frac{\vartheta}{2} \in [\frac{\pi}{2}, \pi)$ and the black edges are right-angled. Again, the path $\vartheta \mapsto \mathcal{F}_\vartheta$ can be arranged so that the three ideal vertices stay fixed. As $\vartheta \to 2\pi$, the polyhedron collapses to the horizontal ideal triangle $\mathcal{T}$, which is a face of $\mathcal{F}_\vartheta$ for all $\vartheta_s \in [\pi, 2\pi)$. Figure 16 gives a geometric picture.

Similarly to the previous section, for $s < 0$ we have a path of AdS polyhedra collapsing to $\mathcal{T}$, and by rescaling opportunely the two paths are joined by a half-pipe polyhedron with the same combinatorics. Again, the black edges are constantly right-angled. In the AdS side, the three vertical triangular faces are timelike, while the remaining three quadrilateral faces (and the ideal triangle $\mathcal{T}$) are spacelike. In the half-pipe limit, the triangular faces are degenerate.

By doubling $\mathcal{F}_\vartheta$ along the three vertical triangular faces, and then doubling the resulting manifold with boundary, we get the desired transition on a 3-manifold homeomorphic to $\mathcal{S}_{0,3} \times S^1$ (where $\mathcal{S}_{0,3}$ is the double of $\mathcal{T}$), with singularity along a theta-graph (which is the double of the red locus in $\mathcal{F}_\vartheta$).

Again, all these statements can be proved directly, but will follow from the fact that $\mathcal{F}_\vartheta$ is isometric to a facet of the 4-dimensional polytope of Section 7.

$$\mathbf{0}^+ = \left(-\sqrt{2}\,|t| : +|t| : +|t| : +|t| : +1\right), \qquad \mathbf{0}^- = \left(-\sqrt{2} : +1 : +1 : +1 : -t\right),$$

$$\mathbf{1}^+ = \left(-\sqrt{2}\,|t| : +|t| : -|t| : +|t| : -1\right), \qquad \mathbf{1}^- = \left(-\sqrt{2} : +1 : -1 : +1 : +t\right),$$

$$\mathbf{2}^+ = \left(-\sqrt{2}\,|t| : +|t| : -|t| : -|t| : +1\right), \qquad \mathbf{2}^- = \left(-\sqrt{2} : +1 : -1 : -1 : -t\right),$$

$$\mathbf{3}^+ = \left(-\sqrt{2}\,|t| : +|t| : +|t| : -|t| : -1\right), \qquad \mathbf{3}^- = \left(-\sqrt{2} : +1 : +1 : -1 : +t\right),$$

$$\mathbf{4}^+ = \left(-\sqrt{2}\,|t| : -|t| : +|t| : -|t| : +1\right), \qquad \mathbf{4}^- = \left(-\sqrt{2} : -1 : +1 : -1 : -t\right),$$

$$\mathbf{5}^+ = \left(-\sqrt{2}\,|t| : -|t| : +|t| : +|t| : -1\right), \qquad \mathbf{5}^- = \left(-\sqrt{2} : -1 : +1 : +1 : +t\right),$$

$$\mathbf{6}^+ = \left(-\sqrt{2}\,|t| : -|t| : -|t| : +|t| : +1\right), \qquad \mathbf{6}^- = \left(-\sqrt{2} : -1 : -1 : +1 : -t\right),$$

$$\mathbf{7}^+ = \left(-\sqrt{2}\,|t| : -|t| : -|t| : -|t| : -1\right), \qquad \mathbf{7}^- = \left(-\sqrt{2} : -1 : -1 : -1 : +t\right),$$

$$\mathbf{A} = \left(-1 : +\sqrt{2} : 0 : 0 : 0\right), \qquad \mathbf{B} = \left(-1 : 0 : +\sqrt{2} : 0 : 0\right),$$

$$\mathbf{C} = \left(-1 : 0 : 0 : +\sqrt{2} : 0\right), \qquad \mathbf{D} = \left(-1 : 0 : 0 : -\sqrt{2} : 0\right),$$

$$\mathbf{E} = \left(-1 : 0 : -\sqrt{2} : 0 : 0\right), \qquad \mathbf{F} = \left(-1 : -\sqrt{2} : 0 : 0 : 0\right).$$

TABLE 2. The half-spaces in S^4 that define the projective polytope $\overline{\mathcal{P}}_t$ are given by these elements of $\mathsf{S}^{4,*}$ and denoted by the same symbols. We will often omit the dependence in t in the symbols $\boldsymbol{i}^+$, $\boldsymbol{i}^-$ and $\boldsymbol{X}$, to simplify the notation.

7. TRANSITION IN DIMENSION FOUR

In this section we prove Theorem 1.1, giving as a byproduct also rigours to the assertions of the previous section about 3-dimensional transition.

7.1. **A deforming polytope.** Recall Section 4 about half-spaces of the projective sphere S^n, and Section 5.1 about projective polytopes. We define

$$\overline{\mathcal{P}}_t \subset \mathsf{S}^4$$

to be the intersection of the 22 half-spaces listed in Table 2, depending on the time parameter

$$t \in I = \left(-1, \tfrac{1}{\sqrt{3}}\right].$$

We set

$$I^- = \left(-1, 0\right), \quad I^+ = \left(0, \tfrac{1}{\sqrt{3}}\right],$$

and

$$\mathcal{P}_t = \begin{cases} \overline{\mathcal{P}}_t \cap \mathbb{H}^4 & \text{when } t \in I^+ \cup \{0\}, \\ \overline{\mathcal{P}}_t \cap \mathbb{A}\mathrm{d}\mathbb{S}^4 & \text{when } t \in I^- \cup \{0\}. \end{cases}$$

We will see that this last definition is well posed as $t = 0$. It will be clear later that $\overline{\mathcal{P}}_t$ is the closure in S^4 of $\mathcal{P}_t$.

When $t \in I^+$, each element $(\alpha) \in \mathsf{S}^{4,*}$ in the list of Table 2 satisfies $q_1(\alpha) > 0$, and thus by Lemma 4.3 defines a half-space of $\mathbb{H}^4$. When $t \in I^+$, the set $\mathcal{P}_t \subset \mathbb{H}^4$ is indeed a hyperbolic 4-polytope, first introduced in [KS10] and then studied in [MR18]. The set of half-spaces of Table 2 is minimal for $t \neq 0$; in other words, none of them contains any other — this is shown in [MR18, Proposition 3.3] for $t \in I^+$ and holds for $t \in I^-$ by a straightforward adaptation of the proof.

Throughout the remainder of the paper, we will denote

$$\iota(\mathbb{H}^3) = \{x_4 = 0\} \subset \mathbb{H}^4, \mathsf{HP}^4, \mathbb{AdS}^4,$$

simply as $\mathbb{H}^3$, where the isometric embedding ι is defined by (3) in Section 2.8. As $t \to 0^+$, the polytope $\mathcal{P}_t$ collapses to a 3-dimensional polytope in the hyperplane $\mathbb{H}^3 \subset \mathbb{H}^4$.

Proposition 7.1 ([KS10, MR18]). *When $t \in I^+$, the set $\mathcal{P}_t$ is a finite-volume hyperbolic 4-polytope, whose combinatorics does not depend on $t \in I^+$. The set $\mathcal{P}_0$ is a finite-volume 3-polytope in $\mathbb{H}^3 \subset \mathbb{H}^4$.*

In the next sections, we will show that when $t \in I^-$ the behaviour of $\mathcal{P}_t$ is analogue, in the AdS setting, to that when $t \in I^+$ given by Proposition 7.1.

Remark 7.2. The path $t \mapsto \mathcal{P}_t \subset \mathbb{H}^4$ of hyperbolic polytopes extends beyond $t = \frac{1}{\sqrt{3}}$ to all $t \in (0, 1]$. When $t > \frac{1}{\sqrt{3}}$ the combinatorics changes a few times, and moreover when $t > \frac{1}{\sqrt{2}}$ the volume becomes infinite. This whole path of hyperbolic polytopes was discovered by Kerckhoff and Storm [KS10].

The smaller polytope $\mathcal{P}_1 \cap \boldsymbol{G} \cap \boldsymbol{H}$ is the ideal right-angled 24-cell, where the half-spaces $\boldsymbol{G} = (-1 : 0 : 0 : 0 : -\sqrt{2})$ and $\boldsymbol{H} = (-1 : 0 : 0 : 0 : \sqrt{2})$ correspond to two opposite facets. The partition

$$\{\boldsymbol{0}^+, \dots, \boldsymbol{7}^+\} \sqcup \{\boldsymbol{0}^-, \dots, \boldsymbol{7}^-\} \sqcup \{\boldsymbol{A}, \dots, \boldsymbol{H}\}$$

gives the standard 3-colouring of the facets of the 24-cell: if two hyperplanes belong to the same octet, then they are disjoint in $\mathbb{H}^4$.

Moreover, it is easily checked that all the orthogonality relations that occur when $t = 1$ between any two vectors in Table 2 are maintained for all $t \in (-1, 1]$, with respect to the bilinear form of signature $- + + + +$ when $t \in [0, 1)$, and $- + + + -$ when $t \in (-1, 0]$.

7.2. **Combinatorics of the polytope.** The main goals here are to prove that when $t \in I^-$ the set $\mathcal{P}_t \subset \mathbb{AdS}^4$ is a deforming AdS 4-polytope, that the combinatorics of $\mathcal{P}_t$ is independent on $t \in I \smallsetminus \{0\}$, and that the rescaled limit (see Section 2.7)

$$\lim_{t \to 0} \mathfrak{r}_{|t|}(\mathcal{P}_t) \subset \mathsf{HP}^4$$

is a half-pipe polytope with the same combinatorics of $\mathcal{P}_t$ with $t \neq 0$. In particular, we will show that $\{\mathfrak{r}_{|t|}(\mathcal{P}_t)\}_{t \in I}$ is a path of projective 4-polytopes (extended to $t = 0$ by continuity) whose combinatorics is constant. For easiness of the reader, we record the list of rescaled half-spaces defining $\mathfrak{r}_{|t|}(\mathcal{P}_t)$ in Table 3, calculated using Lemma 4.1.

All these facts will follow from the following proposition (recall that we denote by A^4 the affine chart $\{x_0 > 0\} \subset \mathsf{S}^4$):

Proposition 7.3. *The set $\mathfrak{r}_{|t|}(\overline{\mathcal{P}}_t)$ is contained in $\overline{\mathbb{X}^4_t} \cap \mathsf{A}^4$, and is a 4-polytope whose combinatorics does not depend on $t \in I$.*

Remark 7.4. Recall Definition 2.11 of geometric transition. Proposition 7.3 implies that we already have a transition on the interior of $\mathcal{P}_t$.

Before proving Proposition 7.3, let us begin with a simple lemma.

Lemma 7.5. *For all $t \in I$, the set $\mathfrak{r}_{|t|}(\overline{\mathcal{P}}_t) \subset \mathsf{S}^4$ is a 4-polytope.*

Proof. It suffices to show that $\mathfrak{r}_{|t|}(\overline{\mathcal{P}}_t)$ has non-empty interior. From Table 3, a small neighbourhood of the point $[1 : 0 : 0 : 0 : 0] \in \mathsf{S}^4$ is contained in $\mathfrak{r}_{|t|}(\overline{\mathcal{P}}_t)$ because the first entry of each vector of Table 3 is negative. □

$$\mathfrak{r}_{|t|}\mathbf{0}^+ = \left(-\sqrt{2} : +1 : +1 : +1 : +1\right), \qquad \mathfrak{r}_{|t|}\mathbf{0}^- = \left(-\sqrt{2} : +1 : +1 : +1 : -t|t|\right),$$

$$\mathfrak{r}_{|t|}\mathbf{1}^+ = \left(-\sqrt{2} : +1 : -1 : +1 : -1\right), \qquad \mathfrak{r}_{|t|}\mathbf{1}^- = \left(-\sqrt{2} : +1 : -1 : +1 : +t|t|\right),$$

$$\mathfrak{r}_{|t|}\mathbf{2}^+ = \left(-\sqrt{2} : +1 : -1 : -1 : +1\right), \qquad \mathfrak{r}_{|t|}\mathbf{2}^- = \left(-\sqrt{2} : +1 : -1 : -1 : -t|t|\right),$$

$$\mathfrak{r}_{|t|}\mathbf{3}^+ = \left(-\sqrt{2} : +1 : +1 : -1 : -1\right), \qquad \mathfrak{r}_{|t|}\mathbf{3}^- = \left(-\sqrt{2} : +1 : +1 : -1 : +t|t|\right),$$

$$\mathfrak{r}_{|t|}\mathbf{4}^+ = \left(-\sqrt{2} : -1 : +1 : -1 : +1\right), \qquad \mathfrak{r}_{|t|}\mathbf{4}^- = \left(-\sqrt{2} : -1 : +1 : -1 : -t|t|\right),$$

$$\mathfrak{r}_{|t|}\mathbf{5}^+ = \left(-\sqrt{2} : -1 : +1 : +1 : -1\right), \qquad \mathfrak{r}_{|t|}\mathbf{5}^- = \left(-\sqrt{2} : -1 : +1 : +1 : +t|t|\right),$$

$$\mathfrak{r}_{|t|}\mathbf{6}^+ = \left(-\sqrt{2} : -1 : -1 : +1 : +1\right), \qquad \mathfrak{r}_{|t|}\mathbf{6}^- = \left(-\sqrt{2} : -1 : -1 : +1 : -t|t|\right),$$

$$\mathfrak{r}_{|t|}\mathbf{7}^+ = \left(-\sqrt{2} : -1 : -1 : -1 : -1\right), \qquad \mathfrak{r}_{|t|}\mathbf{7}^- = \left(-\sqrt{2} : -1 : -1 : -1 : +t|t|\right),$$

$$\mathfrak{r}_{|t|}\mathbf{A} = \left(-1 : +\sqrt{2} : 0 : 0 : 0\right), \qquad \mathfrak{r}_{|t|}\mathbf{B} = \left(-1 : 0 : +\sqrt{2} : 0 : 0\right),$$

$$\mathfrak{r}_{|t|}\mathbf{C} = \left(-1 : 0 : 0 : +\sqrt{2} : 0\right), \qquad \mathfrak{r}_{|t|}\mathbf{D} = \left(-1 : 0 : 0 : -\sqrt{2} : 0\right),$$

$$\mathfrak{r}_{|t|}\mathbf{E} = \left(-1 : 0 : -\sqrt{2} : 0 : 0\right), \qquad \mathfrak{r}_{|t|}\mathbf{F} = \left(-1 : -\sqrt{2} : 0 : 0 : 0\right).$$

TABLE 3. The half-spaces in S^4 defining $\mathfrak{r}_{|t|}(\mathcal{P}_t)$, by a direct application of Lemma 4.1 to Table 2.

As in [KS10, MR18], we now descibe the symmetries of the polytope $\overline{\mathcal{P}}_t$ and of its rescaled $\mathfrak{r}_{|t|}(\overline{\mathcal{P}}_t)$ which are useful to reduce the number of computations. We refer to [KS10, Section 4] and [MR18, Section 3.2] for details in the hyperbolic case.

Let us introduce three auxiliary half-spaces $\mathbf{L}$, $\mathbf{M}$ and $\mathbf{N}$, defined in Equation (8). Observe that they are all left invariant by $\mathfrak{r}_{|t|}$.

$$\begin{aligned} \mathbf{L} &= (0 : -1 : +1 : 0 : 0), \\ \mathbf{M} &= (0 : 0 : -1 : +1 : 0), \\ \mathbf{N} &= (0 : 0 : -1 : -1 : 0). \end{aligned} \tag{8}$$

The following projective involutions of S^4

$$\begin{aligned} r_{\mathbf{L}} &: [x_0 : x_1 : x_2 : x_3 : x_4] \longmapsto [x_0 : x_2 : x_1 : x_3 : x_4], \\ r_{\mathbf{M}} &: [x_0 : x_1 : x_2 : x_3 : x_4] \longmapsto [x_0 : x_1 : x_3 : x_2 : x_4], \\ r_{\mathbf{N}} &: [x_0 : x_1 : x_2 : x_3 : x_4] \longmapsto [x_0 : x_1 : -x_3 : -x_2 : x_4], \\ R &: [x_0 : x_1 : x_2 : x_3 : x_4] \longmapsto [x_0 : x_1 : x_2 : -x_3 : -x_4] \end{aligned}$$

commute with $\mathfrak{r}_{|t|}$, preserve the hyperplane $\mathbb{H}^3$, and all belong to $\mathrm{Isom}(\mathbb{H}^4)$, G_{HP^4} and $\mathrm{Isom}(\mathbb{AdS}^4)$. As the notation suggests, $r_{\mathbf{L}}, r_{\mathbf{M}}$ and $r_{\mathbf{N}}$ are reflections along the hyperplanes $\partial\mathbf{L}$, $\partial\mathbf{M}$ and $\partial\mathbf{N}$, respectively. The map R, instead, is a rotation (called "roll symmetry" in [KS10]). The group $\langle r_{\mathbf{L}}, r_{\mathbf{M}}, r_{\mathbf{N}} \rangle < \mathrm{Aut}(\mathsf{S}^4)$ is isomorphic to the symmetric group $\mathfrak{S}_4$ on 4 elements.

Lemma 7.6. *The maps $r_{\mathbf{L}}, r_{\mathbf{M}}, r_{\mathbf{N}}$ and R preserve $\overline{\mathcal{P}}_t$ and $\mathfrak{r}_{|t|}(\overline{\mathcal{P}}_t)$ for all $t \in I$. Moreover, the set*

$$\overline{\mathcal{Q}}_t = \mathbf{0}^+ \cap \mathbf{0}^- \cap \mathbf{3}^+ \cap \mathbf{3}^- \cap \mathbf{A} \cap \mathbf{L} \cap \mathbf{M} \cap \mathbf{N} \subset \mathsf{S}^4$$

is a fundamental domain for the action of the group $\langle r_{\boldsymbol{L}}, r_{\boldsymbol{M}}, r_{\boldsymbol{N}}\rangle < \mathrm{Aut}(\mathsf{S}^4)$ on $\overline{\mathcal{P}}_t$. More-over, $\mathfrak{r}_{|t|}(\overline{\mathcal{Q}}_t)$ is a fundamental domain for the action of the group $\langle r_{\boldsymbol{L}}, r_{\boldsymbol{M}}, r_{\boldsymbol{N}}\rangle < \mathrm{Aut}(\mathsf{S}^4)$ on $\mathfrak{r}_{|t|}(\overline{\mathcal{P}}_t)$.

Proof. This is already proved for $t \in I^+$ in [KS10, Section 4] and [MR18, Section 3.2]. To conclude, it suffices to observe that the action of $\langle r_{\boldsymbol{L}}, r_{\boldsymbol{M}}, r_{\boldsymbol{N}}\rangle$ on the set of vectors in Table 2 does not depend on $t \in I$. The second statement follows as a consequence, using that $\mathfrak{r}_{|t|}$ commutes with $r_{\boldsymbol{L}}, r_{\boldsymbol{M}}$ and $r_{\boldsymbol{N}}$. $\qquad\square$

Lemma 7.7. *For all $t \in I^-$, the sets $\overline{\mathcal{P}}_t$ and $\mathfrak{r}_{|t|}(\overline{\mathcal{P}}_t)$ are contained in the affine chart A^4.*

Proof. Since the maps $r_{\boldsymbol{L}}, r_{\boldsymbol{M}}, r_{\boldsymbol{N}}, \mathfrak{r}_{|t|} \in \mathrm{Aut}(\mathsf{S}^4)$ preserve the affine chart A^4, it suffices to show that $\mathfrak{r}_{|t|}(\overline{\mathcal{Q}}_t) \subset \mathsf{A}^4$. By looking at Table 3 and Equation (8), $\mathfrak{r}_{|t|}(\overline{\mathcal{Q}}_t)$ is defined by the following inequalities:

$$-\sqrt{2}x_0 + x_1 + x_2 + x_3 + x_4 \le 0, \quad -\sqrt{2}x_0 + x_1 + x_2 - x_3 - x_4 \le 0, \tag{9}$$

$$-\sqrt{2}x_0 + x_1 + x_2 + x_3 + t^2 x_4 \le 0, \quad -\sqrt{2}x_0 + x_1 + x_2 - x_3 - t^2 x_4 \le 0, \tag{10}$$

$$-x_0 + \sqrt{2}x_1 \le 0, \quad -x_1 + x_2 \le 0, \quad -x_2 + x_3 \le 0, \quad -x_2 - x_3 \le 0. \tag{11}$$

Suppose by contradiction that $x_0 \le 0$. By (11), we would also have $x_1, x_2, x_3 \le 0$. Together with the last inequality of (11), this gives $x_2 = x_3 = 0$. By the second inequality of (11), we have also $x_1 = 0$. By the first inequality of (11), we have also $x_0 = 0$. Substituting $x_0 = x_1 = x_2 = x_3 = 0$ in (9), we have also $x_4 = 0$, and this is absurd. $\qquad\square$

We will thus be free to use the affine coordinates $y_1, \ldots, y_4$ of A^4, where $y_i = x_i/x_0$. Let us now analyse the vertices of $\overline{\mathcal{P}}_t$.

Lemma 7.8. *For all $t \in I$, the polytope $\mathfrak{r}_{|t|}(\overline{\mathcal{P}}_t)$ has 46 vertices, of which 12 belong to $\partial \mathbb{X}_t^4$ and 34 belong to $\mathbb{X}_t^4$.*

Proof. This is already proven in [MR18, Proposition 3.16] for $t \in I^+$, by applying to $\mathcal{Q}_t \subset \mathbb{H}^4$ Vinberg's theory of acute-angled hyperbolic polytopes [Vin85] and then by letting the group $\langle r_{\boldsymbol{L}}, r_{\boldsymbol{M}}, r_{\boldsymbol{N}}\rangle$ act. We cannot do the same for $t \in I^- \cup \{0\}$, being now in the AdS (or HP) setting, so in this case we proceed as follows.

(1) For every $k = 4, 5, 6, 7, 8$ and every set $\{\boldsymbol{H}_1, \ldots, \boldsymbol{H}_k\}$ of bounding hyperplanes of $\mathfrak{r}_{|t|}(\overline{\mathcal{Q}}_t)$, we consider the linear system in A^4 defining $\bigcap_i \partial \boldsymbol{H}_i$.
(2) Every time such linear system has a unique solution, we check if the solution belongs to $\mathfrak{r}_{|t|}(\overline{\mathcal{Q}}_t)$.
(3) We collect all such points, which are the 13 vertices of $\mathfrak{r}_{|t|}(\overline{\mathcal{Q}}_t)$.
(4) We check that one vertex belongs to $\partial \mathbb{X}_t^4$, while the remaing 12 belong to $\mathbb{X}_t^4$.
(5) We select the vertices of $\mathfrak{r}_{|t|}(\overline{\mathcal{Q}}_t)$ which are vertices of $\overline{\mathcal{P}}_t$.
(6) We let the group $\langle r_{\boldsymbol{L}}, r_{\boldsymbol{M}}, r_{\boldsymbol{N}}\rangle$ act on these latter points, to finally find all the vertices of $\mathfrak{r}_{|t|}(\overline{\mathcal{P}}_t)$.

The final output is reported in Table 4. Although this procedure is very simple, the number of computations is terribly big, so we omit the complete proof. The details can be checked through a computer (see [RSb, Appendix A]). $\qquad\square$

Note that the previous lemma implies that $\mathfrak{r}_{|t|}(\overline{\mathcal{P}}_t) \subset \overline{\mathbb{X}_t^4} \cap \mathsf{A}^4$ when $t \in I^+ \cup \{0\}$, since in that case $\overline{\mathbb{X}_t^4} \subset \mathsf{A}^4$ is convex. We cannot directly conclude in the same way when $t \in I^-$, as $\overline{\mathbb{X}_t^4} \cap \mathsf{A}^4$ is not convex when $t < 0$.

$$
\begin{aligned}
\mathcal{V}_{\mathbf{0^+3^+0^-3^-}AL} &= \left(\tfrac{\sqrt{2}}{2},\ \tfrac{\sqrt{2}}{2},\ 0,\ 0\right), \\
\mathcal{V}_{\mathbf{0^+0^-}AM} &= \left(\tfrac{\sqrt{2}}{2},\ \tfrac{\sqrt{2}}{4},\ \tfrac{\sqrt{2}}{4},\ 0\right), \\
\mathcal{V}_{\mathbf{0^+0^-}LM} &= \left(\tfrac{\sqrt{2}}{3},\ \tfrac{\sqrt{2}}{3},\ \tfrac{\sqrt{2}}{3},\ 0\right), \\
\mathcal{V}_{\mathbf{0^+3^-}AN} &= \left(\tfrac{\sqrt{2}}{2},\ \tfrac{\sqrt{2}}{4}(t^2+1),\ -\tfrac{\sqrt{2}}{4}(t^2+1),\ \tfrac{\sqrt{2}}{4}\right), \\
\mathcal{V}_{\mathbf{0^+3^-}LN} &= \left(\sqrt{2}\tfrac{t^2+1}{t^2+3},\ \sqrt{2}\tfrac{t^2+1}{t^2+3},\ -\sqrt{2}\tfrac{t^2+1}{t^2+3},\ \tfrac{2\sqrt{2}}{t^2+3}\right), \\
\mathcal{V}_{\mathbf{0^+}AMN} &= \left(\tfrac{\sqrt{2}}{2},\ 0,\ 0,\ \tfrac{\sqrt{2}}{2}\right), \\
\mathcal{V}_{\mathbf{0^+}LMN} &= \left(0,\ 0,\ 0,\ \sqrt{2}\right), \\
\mathcal{V}_{\mathbf{3^+0^-}AM} &= \left(\tfrac{\sqrt{2}}{2},\ \tfrac{\sqrt{2}}{4}(t^2+1),\ \tfrac{\sqrt{2}}{4}(t^2+1),\ -\tfrac{\sqrt{2}}{2}\right), \\
\mathcal{V}_{\mathbf{3^+0^-}LM} &= \left(\sqrt{2}\tfrac{t^2+1}{t^2+3},\ \sqrt{2}\tfrac{t^2+1}{t^2+3},\ \sqrt{2}\tfrac{t^2+1}{t^2+3},\ -\tfrac{2\sqrt{2}}{t^2+3}\right), \\
\mathcal{V}_{\mathbf{3^+3^-}AN} &= \left(\tfrac{\sqrt{2}}{2},\ \tfrac{\sqrt{2}}{4},\ -\tfrac{\sqrt{2}}{4},\ 0\right), \\
\mathcal{V}_{\mathbf{3^+3^-}LN} &= \left(\tfrac{\sqrt{2}}{3},\ \tfrac{\sqrt{2}}{3},\ -\tfrac{\sqrt{2}}{3},\ 0\right), \\
\mathcal{V}_{\mathbf{3^+}AMN} &= \left(\tfrac{\sqrt{2}}{2},\ 0,\ 0,\ -\tfrac{\sqrt{2}}{2}\right), \\
\mathcal{V}_{\mathbf{3^+}LMN} &= \left(0,\ 0,\ 0,\ -\sqrt{2}\right).
\end{aligned}
$$

TABLE 4. The vertices of $\mathfrak{r}_{|t|}(\overline{\mathcal{Q}}_t)$ in affine coordinates.

Lemma 7.9. *For all $t \in I$, we have*
$$
\mathfrak{r}_{|t|}(\overline{\mathcal{Q}}_t) \cap \partial \mathbb{X}_t^4 = \{[2 : \sqrt{2} : \sqrt{2} : 0 : 0]\}.
$$

Proof. This is already proven in [MR18] when $t \in I^+$. So, let us assume that $t \in I^- \cup \{0\}$. In affine coordinates, (9) and (11) read as:
$$
-\sqrt{2} + y_1 + y_2 + y_3 + y_4 \le 0, \quad -\sqrt{2} + y_1 + y_2 - y_3 - y_4 \le 0,
$$
$$
-y_2 \le y_3 \le y_2 \le y_1 \le \tfrac{\sqrt{2}}{2}.
$$
By summing the first two equations and using the third, we get $y_1 = y_2 = \sqrt{2}/2$. This implies $y_3 + y_4 = 0$. Now, the affine coordinates of a point in $\partial \mathbb{X}_t^4$ satisfy
$$
y_1^2 + y_2^2 + y_3^2 - t^2 y_4^2 = 1.
$$
This implies $y_3^2 - t^2 y_4^2 = 0$. Together with $y_3 + y_4 = 0$, we get $y_3 = y_4 = 0$ since $t^2 \ne 1$. This concludes the proof. $\qquad\square$

We are finally ready to prove Proposition 7.3.

Proof of Proposition 7.3. By Lemma 7.7, $\mathfrak{r}_{|t|}(\overline{\mathcal{P}}_t) \subset \mathsf{A}^4$. Recall that $[1 : 0 : 0 : 0 : 0] \in \mathfrak{r}_{|t|}(\mathcal{P}_t) \cap \mathbb{X}_t^4$. By Lemma 7.9, the intersection $\mathfrak{r}_{|t|}(\overline{\mathcal{P}}_t) \cap \partial \mathbb{X}_t^4$ consists solely of vertices of $\mathfrak{r}_{|t|}(\overline{\mathcal{P}}_t)$, hence we have also $\mathfrak{r}_{|t|}(\overline{\mathcal{P}}_t) \subset \overline{\mathbb{X}_t^4}$. Thus, $\mathfrak{r}_{|t|}(\overline{\mathcal{P}}_t) \subset \overline{\mathbb{X}_t^4} \cap \mathsf{A}^4$. The combinatorics of $\mathfrak{r}_{|t|}(\overline{\mathcal{P}}_t)$ is constant by Lemma 7.8. The proof is complete. $\qquad\square$

In contrast with $\overline{\mathcal{P}}_t$, the polytope $\mathcal{P}_t$ is simple [MR18, Proposition 3.12]. Moreover, each ideal vertex of $\mathcal{P}_t$ belongs to exactly 6 facets of $\overline{\mathcal{P}}_t$ [MR18, Proposition 3.16]. (We applied
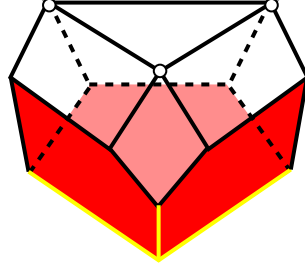
FIGURE 17. A facet $\mathcal{F}_{\boldsymbol{i}^+}$, $\boldsymbol{i}^+ \in \{\boldsymbol{0}^+, \dots, \boldsymbol{7}^+\}$, of the 4-polytope $\mathcal{P}_t$. The white dots represent ideal vertices, the black edges are right-angled, and the yellow edges have some other varying dihedral angle. The three red pentagons are ridges of $\mathcal{P}_t$ of type $\mathcal{R}_{\boldsymbol{i}^+\boldsymbol{j}^+}$, and have varying dihedral angle θ_t or φ_t (see Proposition 7.12). Each of the three quadrilaterals with one ideal vertex (resp. two ideal vertices) is a ridge of $\mathcal{P}_t$ of type $\mathcal{R}_{\boldsymbol{i}^+\boldsymbol{j}^-}$ (resp. $\mathcal{R}_{\boldsymbol{i}^+\boldsymbol{X}}$). The horizontal ideal triangle is the ridge $\mathcal{R}_{\boldsymbol{i}^+\boldsymbol{i}^-}$.

Proposition 7.3 to conclude when $t \in I^-$.) We adopt the following notation for the faces of $\mathcal{P}_t$ when $t \neq 0$ (and similarly for the rescaled limit $\lim_{t\to 0} \mathfrak{r}_{|t|}\mathcal{P}_t$):

- facets: $\mathcal{F}_{\boldsymbol{H}} = \partial \boldsymbol{H} \cap \mathcal{P}_t$,
- ridges: $\mathcal{R}_{\boldsymbol{H}_1\boldsymbol{H}_2} = \partial \boldsymbol{H}_1 \cap \partial \boldsymbol{H}_2 \cap \mathcal{P}_t$,
- edges: $\mathcal{E}_{\boldsymbol{H}_1\boldsymbol{H}_2\boldsymbol{H}_3} = \partial \boldsymbol{H}_1 \cap \partial \boldsymbol{H}_2 \cap \partial \boldsymbol{H}_3 \cap \mathcal{P}_t$,
- finite vertices: $\mathcal{V}_{\boldsymbol{H}_1\dots\boldsymbol{H}_4} = \partial \boldsymbol{H}_1 \cap \dots \cap \partial \boldsymbol{H}_4 \cap \mathcal{P}_t$,
- ideal vertices: $\mathcal{V}_{\boldsymbol{H}_1\dots\boldsymbol{H}_6} = \partial \boldsymbol{H}_1 \cap \dots \cap \partial \boldsymbol{H}_6 \cap \overline{\mathcal{P}}_t$,

where $\boldsymbol{H}, \boldsymbol{H}_i \subset \mathsf{S}^4$ are half-spaces from the list in Table 2.

We conclude the section with a combinatorial description of the facets of the polytope $\mathcal{P}_t$. This follows by applying Proposition 7.3 to [MR18, Proposition 3.16], where the combinatorics was studied for $t \in I^+$.

Proposition 7.10. *For all $t \in I$, the combinatorics of each of the 22 facets $\mathcal{F}_{\boldsymbol{X}}$, $\mathcal{F}_{\boldsymbol{i}^-}$ and $\mathcal{F}_{\boldsymbol{i}^+}$ of $\mathfrak{r}_{|t|}\mathcal{P}_t$ where $\boldsymbol{i} \in \{\boldsymbol{0}, \dots, \boldsymbol{7}\}$ and $\boldsymbol{X} \in \{\boldsymbol{A}, \dots, \boldsymbol{F}\}$, is described in Figures 12, 15 and 17, respectively.*

7.3. **Geometry of the polytope.** We continue to describe the polytope $\mathcal{P}_t$. Recall Sections 4.2 and 4.8 about hyperplanes and angles in $\mathbb{H}^n$, $\mathbb{A}\mathrm{d}\mathbb{S}^n$ and HP^n. By applying Lemmas 4.5 and 4.8 to the list of vectors in Tables 2 and 3, we get:

Proposition 7.11. *When $t \in I^-$, each hyperplane $\partial \boldsymbol{i}^+ \cap \mathbb{A}\mathrm{d}\mathbb{S}^4$ is spacelike, while each hyperplane $\partial \boldsymbol{i}^- \cap \mathbb{A}\mathrm{d}\mathbb{S}^4$ and $\partial \boldsymbol{X} \cap \mathbb{A}\mathrm{d}\mathbb{S}^4$ is timelike, for all $\boldsymbol{i} \in \{\boldsymbol{0}, \dots, \boldsymbol{7}\}$ and $\boldsymbol{X} \in \{\boldsymbol{A}, \dots, \boldsymbol{F}\}$.*

Similarly when $t = 0$, the rescaled limits of $\partial \boldsymbol{i}^+$ are non-degenerate hyperplanes in HP^4, while the rescaled limits of $\partial \boldsymbol{i}^-$ and $\partial \boldsymbol{X}$ are degenerate hyperplanes.

We will also need the following:

Proposition 7.12. *The constant dihedral angles of $\mathcal{P}_t$ are right. The non-constant ones equal $\theta_t \in [\frac{\pi}{2}, \pi)$ when $t \in I^+$, and $\varphi_t \in (0, +\infty)$ when $t \in I^-$, where*

$$\cos \theta_t = \frac{3t^2 - 1}{1 + t^2} \quad and \quad \cosh \varphi_t = \frac{3t^2 + 1}{1 - t^2}.$$

A ridge is compact if and only if its dihedral angle is non-constant, and such ridges consist precisely of $\mathcal{R}_{\boldsymbol{i}^+\boldsymbol{j}^+}$ for all distinct $\boldsymbol{i}^+, \boldsymbol{j}^+ \in \{\boldsymbol{0}^+, \dots, \boldsymbol{7}^+\}$ such that $i \equiv j \pmod 2$.
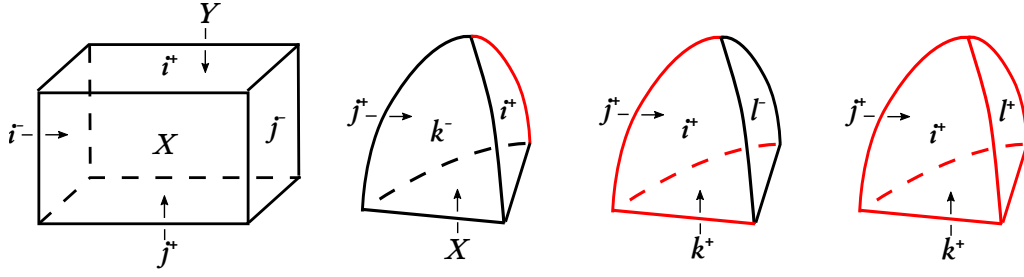
FIGURE 18. The links of the vertices of $\mathcal{P}_t$ (see Proposition 7.13). When $t \in I^+$ (resp. $t \in I^-$) the link of an ideal vertex is a Euclidean (resp. Minkowski) right paralleleped, and the link of a finite vertex is a spherical tetrahedron (resp. de Sitter tetrahedron with spacelike facets). The black edges are right-angled, and the red edges have varying dihedral angle.

Proof. This is proven for $t \in I^+$ in [MR18, Proposition 3.10]. Such ridges are compact also when $t \in I^-$ by Proposition 7.3. By applying Lemma 4.6 to the list of vectors in Table 2, we conclude also for $t \in I^-$. (In fact, we have already observed in Remark 7.2 that the orthogonality between the vectors of Table 2 is maintained when $t \in (-1, 0)$ for the bilinear form of signature $-+++-$.) $\square$

We now describe the links of the vertices of $\mathcal{P}_t$, whose geometric structures have been described in Section 3 for ideal vertices and Section 5 for finite vertices. These are depicted in Figures 18, 19 and 20 and described by the following proposition:

Proposition 7.13. *The 46 vertices of $\mathcal{P}_t$ are divided by the similarity class of their link in:*

- *12 ideal vertices of type $\mathcal{V}_{i^+ i^- j^+ j^- XY}$,*
- *24 finite vertices of type $\mathcal{V}_{i^+ j^+ k^- X}$,*
- *8 finite vertices of type $\mathcal{V}_{i^+ j^+ k^+ \ell^-}$,*
- *2 finite vertices of type $\mathcal{V}_{i^+ j^+ k^+ \ell^+}$,*

The link of each ideal vertex is a rectangular parallelepiped (which in a horospherical section is Euclidean when $t \in I^+$, and Minkowski when $t \in I^-$), while the link each finite vertex is a tetrahedron (which is spherical when $t \in I^+$, and HS when $t \in I^-$). A similar statement holds for the rescaled limit $\lim_{t \to 0} \mathfrak{r}_{|t|} \mathcal{P}_t$ in the half-pipe setting.

Proof. These facts are proven in [MR18, Proposition 3.16] for $t \in I^+$. By applying Propositions 7.3, 7.11 and 7.12, we conclude also for $t \in I^-$ and for the rescaled limit. $\square$

As a consequence of Proposition 7.13, we get:

Corollary 7.14. *When $t \in I^-$, the Anti-de Sitter polytope $\mathcal{P}_t \subset \mathbb{A}d\mathbb{S}^4$ has finite volume. The same holds for the half-pipe polytope $\lim_{t \to 0} \mathfrak{r}_{|t|}(\mathcal{P}_t) \subset \mathsf{HP}^4$.*

Proof. By Proposition 7.1, when $t \in I^+$ the hyperbolic polytope $\mathcal{P}_t$ has finite volume. Equivalently, each edge of $\mathcal{P}_t$ joins two (finite or ideal) vertices of $\mathcal{P}_t$. By Proposition 7.3, this last fact also holds in $\mathbb{A}d\mathbb{S}^4$ when $t \in I^-$ and in HP^4 for the rescaled limit. By truncating the ends of $\mathcal{P}_t$ (resp. $\lim_{t \to 0} \mathfrak{r}_{|t|}(\mathcal{P}_t)$) with horospheres (see Section 3.1), we have decomposed the polytope in a compact part plus 12 regions, each isometric to the fundamental domain of a cusp in an Anti-de Sitter (resp. half-pipe) 4-manifold (see Definition 3.6). Therefore (see Remark 3.7), the polytope has finite volume. $\square$
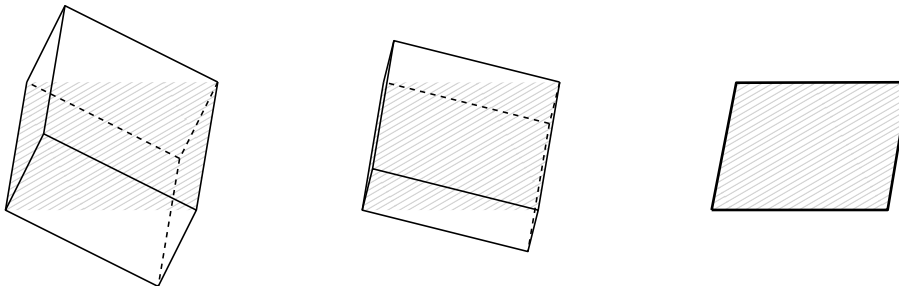
FIGURE 19. The link of an ideal vertex of $\mathcal{P}_t$, obtained by intersecting $\mathcal{P}_t$ with a horosphere. The further intersection with $\mathbb{H}^3$, which is constant in t, is a rectangle (shaded in the picture). When $t \to 0$, the rectangular parallepiped collapses to this rectangle.
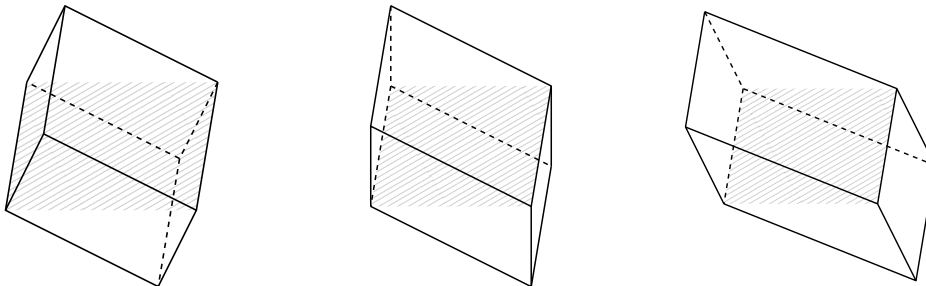

FIGURE 20. After rescaling, the geometry of the link of an ideal vertex transitions from Euclidean (left) to Minkoskian (right), via Galilean geometry (centre). The intersection with the fixed copy of $\mathbb{H}^3$ is shaded. This is an example of the transition explained in Section 3.2.

7.4. **Orbifold transition.** Roughly speaking, a (G, X)-*orbifold* is a space locally modelled on quotients of X by finite subgroups of G. We refer to [Thu79, Cho04] for the details.

The geometry of $\mathcal{P}_t$ gives the complement of the ridges with non-constant dihedral angle (see Proposition 7.12) a natural structure of orbifold (this is different, but somehow related, to the concept of "mirror polytope" [Mar17, CLM20]), and this fact will be convenient in the sequel.

Let us first prove a preliminary lemma. Recall Section 4.5 about reflections and their limits. For the sake of clarity, we will make explicit the dependence of the half-spaces of Table 2 in t, by a subscript $\boldsymbol{H}_t$.

Lemma 7.15. *For every half-space $\boldsymbol{H}$ of Table 2, let $r_{\boldsymbol{H}} = r_{\boldsymbol{H}}(t)$ be the reflection in* $\mathrm{Isom}(\mathbb{H}^4)$ *for $t \in I^+$ and in $\mathrm{Isom}(\mathbb{A}\mathrm{d}\mathbb{S}^4)$ for $t \in I^-$ which fixes $\partial \boldsymbol{H}$. Then $\mathfrak{r}_{|t|} r_{\boldsymbol{H}}(t) \mathfrak{r}_{|t|}^{-1}$ extends to a C^1 path in $\mathrm{Aut}(\mathsf{S}^4)$ for $t \in I^- \cup \{0\} \cup I^+$.*

Observe that Lemma 7.15 does not follow immediately from the convergence of the hyperplanes $\mathfrak{r}_{|t|}(\partial \boldsymbol{H}_t)$ to a half-pipe hyperplane because, as remarked in Section 4.13, in half-pipe geometry there is *not* a uniquely determined reflection in a hyperplane.

Proof. Let us start by the case $\boldsymbol{H} = \boldsymbol{i}^- \in \boldsymbol{i} \in \{\boldsymbol{0}^-, \dots, \boldsymbol{7}^-\}$. For $t \in I^+$, the hyperbolic reflection $r_{\boldsymbol{i}^-}$ (for which we will make explicit the dependence on t) can be written as the matrix

$$r_{\boldsymbol{i}^-}(t) = \mathrm{id} - 2J_1 \alpha_i(t) \alpha_i(t)^T , \tag{12}$$

where $J_1 = \text{diag}(-1, 1, 1, 1, 1)$ and

$$\alpha_i(t)^T = \frac{1}{\sqrt{1 + t^2}} \left(-\sqrt{2}, \pm 1, \pm 1, \pm 1, \pm t \right)$$

is obtained from the vector defining $\boldsymbol{i}^-$ (see Table 2) by normalising with respect to the Minkowski product of $\mathbb{R}^{1,4}$. (The signs in the $\pm$ symbols are fixed once and forever according to the choice of $\boldsymbol{i}^-$.) Indeed, one can check (using that $\alpha_i(t)^T J_1 \alpha_i(t) = 1$) that the expression of Equation (12) maps $J_1 \alpha_i(t)$ to its opposite, whereas it fixes every $v \in \partial \boldsymbol{i}^-$, since v satisfies $\alpha_i(t)^T v = 0$.

Similarly, when $t \in I^-$ the AdS reflection can be expressed as

$$r_{\boldsymbol{i}^-}(t) = \text{id} - 2J_{-1}\alpha_i(t)\alpha_i(t)^T , \tag{13}$$

where $J_{-1} = \text{diag}(-1, 1, 1, 1, -1)$ and

$$\alpha_i(t) = \frac{1}{\sqrt{1 - t^2}} \left(-\sqrt{2} : \pm 1 : \pm 1 : \pm 1 : \pm t \right) .$$

Hence we get the expression (for $t \neq 0$):

$$\mathfrak{r}_{|t|} r_{\boldsymbol{i}^-}(t) \mathfrak{r}_{|t|}^{-1} = \text{id} - 2 \left[J_{\text{sign}(t)} \mathfrak{r}_{|t|} \alpha_i(t) \right] \left[\mathfrak{r}_{|t|}^{-1} \alpha_i(t)^T \right] .$$

The term in the first square bracket thus reads for both $t > 0$ and $t < 0$ as the column vector:

$$\frac{1}{\sqrt{1 + t|t|}} \left(\sqrt{2} : \pm 1 : \pm 1 : \pm 1 : \pm 1 \right)$$

while the second square bracket has the form (horizontal vector):

$$\frac{1}{\sqrt{1 + t|t|}} \left(-\sqrt{2} : \pm 1 : \pm 1 : \pm 1 : \pm t|t| \right) .$$

Since both extend C^1 to $t = 0$, so does $\mathfrak{r}_{|t|} r_{\boldsymbol{i}^-}(t) \mathfrak{r}_{|t|}^{-1}$.

For $\boldsymbol{H} = \boldsymbol{X} \in \boldsymbol{X} \in \{\boldsymbol{A}, \ldots, \boldsymbol{F}\}$, the path $\mathfrak{r}_{|t|} r_{\boldsymbol{X}} \mathfrak{r}_{|t|}^{-1}$ is actually constant, since $\boldsymbol{X}$ does not depend on t and it can be easily checked that the hyperbolic and AdS reflections, expressed as in Equations (12) and (13), coincide and commute with $\mathfrak{r}_{|t|}$. Finally, for the case $\boldsymbol{H} = \boldsymbol{i}^+ \in \{\boldsymbol{0}^+, \ldots, \boldsymbol{7}^+\}$, when $t \in I^-$ there is a small difference in the formula of Equation (12), which now becomes

$$r_{\boldsymbol{i}^+}(t) = \text{id} + 2J_{-1}\alpha_i(t)\alpha_i(t)^T , \tag{14}$$

due to the fact that the $\boldsymbol{i}^-$ are timelike while the $\boldsymbol{i}^+$ are spacelike, and again the rescaled limit is the same as for $t \in I^+$. With this caveat, it can be checked directly that all the entries in $\mathfrak{r}_{|t|} r_{\boldsymbol{i}^+}(t) \mathfrak{r}_{|t|}^{-1}$ are, up to constants, either of the form $1/\sqrt{1 + t|t|}$ or of the form $t|t|/\sqrt{1 + t|t|}$, and thus the path is C^1 in $\text{Aut}(\mathsf{S}^4)$. $\square$

From the proof of Lemma 7.15, we see also that the convergence is not C^2.

Remark 7.16. The proof of Lemma 7.15 enables us to compute also the limits of $\mathfrak{r}_{|t|} r_{\boldsymbol{H}}(t) \mathfrak{r}_{|t|}^{-1}$, as $t \to 0$ in the half-pipe group G_{HP^4}. In fact, for the reflections along the hyperplanes $\boldsymbol{i}^-$, we obtain immediately

$$\lim_{t \to 0} \mathfrak{r}_{|t|} r_{\boldsymbol{i}^-}(t) \mathfrak{r}_{|t|}^{-1} = \left(\begin{array}{c|c} \text{id} - 2Jv_iv_i^T & \begin{matrix} 0 \\ \vdots \\ 0 \end{matrix} \\ \hline \cdots \quad \pm 2v_i^T \quad \cdots & 1 \end{array} \right) = \phi(r_i, \mp 2Jv_i) , \tag{15}$$

where we put $v_i^T = (-\sqrt{2}, \pm 1, \pm 1, \pm 1)$ (namely, the first four terms of the corresponding vector in Table 2, and $r_i = \mathrm{id} - 2Jv_iv_i^T$ is the reflection in $\mathbb{H}^3$ in the plane determined by v_i, for $J = \mathrm{diag}(-1, 1, 1, 1)$. The sign in Equation (15) depends on the oddity of i, since it follows from the sign in the last entry of $\alpha_i(t)$, and in fact the correct sign is $(-1)^{i+1}$. In the last equality, we applied the isomorphism ϕ of Lemma 2.8.

For any half-space $\boldsymbol{X} \in \{\boldsymbol{A}, \dots, \boldsymbol{F}\}$, the same computation shows easily that

$$\lim_{t \to 0} \mathfrak{r}_{|t|} r_{\boldsymbol{X}} \mathfrak{r}_{|t|}^{-1} = \phi(r_{\boldsymbol{X}}, 0) \ ,$$

where $r_{\boldsymbol{X}}$ is now interpreted as the reflection in $\mathbb{H}^3$ associated to the plane $\mathbb{H}^3 \cap \partial \boldsymbol{X}$.

Finally, for the half-spaces of the form $\boldsymbol{i}^+$ the computation is again similar following Lemma 7.15. One obtains

$$\lim_{t \to 0} \mathfrak{r}_{|t|} r_{\boldsymbol{i}^+}(t) \mathfrak{r}_{|t|}^{-1} = \left(\begin{array}{ccc|c} & & & 0 \\ & \mathrm{id} & & \vdots \\ & & & 0 \\ \hline \dots & \mp 2v_i^T & \dots & -1 \end{array} \right) = \phi(-\mathrm{id}, \mp 2Jv_i) \ ,$$

where v_i is defined as above.

We are ready to describe the natural orbifold structure on a subset of $\mathcal{P}_t$.

Proposition 7.17. *The set*

$$\mathcal{P}_t^\times = \mathcal{P}_t \smallsetminus \bigcup_{i \neq j} \mathcal{R}_{\boldsymbol{i}^+ \boldsymbol{j}^+}$$

is isometric to a hyperbolic orbifold when $t \in I^+$, and to an Anti-de Sitter orbifold when $t \in I^-$. Similarly, the rescaled limit $\lim_{t \to 0} \mathfrak{r}_{|t|} \mathcal{P}_t^\times$ has a natural structure of half-pipe orbifold.

Proof. When $t \in I^+$ (resp. $t \in I^-$), we associate to each facet $\mathcal{F}_{\boldsymbol{H}}$ of $\mathcal{P}_t$ the unique hyperbolic (resp. AdS) reflection $r_{\boldsymbol{H}}$ that fixes the bounding hyperplane $\partial \boldsymbol{H}$. By Lemma 7.15, when $t \to 0^\pm$, the rescaled reflections $\lim_{t \to 0} \mathfrak{r}_{|t|} r_{\boldsymbol{H}}(t) \mathfrak{r}_{|t|}^{-1}$ converge to a half-pipe reflection.

Note that by Proposition 7.13 $\mathcal{P}_t^\times$ does not contain any finite vertex of $\mathcal{P}_t$, hence it only remains to check the orbifold structure at the edges. Now, note that by Proposition 7.10 each edge of $\mathcal{P}_t$ disjoint from each of the ridges $\mathcal{R}_{\boldsymbol{i}^+ \boldsymbol{j}^+}$ is of type $\mathcal{E}_{\boldsymbol{i}^+ \boldsymbol{j}^- \boldsymbol{X}}$. Moreover, since the hyperbolic (resp. AdS) hyperplanes $\partial \boldsymbol{0}^+$, $\partial \boldsymbol{1}^-$ and $\partial \boldsymbol{A}$ are pairwise orthogonal for all t, the corresponding hyperbolic (resp. AdS) reflections commute. So we have

$$\Delta_t = \langle r_{\boldsymbol{0}^+}, r_{\boldsymbol{1}^-}, r_{\boldsymbol{A}} \rangle \cong (\mathbb{Z}/2\mathbb{Z})^3,$$

and similarly for the rescaled limit $\lim_{t \to 0} \mathfrak{r}_{|t|} \Delta_t \mathfrak{r}_{|t|}^{-1}$.

By symmetry and Proposition 7.12 (and also Proposition 7.11 in the AdS case) the conjugacy class of Δ_t in $\mathrm{Isom}(\mathbb{H}^4)$ or $\mathrm{Isom}(\mathbb{AdS}^4)$ does not depend on the chosen triple of reflections $r_{\boldsymbol{i}^+}, r_{\boldsymbol{j}^-}, r_{\boldsymbol{X}}$ such that there is an edge $\mathcal{E}_{\boldsymbol{i}^+ \boldsymbol{j}^- \boldsymbol{X}}$ of the polytope.

In this way, $\mathcal{P}_t^\times$ (together with the associated reflections) is locally modelled on

$$\mathbb{H}^4/_{\Delta_t} \quad \text{and} \quad \mathbb{AdS}^4/_{\Delta_t}$$

when $t \in I^+$ and $t \in I^-$, respectively. Similarly, $\lim_{t \to 0} \mathfrak{r}_{|t|} \mathcal{P}_t^\times$ is locally modelled on

$$\mathsf{HP}^4/_{\lim_{t \to 0} \mathfrak{r}_{|t|} \Delta_t \mathfrak{r}_{|t|}^{-1}}.$$

The proof is complete. $\qquad\square$

Remark 7.18. By an opportune orbifold version of Definition 2.11, the path $t \mapsto \mathcal{P}_t^\times$ defines a geometric transition on an orbifold. Moreover, the transition is C^1. Indeed, the holonomy
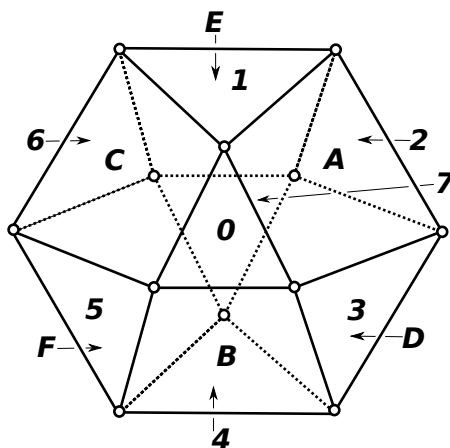
FIGURE 21. The ideal right-angled cuboctahedron $\mathcal{C} = \mathcal{P}_t \cap \mathbb{H}^3 = \mathcal{P}_0$. A quadrilateral face with label $\boldsymbol{X} \in \{\boldsymbol{A}, \ldots, \boldsymbol{F}\}$ coincides with $\mathcal{F}_{\boldsymbol{X}} \cap \mathbb{H}^3$, while a triangular face with label $\boldsymbol{i} \in \{\boldsymbol{0}, \ldots, \boldsymbol{7}\}$ coincides with the ridge $\mathcal{R}_{\boldsymbol{i}^+ \boldsymbol{i}^-}$ of $\mathcal{P}_t$.

representation depends C^1 on the parameter t as a consequence of Lemma 7.15. The developing map also depends C^1 essentially because the vectors defining the rescaled polytope $\mathfrak{r}_{|t|}(\mathcal{P}_t)$ depend C^1 on t.

Remark 7.19. By Proposition 7.12, the polytope $\mathcal{P}_{1/\sqrt{3}}$ is right-angled. In particular, it can be thought as a hyperbolic 4-orbifold. In contrast with $\mathcal{P}_t^\times$, the orbifold $\mathcal{P}_{1/\sqrt{3}}$ is complete (and clearly $\mathcal{P}_{1/\sqrt{3}}$ is the metric completion of $\mathcal{P}_{1/\sqrt{3}}^\times$).

Remark 7.20. Let us briefly elucidate the geometric structure of the cusp sections of the orbifold $\mathcal{P}_t^\times$ and of its recaled limit. In Figure 20 we showed a horospherical section of an ideal vertex of the polytope $\mathfrak{r}_{|t|}(\mathcal{P}_t)$, for $t < 0$, $t = 0$, $t > 0$. The subgroup of the orbifold fundamental group of $\mathcal{P}_t^\times$ preserving a cusp is isomorphic to the Coxeter group Γ_{cube} generated by reflections in the sides of a Euclidean cube — see [RSa] for more details. In the hyperbolic and AdS case, the restriction of the holonomy representation of the orbifold $\mathcal{P}_t^\times$ to this peripheral subgroup Γ_{cube} maps each generator to a Euclidean or Minkowski reflection in a face of the rectangular parallelepiped (as in Figures 19 and 20).

7.5. **The cuboctahedron.** If a bounded Euclidean polytope $\overline{\mathcal{P}} \subset \mathbb{R}^n$ is *vertex-transitive*, i.e. its symmetry group acts transitively on the set of the vertices, then $\overline{\mathcal{P}}$ is inscribed in a closed ball $\overline{\mathcal{B}}$. Let us identify $\mathbb{R}^n$ with our favourite affine chart $\mathsf{A}^n \subset \mathsf{S}^n$ of the projective sphere. Up to similarity, we can put $\overline{\mathcal{B}} = \overline{\mathbb{H}^n} \subset \mathsf{S}^n$, so that $\mathcal{P} = \overline{\mathcal{P}} \cap \mathbb{H}^n$ is an *ideal* hyperbolic polytope, i.e. all the vertices of $\mathcal{P}$ are ideal. The polytope $\mathcal{P}$ is unique up to isometry of $\mathbb{H}^n$.

A *Euclidean cuboctahedron* $\overline{\mathcal{C}} \subset \mathbb{R}^3$ (see Figure 1) is the convex envelop of the midpoints of the edges of a regular cube (or, equivalently, of a regular octahedron). The polyhedron $\overline{\mathcal{C}}$ is vertex-transitive, and has 14 facets, consisting of 6 squares and 8 triangles.

Let now $\mathcal{C} \subset \mathbb{H}^3$ be the *ideal hyperbolic cuboctahedron*. We shall identify the cuboctahedron $\mathcal{C}$ with $\mathcal{P}_0 \subset \mathbb{H}^3 \subset \mathbb{H}^4, \mathbb{A}\mathrm{d}\mathbb{S}^4$ thanks to the following (see Figure 21):

Proposition 7.21. *The set $\mathcal{P}_t \cap \mathbb{H}^3$ does not depend on $t \in I$ and is isometric to $\mathcal{C}$. Its 6 quadrilateral faces are given by $\mathcal{F}_{\boldsymbol{X}} \cap \mathbb{H}^3$ for all $\boldsymbol{X} \in \{\boldsymbol{A}, \ldots, \boldsymbol{F}\}$, while the 8 triangular faces are the ridges of $\mathcal{P}_t$ of type $\mathcal{R}_{\boldsymbol{i}^+ \boldsymbol{i}^-}$ for all $\boldsymbol{i} \in \{\boldsymbol{0}, \ldots, \boldsymbol{7}\}$. Moreover, we have*

$$\mathcal{P}_t \cap \mathbb{H}^3 = \bigcap_{s \in I} \mathcal{P}_s = \mathcal{P}_0.$$

Proof. It is straightforward to check that the same proof of [MR18, Proposition 3.19] for $t \in I^+ \cup \{0\}$ applies also when $t \in I^-$ (recall the isometric embedding $\iota \colon \mathbb{H}^3 \hookrightarrow \mathbb{X}_t^4$ defined by (3) in Section 2.8). □

A nice feature of the hyperbolic polyhedron $\mathcal{C}$ is that it is right-angled. In particular, there is a unique hyperbolic orbifold $\mathbb{H}^3/_{\Gamma_{\mathrm{co}}}$ isometric to $\mathcal{C}$, where the discrete group $\Gamma_{\mathrm{co}} < \mathrm{Isom}(\mathbb{H}^3)$ is generated by reflections through the bounding hyperplanes of $\mathcal{C}$. We shall thus interpret $\mathcal{C}$ as an orbifold.

7.6. **From polytopes to manifolds.** We now build the cone-manifolds of Theorem 1.1.

Let $\mathcal{N} \to \mathcal{C}$ be an *orbifold covering* for some 3-manifold $\mathcal{N}$; in other words, we can assume to have a torsion-free subgroup $\Gamma < \Gamma_{\mathrm{co}}$ and

$$\mathcal{N} = \mathbb{H}^3/_\Gamma \to \mathbb{H}^3/_{\Gamma_{\mathrm{co}}} = \mathcal{C}.$$

Remark 7.22. The first two points of Theorem 1.1 (that is, when $t \in I^+$) were proven in [MR18, Theorem 1.2] for a particular manifold $\mathcal{N}$ such that $\Gamma < \Gamma_{\mathrm{co}}$ is normal and $\Gamma/\Gamma_{\mathrm{co}} \cong \mathbb{Z}/2\mathbb{Z} \times \mathbb{Z}/2\mathbb{Z}$. Following our arguments, the proof given there can be indeed extended to every $\mathcal{N}$ that orbifold-covers $\mathcal{C}$, as in our hypothesis. Then the main content of our Theorem 1.1 is extending the deformation to half-pipe and Anti-de Sitter geometry, for a rather general choice of $\mathcal{N}$ (see also the discussion of Remark 7.29 for this point).

The covering $\mathcal{N} \to \mathcal{C}$ induces a tessellation of the hyperbolic 3-manifold $\mathcal{N}$ into copies of $\mathcal{C}$. One can think of $\mathcal{N}$ as obtained by pairing the facets of such copies of $\mathcal{C}$ through the maps induced by the identity. The existence (and abundance) of such orbifold-covers from a manifold to $\mathcal{C}$ is a consequence of Selberg's Lemma (and Malcev's Theorem).

Now, we pick a copy of $\mathcal{P}_t$ for each copy of $\mathcal{C}$ in $\mathcal{N}$. Recall that by Propsition 7.21 we put $\mathcal{C} = \mathcal{P}_0 \subset \mathcal{P}_t$. If two copies of $\mathcal{C}$ in $\mathcal{N}$ are adjacent along a quadrilateral face $\mathcal{F}_{\boldsymbol{X}} \cap \mathbb{H}^3$, we glue the corresponding two copies of $\mathcal{P}_t$ along the facet $\mathcal{F}_{\boldsymbol{X}}$ through the map induced by the identity. If two copies of $\mathcal{C}$ in $\mathcal{N}$ are adjacent along a triangular face $\mathcal{R}_{\boldsymbol{i}^+\boldsymbol{i}^-}$, we glue the corresponding two copies of $\mathcal{P}_t$ along the facet $\mathcal{F}_{\boldsymbol{i}^-}$ through the map induced by the identity. We call $\mathcal{X}_t'$ the resulting space. Note that we have paired all the facets of the copies of $\mathcal{P}_t$, with the exception of those of type $\mathcal{F}_{\boldsymbol{0}^+}, \ldots, \mathcal{F}_{\boldsymbol{7}^+}$.

Finally, let $\mathcal{X}_t$ be the space obtained by doubling $\mathcal{X}_t'$ along the unpaired facets. We call also $\mathfrak{r}_{|t|}(\mathcal{X}_t)$ the space obtained similarly to $\mathcal{X}_t$, by taking copies of the rescaled polytope $\mathfrak{r}_{|t|}(\mathcal{P}_t)$ in place of copies of $\mathcal{P}_t$. We have:

Proposition 7.23. *For all $t \in I \smallsetminus \{0\}$, the space $\mathcal{X}_t$ is homeomorphic to $\mathcal{N} \times S^1$. The same holds for the rescaled $\mathfrak{r}_{|t|}(\mathcal{X}_t)$ for all $t \in I$.*

Proof. By the proof of [MR18, Proposition 4.13] and by Proposition 7.3, as $t \neq 0$ there is a homeomorphism $\mathcal{P}_t \to \mathcal{C} \times [-1, 1]$ which restricts to

$$\begin{aligned}
\mathcal{P}_0 &\to \mathcal{C} \times \{0\} && \text{(see Figure 21)}, \\
\mathcal{F}_{\boldsymbol{0}^+} \cup \mathcal{F}_{\boldsymbol{2}^+} \cup \mathcal{F}_{\boldsymbol{4}^+} \cup \mathcal{F}_{\boldsymbol{6}^+} &\to \mathcal{C} \times \{-1\} && \text{(see Figure 22)}, \\
\mathcal{F}_{\boldsymbol{1}^+} \cup \mathcal{F}_{\boldsymbol{3}^+} \cup \mathcal{F}_{\boldsymbol{5}^+} \cup \mathcal{F}_{\boldsymbol{7}^+} &\to \mathcal{C} \times \{1\} && \text{(see Figure 22)}, \\
\mathcal{F}_{\boldsymbol{X}} &\to \mathcal{Q} \times [-1, 1] && \text{(see Figure 12)}, \\
\text{and} \quad \mathcal{F}_{\boldsymbol{i}^-} &\to \mathcal{T} \times [-1, 1] && \text{(see Figure 15)},
\end{aligned}$$

where for each $\boldsymbol{X} \in \{\boldsymbol{A}, \ldots, \boldsymbol{F}\}$ (resp. $\boldsymbol{i}^- \in \{\boldsymbol{0}^-, \ldots, \boldsymbol{7}^-\}$) there is a quadrilateral (resp. triangular) face $\mathcal{Q} \subset \partial\mathcal{C}$ (resp. $\mathcal{T} \subset \partial\mathcal{C}$) of $\mathcal{C}$ (recall Proposition 7.21). This extends to a homeomorphism $\mathcal{X}_t' \to \mathcal{N} \times [-1, 1]$. By doubling, the proof is complete. □
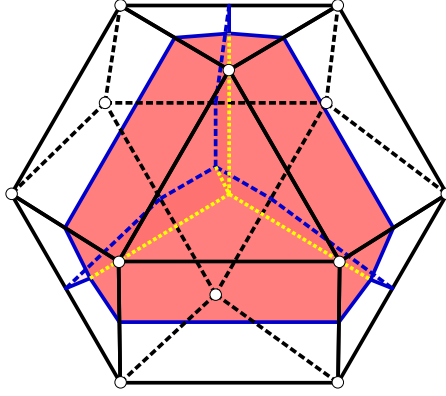
FIGURE 22. The union $\mathcal{C}_0 = \mathcal{F}_{\mathbf{0+}} \cup \mathcal{F}_{\mathbf{2+}} \cup \mathcal{F}_{\mathbf{4+}} \cup \mathcal{F}_{\mathbf{6+}}$ (resp. $\mathcal{C}_1 = \mathcal{F}_{\mathbf{1+}} \cup \mathcal{F}_{\mathbf{3+}} \cup \mathcal{F}_{\mathbf{5+}} \cup \mathcal{F}_{\mathbf{7+}}$) is an ideal right-angled cuboctahedron, pleated along the 6 red pentagons $\mathcal{R}_{\mathbf{i+}\,\mathbf{j+}}$ (each with 3 blue edges and 2 yellow edges in the picture). The facets of $\mathcal{C}_0$ are divided as follows: 4 ideal triangles $\mathcal{R}_{\mathbf{i+}\,\mathbf{i-}}$; 4 ideal triangles, each subdivided by the pleats as $\mathcal{R}_{\mathbf{i+}\boldsymbol{\ell-}} \cup \mathcal{R}_{\mathbf{j+}\boldsymbol{\ell-}} \cup \mathcal{R}_{\mathbf{k+}\boldsymbol{\ell-}}$; 6 ideal quadrilaterals, each subdivided by a pleat as $\mathcal{R}_{\mathbf{i+}\,\mathbf{X}} \cup \mathcal{R}_{\mathbf{j+}\,\mathbf{X}}$. The black edges are edges of the cuboctahedron, while the blue edges are contained in its facets, and the yellow edges intersect in the barycentre $\mathcal{V}_{\mathbf{0+2+4+6+}}$ (resp.$\mathcal{V}_{\mathbf{1+3+5+7+}}$).

7.7. Transition and cone structures.

In this section, we give the promised cone-manifold structure to the space $\mathcal{X}_t$ constructed above and conclude the proof of Theorem 1.1.

For $t \neq 0$, we put

$$\Sigma_t \;=\; \bigcup_{\mathcal{P}_t \text{ in } \mathcal{X}_t} \bigcup_{i \neq j} \mathcal{R}_{\mathbf{i+}\,\mathbf{j+}} \;\subset\; \mathcal{X}_t,$$

where the union runs over all the copies of $\mathcal{P}_t$ in $\mathcal{X}_t$. In other words, $\Sigma_t \subset \mathcal{X}_t$ is the union of the ridges with non-constant dihedral angle of the copies of $\mathcal{P}_t$ in $\mathcal{X}_t$ (see Proposition 7.12), and we have (see Proposition 7.17)

$$\mathcal{X}_t \smallsetminus \Sigma_t \;=\; \bigcup_{\mathcal{P}_t \text{ in } \mathcal{X}_t} \mathcal{P}_t^{\times}.$$

The couple $(\mathcal{X}_t, \Sigma_t)$ is homeomorphic to $(\mathcal{N} \times S^1, \Sigma)$ by Proposition 7.23, where $\Sigma \subset \mathcal{N} \times S^1$ is a foam by Proposition 7.13. If the covering $\mathcal{N} \to \mathcal{C}$ is finite, the foam Σ is compact by Proposition 7.12.

Recall from Proposition 7.17 that $\mathcal{P}_t^{\times}$ has a natural structure of orbifold. We have:

Proposition 7.24. *The natural map $\mathcal{X}_t \smallsetminus \Sigma_t \to \mathcal{P}_t^{\times}$ is an orbifold covering, and similarly for the rescaled limits.*

Proof. We continue to refer to [Thu79, Cho04] for details about orbifolds and their coverings.

By the proof of Proposition 7.17, it suffices to check that locally, near a k-stratum of the orbifold $\mathcal{P}_t^{\times}$, the map $\mathcal{X}_t \smallsetminus \Sigma_t \to \mathcal{P}_t^{\times}$ is modelled on the quotient map $\mathbb{R}^4 \to \mathbb{R}^4/_{(\mathbb{Z}/2\mathbb{Z})^{4-k}}$. Here, the i-th factor of $(\mathbb{Z}/2\mathbb{Z})^{4-k} < (\mathbb{Z}/2\mathbb{Z})^4$ is generated by the reflection $r_i \in \mathrm{O}(4)$ along the hyperplane $\{x_i = 0\} \subset \mathbb{R}^4$. Note that by Proposition 7.13, each stratum of the orbifold $\mathcal{P}_t^{\times}$ is non-compact and has an ideal vertex (in particular, $\mathcal{P}_t^{\times}$ has no 0-strata). This implies that it suffices to consider the case $k = 1$ only.

By symmetry (see Lemma 7.6), we can fix a horosection H of the ideal vertex $\mathcal{V} = \mathcal{V}_{\mathbf{0+0-3+3-}\,\mathbf{AB}}$ of $\mathcal{P}_t$ and look at the effect of the gluing on the copies of the link $\mathcal{L}_{\mathcal{V}} = H \cap \mathcal{P}_t$.
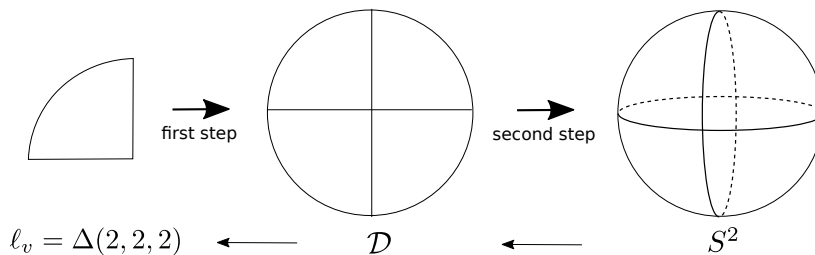
FIGURE 23. The effect of the gluing on the link ℓ_v of a vertex v of the link $\mathcal{L}_\mathcal{V}$ (which is depicted in Figure 18–left) of an ideal vertex $\mathcal{V}$ of $\mathcal{P}_t$ (see the proof of Proposition 7.24). The two top arrows represent the two steps of the construction of $\mathcal{X}_t$, while the bottom ones indicate orbifold coverings.

We also know by Proposition 7.13 that the orbifold structure on $\mathcal{L}_\mathcal{V}$ is that of a right parallelepiped. Again by symmetry, we can fix the vertex $v = v_{\mathbf{0}^-\mathbf{3}^+\mathbf{A}}$ of $\mathcal{L}_\mathcal{V}$ and look at the effect of the gluing of the copies of its link ℓ_v. We refer to Figure 23. Note that the orbifold structure on ℓ_v is that of a mirror triangle $\Delta(2,2,2) = S^2/_{(\mathbb{Z}/2\mathbb{Z})^3}$.

Recall from Section 7.6 that $\mathcal{X}_t$ is built from some copies of $\mathcal{P}_t$ in two steps. When we pair the facets of $\mathcal{P}_t$ of type $\mathcal{F}_\mathbf{X}$ and $\mathcal{F}_{\mathbf{i}^-}$, we glue four copies of ℓ_v around its vertex of type $\mathbf{0}^-\mathbf{A}$ and get a disc $\mathcal{D} = S^2/_{\mathbb{Z}/2\mathbb{Z}}$ with mirror boundary. The reason is that $\mathcal{C}$ is right-angled and $\mathcal{N}$ is a hyperbolic manifold, so each edge of its tessellation into copies of $\mathcal{C}$ has valence 4. By doubling along the unpaired facets, we double $\mathcal{D}$ and get the sphere S^2. Thus, the map $\mathcal{X}_t \smallsetminus \Sigma_t \to \mathcal{P}_t^\times$ induces at v the orbifold covering $S^2 \to \Delta(2,2,2)$, and therefore it is locally modelled on $\mathbb{R}^4 \to \mathbb{R}^4/_{(\mathbb{Z}/2\mathbb{Z})^3}$ near the 1-strata of $\mathcal{P}_t^\times$. The proof is complete. $\square$

Remark 7.25. Recalling Remark 7.19, we have also that $\mathcal{X}_{1/\sqrt{3}} \to \mathcal{P}_{1/\sqrt{3}}$ is an orbifold covering.

Recall now Remark 7.18. By lifting to $\mathcal{X}_t \smallsetminus \Sigma_t$ the geometric structures of the orbifold $\mathcal{P}_t^\times$, and similarly for the rescaled limits, we immediately get:

Corollary 7.26. *The family $\{\mathcal{X}_t \smallsetminus \Sigma_t\}_{t \in I}$ defines a C^1 geometric transition on $\mathcal{N} \times S^1 \smallsetminus \Sigma$.*

Remark 7.27. Recall Sections 3.1, 3.2 and 3.2 about horospheres and transition. From the proof of Proposition 7.24 one can recover the geometric transition on each cusp section of $\mathcal{X}_t$ (see Figure 19 and 20). We have a path of (non-singular) Euclidean structures (on the 3-torus or $\mathcal{K} \times S^1$, where $\mathcal{K}$ is the Klein bottle) collapsing to a Euclidean surface (a flat 2-torus or Klein bottle, which is a cusp section of $\mathcal{N}$), such that by rescaling in the direction of collapse the path extends to Minkowskian structures, via a transitional Galilean structure.

To conclude the proof of Theorem 1.1, it remains to understand what happens near Σ_t. Recall Definition 5.5 of simple hyperbolic, Anti-de Sitter, or half-pipe cone-manifold. Recall also Proposition 7.12 where the explicit expressions of the dihedral angles θ_t and φ_t of $\mathcal{P}_t$ are given. We have:

Proposition 7.28. *When $t \in I^-$, the space $\mathcal{X}_t$ is a simple Anti-de Sitter cone-manifold with spacelike singularity along Σ_t, whose 2-strata have all the same magnitude $\beta_t = -2 \cdot \varphi_t$.*

Similarly, $\mathcal{X}_t$ is a simple hyperbolic cone-manifold with cone angles $\alpha_t = 2 \cdot \theta_t$ when $t \in I^+$, and the rescaled limit $\lim_{t \to 0} \mathfrak{r}_{|t|} \mathcal{X}_t$ is a simple half-pipe cone-manifold.

Proof. Let us fix $t \in I^-$. We will show that $\mathcal{X}_t$ is locally modelled on

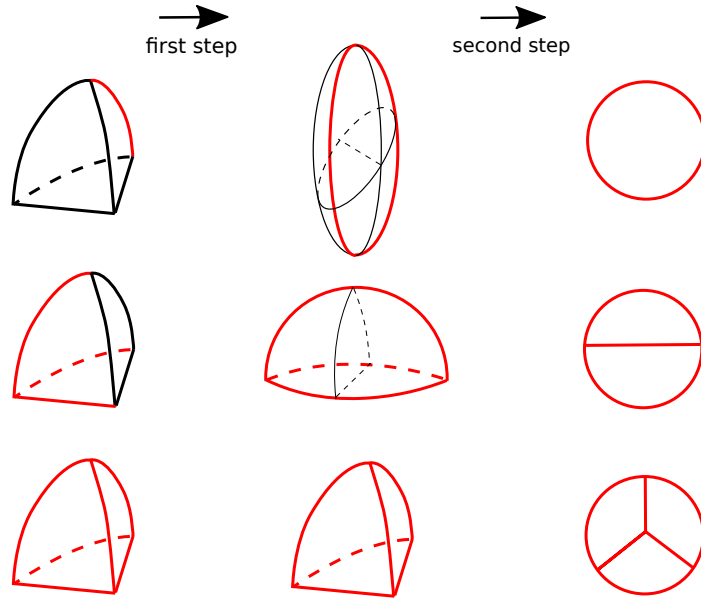$$\mathcal{D} = D(\mathbf{1}^+ \cap \mathbf{3}^+ \cap \mathbf{5}^+ \cap \mathbf{7}^+)$$

FIGURE 24. The effect of the gluing on the link $\mathcal{L}_\mathcal{V}$ of a finite vertex $\mathcal{V}$ of $\mathcal{P}_t$ (see the proof of Proposition 7.28). At each line we see the effect on a different class of vertices (see Figure 18). The two arrows represent the two steps of the construction of $\mathcal{X}_t$. In the first two columns we have some polyhedra, while in the third column we have cone-manifolds homeomorphic to S^3 (the singular locus is a red graph in S^3). These polyhedra and cone-manifolds are spherical when $t \in I^+$, and HS (with spacelike red locus contained in the de Sitter region) when $t \in I^-$. Each of the three cone-manifolds in the third column is the link of a point in a 2- (top), 1- (centre), and 0-stratum (bottom) of the cone-manifold $\mathcal{X}_t$.

in the sense of Definition 5.3, where for each bounding hyperplane of the polytope $\mathbf{1^+} \cap \mathbf{3^+} \cap \mathbf{5^+} \cap \mathbf{7^+} \subset \mathsf{S}^4$ we choose the unique AdS reflection that fixes it (recall Section 4.5 about reflections).

To this purpose, it suffices to look at the effect of the gluing of the copies of $\mathcal{P}_t$ on the link $\mathcal{L}_\mathcal{V}$ of each finite vertex $\mathcal{V}$. By symmetry (Lemma 7.6) and Proposition 7.13, it suffices to consider the vertices $\mathcal{V}_{\mathbf{1^+3^+0^-}A}$, $\mathcal{V}_{\mathbf{1^+3^+5^+0^-}}$ and $\mathcal{V}_{\mathbf{1^+3^+5^+7^+}}$ only. Recall from Section 7.6 that $\mathcal{X}_t$ is built from some copies of $\mathcal{P}_t$ in two steps. We refer to Figure 24.

- If $\mathcal{V} = \mathcal{V}_{\mathbf{1^+3^+0^-}A}$, the same argument in the proof of Proposition 7.24 implies that at the first step we glue 4 copies of $\mathcal{L}_\mathcal{V}$ around its edge of type $\mathbf{0^-}A$. The resulting space is a polyhedron in HS^3 (see Section 5.5) obtained as the intersection of two spacelike half-spaces. At the second step this polyhedron is doubled, and we get an HS cone 3-sphere with singular locus a spacelike unknotted circle in the de Sitter region. This is the link of a point in a 2-stratum of $\mathcal{D}$ (corresponding to $\partial\mathbf{1^+} \cap \partial\mathbf{3^+}$).
- If $\mathcal{V} = \mathcal{V}_{\mathbf{1^+3^+5^+0^-}}$, at the first step we just double $\mathcal{L}_\mathcal{V}$ along its $\mathbf{0^-}$-face, and then double the resulting polyhedron, to get an HS cone-sphere with singular locus a spacelike unknotted theta-graph in the de Sitter region. This is the link of a point in a 1-stratum of $\mathcal{D}$ (corresponding to $\partial\mathbf{1^+} \cap \partial\mathbf{3^+} \cap \partial\mathbf{5^+}$).
- If $\mathcal{V} = \mathcal{V}_{\mathbf{1^+3^+5^+7^+}}$ the link $\mathcal{L}_\mathcal{V}$ is doubled, to get an HS cone-sphere with singular locus a spacelike unknotted complete graph with four vertices in the de Sitter region. This is the link of a vertex of $\mathcal{D}$ (corresponding to $\partial\mathbf{1^+} \cap \partial\mathbf{3^+} \cap \partial\mathbf{5^+} \cap \partial\mathbf{7^+}$).

In particular, giving $\mathcal{X}_t$ the naturally induced stratification, it is locally modelled on $\mathcal{D}$. The proof for $t \in I^-$ is complete.

We omit the details for the hyperbolic and half-pipe case, since the proof goes exactly as in the AdS case with the obvious modifications (see Remark 7.16 regarding the choice of an HP reflection along each bounding hyperplane for the half-pipe case). $\qquad\square$

The cone structure on the links of points of Σ_t is drawn in Figures 25, 26 and 27. As mentioned in Remark 5.6, there is indeed a geometric transition from spherical to HS cone structures, as a singular version of the transition that one can visualise in Figure 10.

By noticing that as $t \to 0$ the cone-manifold $\mathcal{X}_t$ collapses to the hyperbolic 3-manifold $\mathcal{N}$, the proof of Theorem 1.1 is complete. We conclude with a last observation.
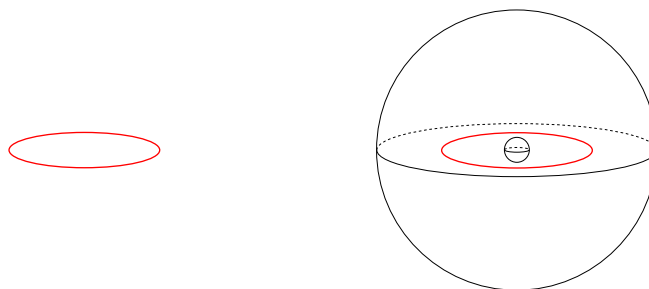

FIGURE 25. The link of a point in a 2-stratum of $\Sigma_t \subset \mathcal{X}_t$ is a cone 3-sphere with singular locus an unknotted circle (drawn in red). The geometry is spherical when $t \in I^+$ (left), and HS when $t \in I^-$ (right). In the HS case, the two balls (one internal and one external) are copies of $\mathbb{H}^3$ and represent the timelike directions — see Section 5.5.
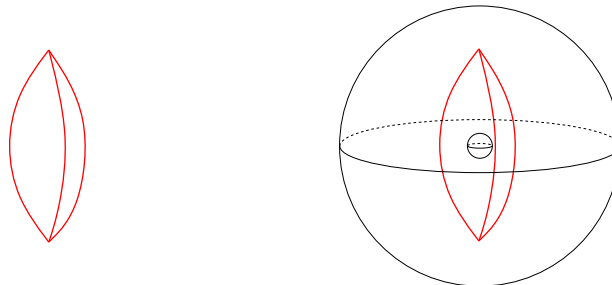

FIGURE 26. The link of a point in an edge (i.e. a 1-stratum) of $\Sigma_t \subset \mathcal{X}_t$, $t \neq 0$, is a cone 3-sphere with singular locus an unknotted theta-graph.
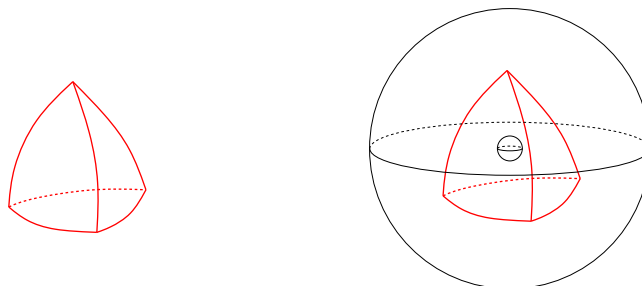

FIGURE 27. The link of a vertex (i.e. a 0-stratum) of $\Sigma_t \subset \mathcal{X}_t$, $t \neq 0$, is a cone 3-sphere with singular locus an unknotted complete graph on four vertices.

Remark 7.29. Theorem 1.1 can be extended as follows. A *cuboctahedral manifold* is a hyperbolic 3-manifold $\mathcal{N}$ that can be tessellated by some copies of the ideal right-angled cuboctahedron $\mathcal{C}$. Note that $\mathcal{C}$ has octahedral symmetry $\mathrm{Isom}(\mathcal{C}) \cong \mathbb{Z}/2\mathbb{Z} \times \mathfrak{S}_4$. Note also that every isometry between two faces of $\mathcal{C}$ is the restriction of a symmetry of $\mathcal{C}$. Moreover, as Figure 21 suggests, we have $\mathrm{Isom}(\mathcal{P}_t) \cong \mathrm{Isom}(\mathcal{C})$ in such a way that every symmetry of $\mathcal{C} = \mathcal{P}_0 \subset \mathcal{P}_t$ (see Proposition 7.21) is the restriction of a symmetry of $\mathcal{P}_t$. (To show this, the same argument of [RS19, Proposition 2.4] applies, by substituting "upper tetrahedral facet" with the link of the vertex $\mathcal{V}_{\mathbf{1}+\mathbf{3}+\mathbf{5}+\mathbf{7}+}$.)

Consider now the natural chequerboard colouring of the triangular faces of $\mathcal{C}$, inherited from that of the octahedron. It is easy to check that a symmetry of $\mathcal{C}$ preserves the chequerboard colouring if and only if its $\mathbb{Z}/2\mathbb{Z}$-factor is trivial. Moreover, this holds if and only if the corresponding symmetry of $\mathcal{P}_t$ preserves the half-space $\{x_4 \geq 0\}$ (and thus fixes the vertex $\mathcal{V}_{\mathbf{1}+\mathbf{3}+\mathbf{5}+\mathbf{7}+}$).

Thanks to this, it is not difficult to conclude that Theorem 1.1 holds for every cuboctahedral manifold $\mathcal{N}$ with a tessellation such that every pairing map between the copies of $\mathcal{C}$ is induced by a symmetry of $\mathcal{C}$ which preserves the chequerboard colouring. More generally, for every cuboctahedral manifold $\mathcal{N}$ one can find a 4-manifold (such that itself or a double covering is homeomorphic to $\mathcal{N} \times S^1$) supporting a geometric transition as in the conclusions of Theorem 1.1.

References

[And70a] E. M. Andreev. Convex polyhedra in Lobačevskiĭ spaces. *Mat. Sb. (N.S.)*, 81 (123):445–478, 1970. 28

[And70b] E. M. Andreev. Convex polyhedra of finite volume in Lobačevskiĭ space. *Mat. Sb. (N.S.)*, 83 (125):256–260, 1970. 28

[AP15] Norbert A'Campo and Athanase Papadopoulos. Transitional geometry. *Sophus Lie and Felix Klein: the Erlangen program and its impact in mathematics and physics*, 23:217, 2015. 1

[BBS11] Thierry Barbot, Francesco Bonsante, and Jean-Marc Schlenker. Collisions of particles in locally AdS spacetimes I. Local description and global examples. *Comm. Math. Phys.*, 308(1):147–200, 2011. 26

[BF18] Thierry Barbot and François Fillastre. Quasi-Fuchsian co-Minkowski manifolds, 2018. To appear in book "In the tradition of Thurston", arXiv:1801.10429. 3, 9

[BH11] M.R. Bridson and A. Häfliger. *Metric Spaces of Non-Positive Curvature*. Grundlehren der mathematischen Wissenschaften. Springer Berlin Heidelberg, 2011. 26

[BLP05] Michel Boileau, Bernhard Leeb, and Joan Porti. Geometrization of 3-dimensional orbifolds. *Ann. of Math. (2)*, 162(1):195–290, 2005. 1, 26

[CDW18] Daryl Cooper, Jeffrey Danciger, and Anna Wienhard. Limits of geometries. *Trans. Amer. Math. Soc.*, 370:6585–6627, 2018. 1, 2, 8, 11

[CHK00] Daryl Cooper, Craig D. Hodgson, and Steven P. Kerckhoff. *Three-dimensional orbifolds and cone-manifolds*, volume 5 of *MSJ Memoirs*. Mathematical Society of Japan, Tokyo, 2000. With a postface by Sadayoshi Kojima. 1, 26

[Cho04] Suhyoung Choi. Geometric structures on orbifolds and holonomy representations. *Geom. Dedicata*, 104:161–199, 2004. 40, 45

[CLM20] S. Choi, G.-S. Lee, and L. Marquis. Convex projective generalized Dehn filling. *Ann. Sci. Éc. Norm. Supér.*, 53:217–266, 2020. 40

[Dan11] Jeffrey Danciger. *Geometric transition: from hyperbolic to AdS geometry*. PhD thesis, Stanford University, 2011. 1, 8, 12, 14, 25, 26

[Dan13] Jeffrey Danciger. A geometric transition from hyperbolic to anti-de Sitter geometry. *Geom. Topol.*, 17(5):3077–3134, 2013. 1, 2, 11, 12, 21, 22, 25, 26, 27

[Dan14] Jeffrey Danciger. Ideal triangulations and geometric transitions. *J. Topol.*, 7(4):1118–1154, 2014. 1, 27

[FS19] François Fillastre and Andrea Seppi. Spherical, hyperbolic, and other projective geometries: convexity, duality, transitions. In *Eighteen essays in non-Euclidean geometry*, volume 29 of *IRMA Lect. Math. Theor. Phys.*, pages 321–409. Eur. Math. Soc., Zürich, 2019. 3, 9, 11, 15

[Hod86]   Craig David Hodgson. *Degeneration and regeneration of hyperbolic structures on three-manifolds (foliations, Dehn surgery)*. ProQuest LLC, Ann Arbor, MI, 1986. Thesis (Ph.D.)–Princeton University. 1

[HPS01]   Michael Heusener, Joan Porti, and Eva Suárez. Regenerating singular hyperbolic structures from Sol. *J. Differential Geom.*, 59(3):439–478, 2001. 1

[KM13]   Alexander Kolpakov and Bruno Martelli. Hyperbolic four-manifolds with one cusp. *Geom. Funct. Anal.*, 23(6):1903–1933, 2013. 28

[Koz13]   Kenji Kozai. *Singular hyperbolic structures on pseudo-Anosov mapping tori*. PhD thesis, Stanford University, 2013. 1

[Koz16]   Kenji Kozai. Hyperbolic structures from sol on pseudo-anosov mapping tori. *Geometry & Topology*, 20(1):437–468, 2016. 1

[KS10]   Steven P. Kerckhoff and Peter A. Storm. From the hyperbolic 24-cell to the cuboctahedron. *Geom. Topol.*, 14(3):1383–1477, 2010. 4, 33, 34, 35, 36

[LMA15a]   María Teresa Lozano and José María Montesinos-Amilibia. Geometric conemanifold structures on $\mathbb{T}_{p/q}$, the result of p/q surgery in the left-handed trefoil knot $\mathbb{T}$. *Journal of Knot Theory and Its Ramifications*, 24(12):1550057, 2015. 1

[LMA15b]   María Teresa Lozano and José María Montesinos-Amilibia. On the degeneration of some 3-manifold geometries via unit groups of quaternion algebras. *Revista de la Real Academia de Ciencias Exactas, Físicas y Naturales. Serie A. Matemáticas*, 109(2):669–715, 2015. 1

[LMR19]   Gye-Seon Lee, Ludovic Marquis, and Stefano Riolo. A small closed convex projective 4-manifold via Dehn filling. 2019. arXiv:1910.11649. 25

[Mar17]   Ludovic Marquis. Coxeter group in Hilbert geometry. *Groups Geom. Dyn.*, 11(3):819–877, 2017. 40

[McM17]   Curtis T. McMullen. The Gauss-Bonnet theorem for cone manifolds and volumes of moduli spaces. *Amer. J. Math.*, 139(1):261–291, 2017. 26

[MR18]   Bruno Martelli and Stefano Riolo. Hyperbolic Dehn filling in dimension four. *Geom. Topol.*, 22(3):1647–1716, 2018. 2, 4, 33, 34, 35, 36, 37, 38, 39, 44

[Por98]   Joan Porti. Regenerating hyperbolic and spherical cone structures from Euclidean ones. *Topology*, 37(2):365–392, 1998. 1

[Por02]   Joan Porti. Regenerating hyperbolic cone structures from Nil. *Geom. Topol.*, 6:815–852, 2002. 1

[Por13]   Joan Porti. Regenerating hyperbolic cone 3-manifolds from dimension 2. *Ann. Inst. Fourier (Grenoble)*, 63(5):1971–2015, 2013. 1

[PW07]   Joan Porti and Hartmut Weiss. Deforming Euclidean cone 3-manifolds. *Geom. Topol.*, 11:1507–1538, 2007. 1

[RSa]   Stefano Riolo and Andrea Seppi. Character varieties of a transitioning Coxeter 4-orbifold. In preparation. 5, 43

[RSb]   Stefano Riolo and Andrea Seppi. Old arXiv version of the present paper. arXiv:1908.05112v1. 36

[RS19]   Stefano Riolo and Leone Slavich. New hyperbolic 4-manifolds of low volume. *Alg. Geom. Topol.*, 19(5):2653–2676, 2019. 49

[Sep20]   Andrea Seppi. Examples of geometric transition from dimension two to four. *To appear, Actes du séminaire Théorie Spectrale et Géométrie, 26 pages*, 2020. 27

[Ser05]   Caroline Series. Limits of quasi-Fuchsian groups with small bending. *Duke Math. J.*, 128(2):285–329, 2005. 1

[The17]   The Sage Developers. *SageMath, the Sage Mathematics Software System (Version 8.1)*, 2017. www.sagemath.org. 4

[Thu79]   W. P. Thurston. The geometry and topology of three-manifolds. Electronic version 1.1, link, 1979. 1, 40, 45

[Thu98]   William P. Thurston. Shapes of polyhedra and triangulations of the sphere. In *The Epstein birthday schrift*, volume 1 of *Geom. Topol. Monogr.*, pages 511–549. Geom. Topol. Publ., Coventry, 1998. 26

[Tre19]   Steve J. Trettel. *Families of geometries, real algebras, and transitions*. PhD thesis, University of California, Santa Barbara, 2019. 1

[Vin85]   E B Vinberg. Hyperbolic reflection groups. *Russian Mathematical Surveys*, 40(1):31, 1985. 36

[Yag79]   I. M. Yaglom. *A simple non-Euclidean geometry and its physical basis*. Springer-Verlag, New York-Heidelberg, 1979. An elementary account of Galilean geometry and the Galilean principle of relativity, Heidelberg Science Library, Translated from the Russian by Abe Shenitzer, With the editorial assistance of Basil Gordon. 4, 15

Stefano Riolo: Institut de Mathématiques, Université de Neuchâtel, Rue Emile-Argand 11, 2000 Neuchâtel, Switzerland
  E-mail address: stefano.riolo@unine.ch

Andrea Seppi: CNRS and Université Grenoble Alpes 100 Rue des Mathématiques, 38610 Gières, France.
  E-mail address: andrea.seppi@univ-grenoble-alpes.fr